Cationically-modified nanoparticles for the pulmonary delivery of the telomerase inhibitor 2'-O-Methyl RNA for the treatment of lung cancer

Dissertation
zur Erlangung des Grades
des Doktors der Naturwissenschaften
der Naturwissenschaftlich-Technischen Fakultät III
Chemie, Pharmazie, Bio- und Werkstoffwissenschaften
der Universität des Saarlandes

von

Noha Nafee

Saarbrücken
2008

Tag des Kolloquiums:	12. Dezember 2008	
Dekan:	Univ.-Prof. Dr. rer. nat. Uli Müller	
Berichterstatter:	Prof. Dr. Claus-Michael Lehr	(1. Gutachter)
	Prof. Dr. Gerhard Wenz	(2. Gutachter)
	Prof. Dr. Rolf Hempelmann	(Vorsitzender)
	Dr. Ulrich F. Schäfer	(Akademischer Mitarbeiter)

Die vorliegende Dissertation entstand unter der Betreuung von

Prof. Dr. Claus-Michael Lehr
Jun. Prof. Dr. Marc Schneider

In der Fachrichtung Biopharmazie und Pharmazeutische Technologie
der Universität des Saarlandes

Bei Herr Prof. Lehr und Herr Jun. Prof. Schneider möchte ich mich für die Überlassung des Themas und die wertvollen Anregungen und Diskussionen herzlich bedanken

Table of contents

SUMMARY

Lung cancer is one of the main causes of cancer-related death worldwide. One of the reasons behind the extensive tumour growth is telomerase enzyme, which is notably expressed in cancer cells. Recent strategies for cancer therapy include, therefore, telomerase inhibition with antisense RNA. A major challenge is the weak cellular uptake of these nucleotide-based drugs which necessitates the choice of appropriate carrier systems. The aim of this study was hence to evaluate chitosan-modified PLGA nanoparticles (cNP) as carrier for the antisense oligonucleotide ***2´-O-Methyl-RNA*** (OMR) and their efficacy as inhalation therapy.

Modification of the process parameters revealed the tuneability of the NP synthesis in terms of size and surface charge. Studying the cellular uptake of fluorescent cNPs with increasing amounts of chitosan showed better uptake in A549 than in Calu-3 cells. Chitosan significantly improved the uptake and binding with OMR; however, higher chitosan content reduced the uptake efficiency. Uptake studies under *in vivo* mimicking conditions using air-interface cultures showed superior cellular uptake of OMR/cNP nanoplexes compared to free OMR. As a proof of the concept, the ability of OMR to reduce telomerase activity was demonstrated.

In conclusion, the concept of telomerase inhibition based on nanoscale delivery of antisense oligonucleotides represents a step forward to a new generation of cancer therapeutics.

ZUSAMMENFASSUNG

Lungenkrebs ist einer der Hauptgründe für krebsbasierten Todesfälle weltweit. Mit einer der Ursachen für das ungehemmte Wachstum von Krebszellen ist das Enzym Telomerase, das in vermehrtem Maße in Krebszellen auftritt. Eine interessante Behandlungsstrategie besteht daher in der Hemmung dieses Enzyms. Eine Hemmung der Telomerase ist mit antisens-RNA möglich. Um solche Arzneistoffe in die Zelle zu transportieren sind jedoch geeignete Trägersysteme notwendig. Das Hauptziel der vorliegenden Arbeit war die Untersuchung von Chitosan-modifizierten PLGA Nanopartikeln (cNP) als Trägersystem für das Antisense-Oligonukleotid 2'-O-Methyl-RNA (OMR) sowie ihres möglichen Einsatzes für einer Inhalationstherapie.

Die Änderung der Prozessparameter erlaubt eine maßgeschneiderte Synthese der cNP hinsichtlich Größe und Ladung. Die Untersuchung der NP in Zellkultur-Modellen ergab eine bessere Aufnahme in A549 als in Calu-3 Zellen. Die zelluläre Aufnahme unter Verwendung von realitätsnahen „Air-interface“-Kulturen zeigte zudem auch eine überlegene Aufnahme von partikelbasierten Systemen im Vergleich zu freien Oligonukleotiden. Außerdem konnte gezeigt werden, dass die Telomerase -Aktivität in diesen Zellen tatsächlich gehemmt war.

In der vorliegenden Arbeit konnte das Konzept der Telomerase-Hemmung zur Krebsbehandlung, basierend auf Komplexen von Antisense-Oligonukleotiden mit nanoskaligen Trägersystemen, erfolgreich *in vitro* demonstriert werden.

Chapter 1

General introduction *

*** Parts of this chapter have been published as book chapters:**

- N. Nafee, M. Schneider, C-M. Lehr. (2008) Charge modification of pharmaceutical nanocarriers: biological implications. In Multifunctional pharmaceutical nanocarriers. V. Torchilin, Ed.; Springer, New York, USA.
- N. Nafee, V. Bhardwaj, M. Schneider. (2008) Transport across biological barriers. In Nanotherapeutics – drug delivery concepts in nanosciences, A. Lamprecht, Ed.; WSPC: Singapore.

I. Lung cancer

Lung cancer is one of the leading causes of cancer-related death worldwide; in the United States, an estimated 213,380 new cases (114,760 men and 98,620 women) of lung and bronchus cancer were diagnosed in 2007 and 160,390 deaths (89,510 in men and 70,880 in women) were registered because of the disease. In the UK, lung cancer is the third most common cause of death after heart disease and pneumonia (nearly 29,000 deaths in 2002 with a male to female ratio of approximately two to one). The incidence and death figures in UK are worse than in Europe and USA (965,241 men and 386,891 women).

The lungs are unique among all organs in having a very high degree of exposure to the internal environment through the pulmonary blood flow and to the outside by exposure to air flow. In patients suffering from metastatic cancer, the lungs are continually exposed to neoplastic cells that are shed from the primary tumor and circulate in their blood. Despite the natural defence mechanism in the lungs, few cells survive and proliferate into metastasis, Figure 1.

(A) **(B)**

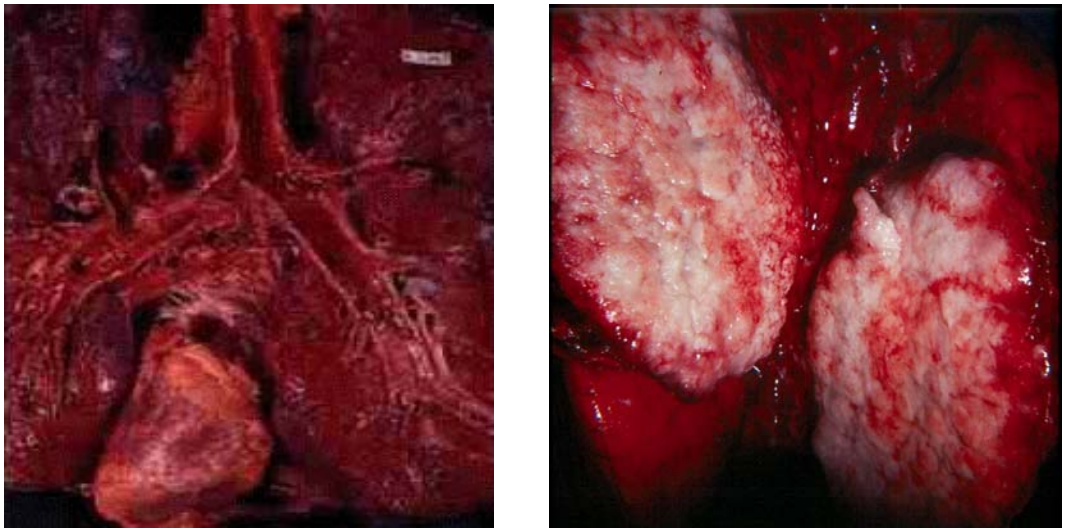

Figure 1: (A) human healthy lung taken from (http://www.freewebs.com), (B) human lung tumor taken from (http://www.taconichills.k12.ny.us/.../lungcancerpic.jpg)

There are two main types of lung cancer based on the characteristics of the disease and its response to treatment; Non-small-cell lung cancer (NSCLC) and Small-cell lung cancer (SCLC). NSCLC accounts for ~85% of all lung cancer; NSCLC patients have poor prognosis with 5-year survival rates of ~14% for all stages. It is subdivided into 3 major types:

- Adenocarcinoma, which arises from mucous glands and scar tissues. It is most frequently occurring in non-smokers, women and elderly.
- Squamous cell (epidermoid) carcinoma, which accounts for 35% of all cancer cases. Cells are usually well differentiated and locally spread.
- Large-cell carcinoma, which accounts for 10% only of all cancer cases and is less well differentiated.

SCLC constitutes ~20% of all cancers. Arising from endocrine cells, these tumors secrete many polypeptide hormones. Some of these hormones provide feedback to the cancer cells and cause tumor growth. Therefore, this type of tumor grows rapidly, taking ~ 3 years from initial malignant change to presentation.

Treatment of lung cancer

Current cancer therapy in general usually involves intrusive processes including application of catheters to allow chemotherapy, initial chemotherapy to shrink any cancer present, surgery to then remove the tumor(s) if possible, followed by more chemotherapy and radiation. The purpose of the chemotherapy and radiation is to kill the tumor cells as these cells are more susceptible to the actions of these drugs and methods because of their growth at a much faster rate than healthy cells, at least in adults.

Due to the importance of the lungs for survival, it is often not possible to remove tumors completely without dramatically reducing the lung function. Therefore, lung tumors are mainly treated by radiation therapy and/or chemotherapy.

Chemotherapy plays an important role in treating many patients with both NSCLC and SCLC. The effectiveness of the treatment is directly related to the treatment's ability to target and to kill the cancer cells while affecting as few healthy cells as possible. However, the regular administration of high doses of these intense drugs is always encountered with some side effects which are sometimes so intense that the patient must discontinue therapy before the drugs have a chance to eradicate the cancer.

Many chemotherapeutics are now available on the market such as paclitaxel, doxorubicin, 5-fluorouracil and camptothecin-based drugs. ***Paclitaxel*** is a microtubule-stabilizing agent which promotes polymerization of tubulin causing cell death by disrupting the dynamics necessary for cell division. It has antineoplastic activity especially against primary epithelial ovarian carcinoma, breast, colon, and non-small cell lung cancers. The currently available formulation includes Chremophor EL containing polyethoxylated castor oil and ethanol for solubilisation. However, Chremophor EL is poorly tolerated and shows side effects such as hypersensitivity reactions, nephrotoxicity and neurotoxicity [1].

One of the most potent and widely used anticancer drugs is ***doxorubicin*** which works by inhibiting the synthesis of nucleic acids within cancer cells [2]. Doxorubicin has a number of undesirable side effects such as cardiotoxicity and myelosuppression which leads to a very narrow therapeutic index. Various researchers have studied ways to target doxorubicin delivery to cancer tissues or at least to diminish its side effects.

Antineoplastic agents Camptothecin-based drugs, specifically ***irinotecan*** (Camptosar) and ***topotecan*** (Hycamptin) have been approved by the FDA and are used most often either in conjunction with ***5-fluorouracil*** as a first therapy or sometimes used alone after 5-fluorouracil has failed. Analogs of these molecules have shown up to 1000- fold higher activity but are a great challenge to delivery because of their extreme hydrophobicity [3].

As mentioned above, the usefulness of cancer chemotherapy is restricted by the dose-limiting toxicity of cytotoxic anticancer drugs and the occurrence of side effects, for example, renal tubular damage induced by cisplatin [4], or peripheral neuropathy induced by cisplatin [5], paclitaxel [6], or oxaliplatin [7]. Therefore, various researchers have studied ways to target these chemotherapeutic drugs to cancer tissues or at least to diminish their side effects. Attempts to explore the potential of specific and target-oriented delivery systems include the use of antibodies [8], monoclonal antibodies [9], growth factors [10] [11], transferrin [12, 13] [14], cytokines [15], folate [16, 17] and low-density lipoprotein (LDL) [18]. Plant lectins, which are proteins that specifically recognize and agglutinate cell-associated carbohydrates, were also suggested to have the potential to select cancer cells [19] [20].

In addition, formulation strategies such as co-solvent systems, emulsification, inclusion in cyclodextrins, micellization, and liposome formation have been studied to alter the pharmacokinetics and the biodistribution of chemotherapeutics. One of the successful approaches for small-molecule drugs has been the use of colloidal drug delivery systems – nanoparticles, in today's parlance - as will be described in the next section.

One of the best and most recent prospects for attaining versatile targeted therapeutics is the use of **antisense oligonucleotides** as therapeutic agents against cancer [21]. This is because, theoretically, they can be adapted to control genetic processes in a manner that regulates any pathological process in any disease, and in a highly selective way that minimizes unwanted side effects. Unlike conventional drugs acting on proteins, nucleic acids can be used for either 'gain of function' actions, i.e. gene therapy, or 'loss of function' activity, such as antisense oligonucleotides that require a match only to a short, unique sequence in the gene [22]. A more precise, stable and highly efficient 'knockdown effect' was introduced using small-interfering RNA (siRNA). The short double-stranded

siRNA (around 22 nucleotides long) is taken up by a protein complex in the cytoplasm called RNA-induced silencing complex (RISC) that unwinds the dsRNA oligonucleotide, uses one strand to identify mRNA with a matching sequence segment, catalytically degrades the mRNA and thus abolishes the expression of the encoded protein [23].

Nowadays promising approaches focus on such therapies that target specific proteins and pathways involved in the growth and proliferation of cancer cells. Much interest has recently focused on ***telomerase***, a ribonucleoprotein that adds telomeric repeats to the end of the telomeres [24] and therefore prevents telomere shortening occurring during replication of the cell cycle. The ribonucleoprotein complex consists of two major components, the protein subunit human telomerase reverse trancriptase (hTERT) which has catalytic activity [25, 26] and the human telomerase RNA component (hTR) which serves as a template for the synthesis of telomeric repeats [27], Figure 2.

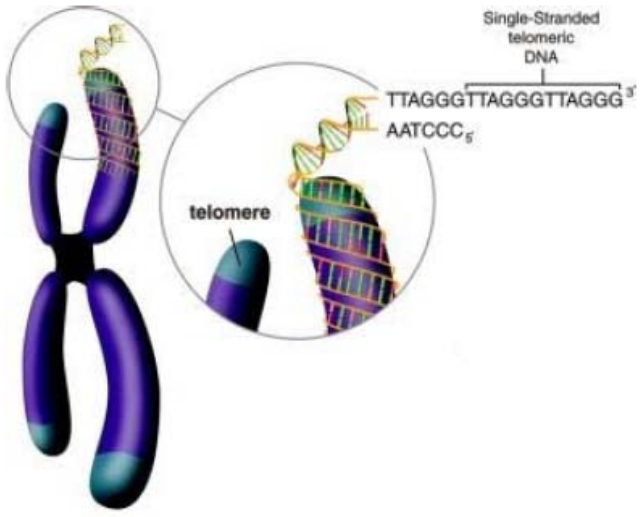

<u>Figure 2:</u> Schematic presentation of telomere on the chromosome ends.

Telomerase activity has been detected in most human cancers and cancer cell lines as well as in stem cells and regenerative tissues, but not in most normal somatic cells [28]. Telomerase activity is required for continuous cell proliferation and allows cells to

overcome senescence. Therefore, activation of telomerase is considered to be one of the key mechanisms leading to immortalization of tumor cells and tumor progression. Telomerase activity has been detected in 80% of NSCLC but not in non-cancerous lung tissue. Furthermore, it has been shown that telomerase activity is associated with advanced stage of NSCLC patients and poor prognosis. These findings suggest that telomerase may represent a promising target for anticancer treatment.

In recent years, several classes of ***telomerase inhibitors*** targeting different sites of the telomerase complex or the telomeres have been evaluated [29]. The RNA template hTR is an ideal target for inhibition by oligonucleotides because it is intrinsically accessible to nucleic acids. The antisense oligonucleotide ***2′-O-methyl-RNA*** (OMR) with a phosphorothioate backbone is a potent and sequence-selective inhibitor of telomerase. 2′-O-methyl-RNA binds to the complementary hTR template sequence with high affinity acting as a competitive enzyme inhibitor of telomerase [30]. However, the application of these nucleotide based drugs is limited by many problems namely their premature degradation in the body and their poor cellular uptake [23]. Accordingly, successful delivery of such drugs requires the proper choice of the suitable carrier system that targets them to their site of action.

Nowadays, nanocarriers have gained a great attention as promising gene delivery systems for both plasmid DNA and antisense oligonucleotides, among which nanoparticles have shown broad application. On this basis, our main goal is the application of nanoparticles as carrier for the antisense oligonucleotides, OMR. PLGA nanoparticles were extensively applied as efficient, biodegradable delivery system. However, the negative surface charge of these particles limits their binding potential to the negatively charged plasmid and minimizes their interaction with the cell membrane. The surface modification of these particles with a cationic polymer would be expected to improve their interaction with the oligonucleotides and enhance their internalization by the targeted cells. Owing to

its relative safety, permeability enhancing properties, and efficiency as gene carrier, chitosan was selected as the cationic polymer to modify the surface charge of PLGA nanoparticles.

Improvement of the cellular uptake of the nanoparticles necessitates the reduction of their size. In addition, more effective binding with OMR requires the augmentation of the surface charge. Therefore, the impact of the formulation parameters on the colloidal characteristics of chitosan-modified PLGA nanoparticles (cNP) needs to be essentially studied in order to obtain tuneable delivery system in dependence of the payload. Thereafter, the influence of these properties on the binding and uptake of the antisense oligonucleotides is to be investigated. Meanwhile, the most suitable purification techniques from the unbound polymers are to be selected and the possible cytotoxic effects caused by the nanoparticles need to be explored. The use of OMR/cNP nanoplexes for the treatment of lung cancer involves the possibility to apply them in the form of inhalation therapy. For this reason, the proper choice of the nebulization technique/device that retains the colloidal characters of the particles is considered to be a matter of interest. A step forward to the *in vivo* conditions is then to test the uptake of these nanoplexes in air interface-cultured cell lines.

II. State of the art - Nanocarriers & targeted treatment of lung cancer

The use of various pharmaceutical carriers to enhance the *in vivo* efficiency of many drugs and drug administration protocols has been well established during the last decade in both pharmaceutical research and clinical setting. Among these carriers, pharmaceutical nanocarriers have been recently developed and have shown tremendous progress in drug and gene delivery. Nanotechnology focuses on formulating therapeutic agents in biocompatible nanocomposites such as nanoparticles, nanocapsules, nanoemulsions, liposomes, micellar systems, and conjugates [31].

In the context of cancer therapy, nanocarriers improved the effect of chemotherapeutic agents through their protection during blood circulation, better delivery to the diseased area, higher encapsulation efficiency, or prolonged release of the therapeutic payload, Figure 3. Numerous examples in this context were reviewed in details by Brannon-Peppas and Blanchette [13].

Many years of work have yielded several successful products, including Ambisome™ (Liposomal Amphotericin B), Doxil™ (Stealth™ liposomal doxorubicin) and, recently, Abraxane™ (nanoparticle albumin paclitaxel). These 'passive' nanoparticle formulations improve the drug pharmacokinetics and tissue distribution, eventually releasing the drug into surrounding tissues due to the lack of targeting moities.

While some of these nanocarriers have already made their way into clinics, there are still others under preclinical development and research. Among the recent advances in this area hydrophobically-modified glycol chitosan nanoparticles loaded with docetaxel [32], ligand based dendrimers [33], long circulating stealth immunoliposomes [34], immunonanoparticles [35] can be mentioned.

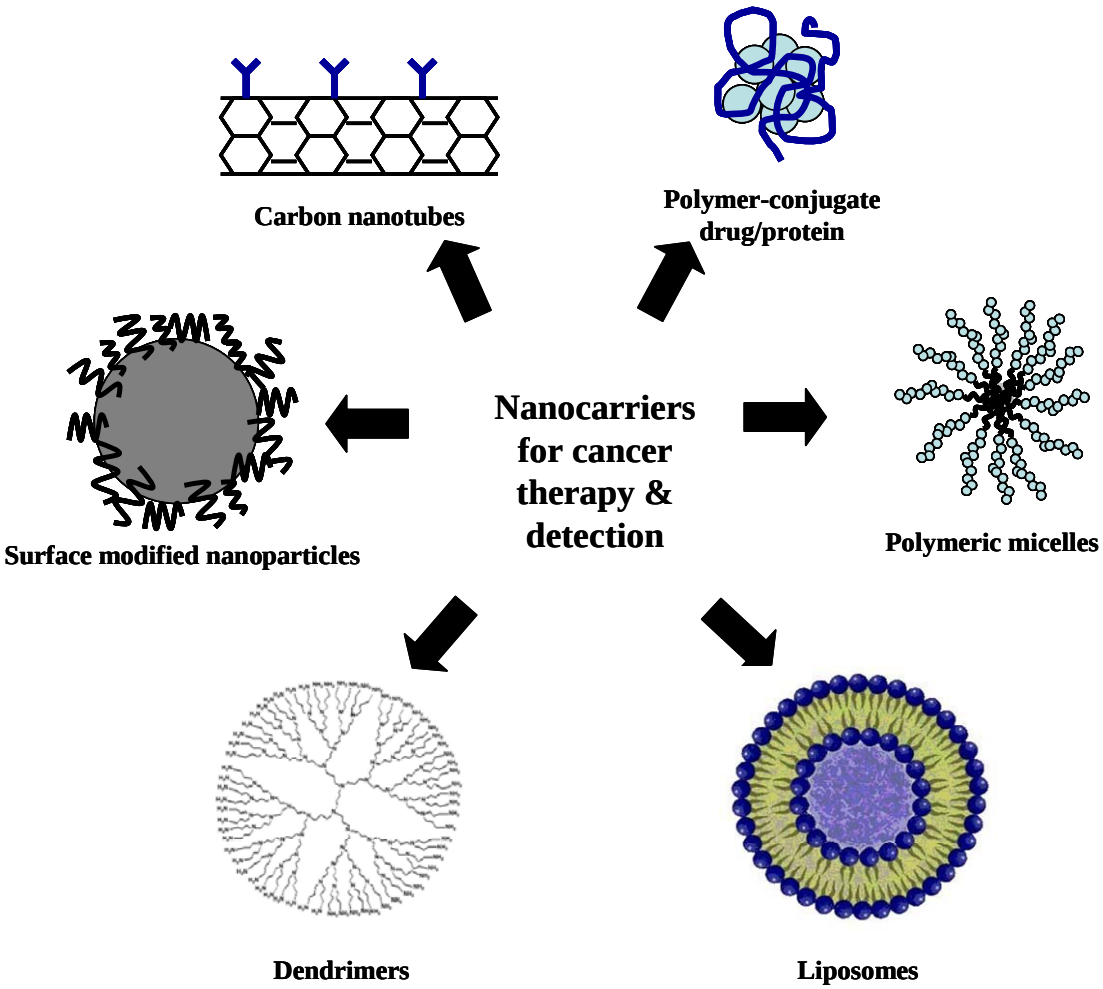

Figure 3: Different types of nanocarriers applied for cancer detection and therapy

More recently, is the treatment of cancer through the application of nucleotide based drugs having the ability to interfere with the pathway of cancer cells. Essentially, this group of compounds needs to be delivered intracellularly and in case of siRNA to the cytosol to exert their action. Figure 4 shows the many barriers to using siRNA as a therapeutic. The first hurdle for these nucleic acids, surprisingly, is just keeping them from being removed from the blood and excreted by the kidney. They are also subject to enzymatic degradation and must be kept from being distributed too widely, so that they can be concentrated at the pathological tissue. Moreover, the application of therapies based on antisense oligonucleotides is hampered by their instability to cellular nuclease and their weak penetration to the lipophilic cellular membrane. Overcoming these hurdles has posed

the greatest barriers to oligonucleotide therapeutics. Nanoparticles seem to be among the right choices for this purpose since they have similar sizes compared to certain viruses which are the natural but pathogenic gene delivery systems [23].

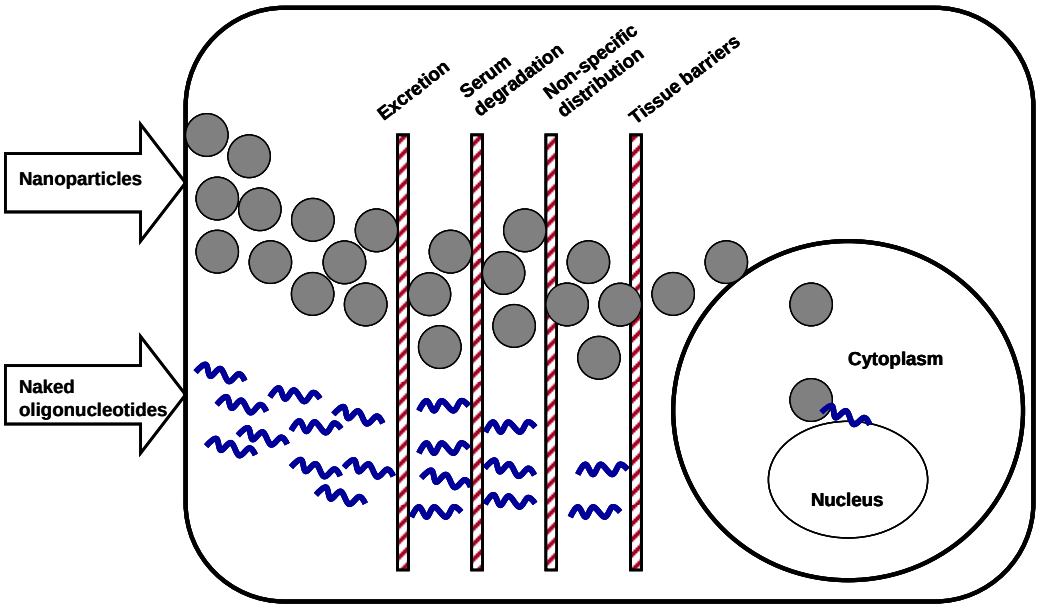

Figure 4: Schematic presentation role of nanoparticles in overcoming the different hurdles of intracellular delivery of nucleotide-based drugs

Improved efficacy of these nanocarriers can be achieved by the association of different functional groups that increase the targetability, the longevity and/or the intracellular penetration of the nanocarriers. For example, plasmid pCMVLuc which codes for luciferase production was incorporated into nanoparticles composed of polyethylenimine (PEI) linked to poly(ethylene glycol) (PEG) which are then coated with either transferrin or epithelial growth factor. *In vivo* studies in mice showed that the gene expression from administration of targeted systems was 10–100 higher in tumors than in other organs [36]. Similarly, Gopalan et al. [37] used DOTAP:cholesterol nanoparticles as an alternate non-immunogenic gene delivery vector for the systemic therapy of lung cancer. In another study, Kaul et al [38] encapsulated reporter plasmid DNA encoding for β-galactosidase (pCMV-β) in gelatine and PEGylated gelatine nanoparticles for Lewis lung carcinoma.

Recently, a ligand targeted and sterically stabilized nanoparticles formulation for the targeted delivery of antisense oligodeoxynucleotides and small interference RNA into lung cancer cells was developed [39].

Decisive parameters for improved cellular uptake of nanoparticles

Due to their subcellular size, nanoparticles can penetrate into tissues and be efficiently taken up by the cells. By modulating polymer characteristics or surface properties one can control the release of therapeutic agent and/or deliver it to distant target sites.

1. Size-dependent uptake of nanocarriers

Size is considered to be of utmost importance and it was demonstrated repeatedly that small particles are more efficiently taken up into cells [31] or accumulated in tissue [40] than larger particles. In some cell lines (e.g. Hepa 1-6, HepG2, and KLN 205), only the submicron size particles are taken up efficiently but not microparticles [41].

Prabha et al. [42] investigated the gene transfection levels of different size fractions of PLGA nanoparticles and found that the lower size nanoparticle fraction resulted in a 27-fold higher transfection in COS-7 cells and 4-fold higher transfection in HEK293 cells for the same dose of nanoparticles. Similarly, the efficiency of uptake of 100 nm size particles was 15-250 fold greater than larger size (1 and 10 μm) microparticles [43]. Nanoparticles were also able to penetrate throughout the submucosal layers while the larger size microparticles were predominantly localized in the epithelium lining [43]. In addition, chitosan nanoparticles are shown to be internalized into intestinal, nasal, and ocular epithelial cells [44, 45]. Furthermore, cationically-modified silica nanoparticles with sizes between 10 and 100 nm complexed with plasmid DNA were found to be colocalized inside and around the nucleus and to promote gene expression in COS-1 cells [46].

Even though size plays a crucial role, other factors such as surface chemistry and charge influence the important molecular routes as well in a non negligible way [47, 48] and need to be considered for the optimal design of the carrier system.

2. Surface modification of nanocarriers

Surface modification of pharmaceutical nanocarriers, such as liposomes, micelles, nanocapsules, polymeric nanoparticles, solid lipid particles, and niosomes, is normally used to control their biological properties in a desirable fashion and to simultaneously make them perform various therapeutically or diagnostically important functions. The most important results of such modification include an increased stability and half-life of drug carriers in the circulation, required biodistribution, passive or active targeting into the required pathological zone, responsiveness to local physiological stimuli, and ability to serve as contrast agents for various imaging modalities (gamma-scintigraphy, magnetic resonance imaging, computed tomography, ultra-sonography).

Polyion complex micelles (PIC) using Poly (L-lysine) (PLL)-PEG block copolymer, in which PLL segments and plasmid DNA formed a hydrophobic core by charge neutralization and PEG plays a role as a surrounding hydrophilic shell layer showed a prolonged *in vivo* circulation time after systemic administration [49], whereas polyethyleneimine (PEI)-grafted PEGs were synthesized to address the cytotoxicity and aggregation problems of PEI [50].

Liposomes have been demonstrated to be an efficient drug and gene carrier system [51, 52]. Surface modification of liposomes achieved by inserting PEG, dextran, galactose or mannose to the surface was found to increase liposome stability and to introduce some specificity in binding to particular cell types [53-55]. Ligand-targeted stealth liposomes utilizing targeting moieties like transferrin coupled to the liposome surface were shown to

selectively deliver their payload to target tumor cells via receptor-mediated internalization for the treatment of lung cancer, murine bladder tumor, adult T-cell leukaemia [12, 56].

2.1. Charge modification of nanocarriers

One of the most basic and crucial properties influencing the environmental interaction of nanoparticulate matter is their charge. This is attributed to the stability of the suspension which is achieved by electrostatic repulsion or, less often, by steric hindrance. Therefore, the surface charge of the nanoscale particles is a standard parameter to be characterized and reported. Positively charged carriers are mainly employed for complexation purposes; this especially holds for the intracellular delivery of genetic material (RNA, DNA, and oligonucleotides) which is typically negatively charged [57].

Charge is a key parameter assumed to play an essential role in cellular drug/gene delivery [47, 48, 58] and is also known to have an influence on the cytotoxicity [59-63] as well as the barrier integrity [60, 64]. In addition, it is known that a charge facilitates the transfection to cells [65-69]. Therefore, trials to augment the surface charge in order to enhance the transfection efficiency of the nanoplexes should not negatively affect the safety aspects of these carriers [70, 71].

Poly (lactic-co-glycolic acid) *(PLGA)* is one of the most common biodegradable polymers used for drug delivery purposes. Typically possessing a negative surface charge, interaction of PLGA nanoparticles with the negatively charged DNA is limited and their transport through the cell membrane is restricted. A novel cationic modification of PLGA was recently developed based on poly[vinyl-3-(dialkylamino)alkylcarbamate-*co*-vinyl acetate-*co*-vinyl alcohol]-graft-poly(D,L-lactide-*co*-glycolide) [72]. The branched polyesters are biodegradable and positively charged depending on the type and degree of amine substitution. Accordingly, they have been successfully used for DNA delivery [73], transmucosal insulin delivery [74] and pulmonary drug delivery [75]. Similarly, ***poly ε-***

caprolactone nanoparticles coated with trimethyl chitosan proved to bind efficiently DNA and enhance its internalization by COS-1 cells [76].

Chitosan has a strong affinity for DNA and protect against the degradation with DNAse. Attempts have been recently made to provide cell-specific targeting and/or improved transfection efficiency. For instance, methylation [77], PEGylation [78], thiolation, mannosylation [79] and galactosylation of chitosan [80, 81], Figure 5, were aiming for fine-tuned adjustments towards targeted delivery of therapeutic genes despite the partial reduction in the net positive charge [45, 82]. ***Chitosan nanoparticles*** were widely used for the delivery of macromolecules such as vaccines and proteins across the oral and nasal mucosa [83]. For example, ovalbumin was adsorbed on the surface of chitosan particles to enhance their uptake by the M-cells of the Peyer's patches. Additional coating of particles with sodium alginate was able to prevent the burst release of the loaded antigen and improve the nanoparticle stability in gastrointestinal fluid [84]. One other way to enhance the interaction of chitosan nanoparticles with M-cells is their coating with carbohydrates having an affinity for the mannose receptors in the epithelial cells like glucomannan. Coating was evidenced by the conversion of the zeta potential to negative values. These particles were efficiently loaded with the inmunomodulatory protein complex P1 for the peroral administration [85].

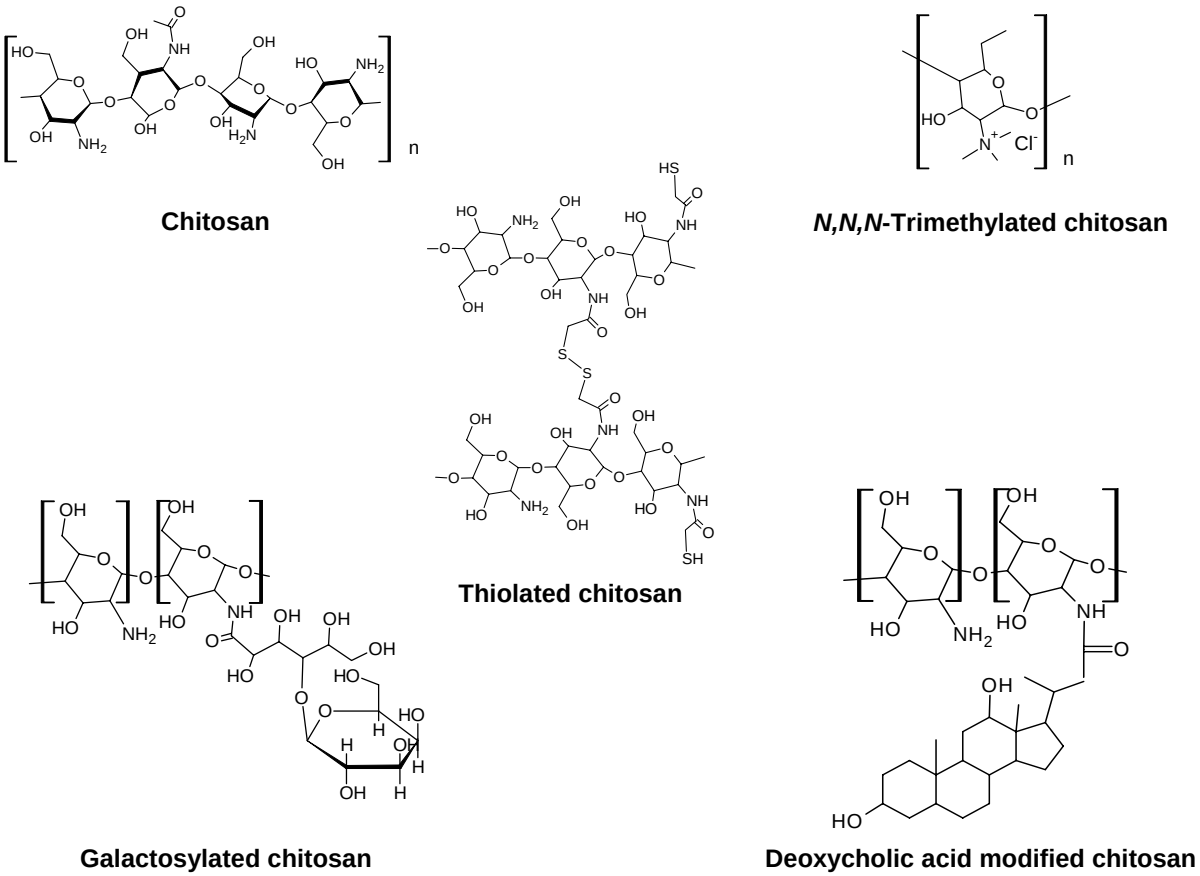

Figure 5: Chemical structure of chitosan and different modified chitosans

2.2. Multifunctional nanocarriers

Numerous studies described modified nanocarriers as well as their use for the delivery of various drugs and genes. However, to encounter the complexity of biological systems, environments of different polarities, pH values, viscosities, and presence of molecular targets, modern nanocarrier systems need to combine a multitude of functionalities. Therefore, looking into the future of the whole field of drug delivery, we have to think about the development of the next generation of pharmaceutical nanocarriers, combining variety of properties and allowing for the simultaneous performance of multiple functions. Multicomponent targeting, exploiting the huge available surface of the nanoscale transport vehicles, the use of different ligands and surrounding susceptible molecules is considered to be essential for future improvements [86, 87]. All these factors need be considered and

adapted to the target area designing multifunctional nanocarrier systems. The most important results of such modification include an increased stability and half-life of drug carriers in the circulation, required biodistribution, passive or active targeting into the required pathological zone, responsiveness to local physiological stimuli, and ability to serve as contrast agents for various imaging modalities (gamma-scintigraphy, magnetic resonance imaging, computed tomography, ultra-sonography), Figure 6.

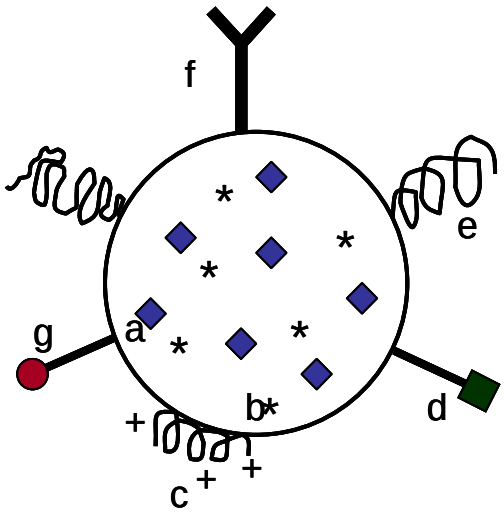

Figure 6: Schematic presentation of multifunctional pharmaceutical nanocarriers (a: drug loaded into the carrier, b: magnetic particles loaded into the nanocarrier, c: charged polymer on the surface, d: cell penetrating peptide, e: surface attached polymer e.g. PEG for long circulating nanocarrier, f: monoclonal antibody on surface of immunocarrier, g: heavy metal atom for contrast gamma- or MR imaging)

Recently, Li et al [88] have developed a self-assembled non-viral nanoparticle formulation, which was prepared by condensing the siRNA and calf thymus DNA with protamine into a compact complex, followed by coating with cationic liposomes [39]. To further stabilize the formulation, PEG conjugated lipids were post-inserted into the outer lipid membrane. A targeting ligand (anisamide) was conjugated to the distal end of PEG for targeting sigma receptor expressing tumor cells. The targeted nanoparticle formulation was shown to selectively deliver siRNA to receptor positive tumor cells *in vitro* [39, 88]

and *in vivo* [89]. In addition, a single I.V. injection of the targeted nanoparticles resulted in 70-80% gene silencing in an experimental metastatic tumor, B16F10 lung metastasis in mice and prolonged the survival time of the animals by 30% [90].

Mechanism of uptake of nanocarriers

1. Biodistribution

Nanoparticles will usually be taken up by the liver, spleen and other parts of the reticuloendothelial system (RES) depending on their surface characteristics. Particles with more hydrophobic surfaces will preferentially be taken up by the liver, followed by the spleen and lungs [91]. Hydrophilic nanoparticles (35 nm diameter), such as those prepared from poly(vinyl pyrrolidone), show less than 1% uptake by the spleen and liver and 8 h after injection show 5–10% still circulating in the bloodstream. However, nanoparticles prepared of 50% PNVP and 50% N-isopropyl acrylamide (45 or 126 nm diameter) instead showed preferential uptake by the liver [92]. Particles with longer circulation times, and hence greater ability to target the site of interest, should be 100 nm or less in diameter and have a hydrophilic surface in order to reduce clearance by macrophages [93]. Therefore, coating of nanoparticle surface with hydrophilic polymers can create a cloud of chains at the particle surface which will repel plasma proteins and work in this area began by adsorbing surfactants to the nanoparticles surface. Other trials include forming the particles from branched or block copolymers with hydrophilic and hydrophobic domains.

2. Opsonization

One of the most important biological barriers to controlled drug or gene delivery is the process of opsonization. This is the process by which a foreign organism or particle becomes covered with opsonin proteins, thereby making it more visible to phagocytic cells [94]. A widely used method to slow the opsonization of nanoparticles is the use hydrophilic polymers such as PEG, poloxamers and poloxamines, which can block the

electrostatic and hydrophobic interaction of opsonin with the particle surface and hence imparts stealth and sterically stabilized properties to the nanoparticles [95]. The characteristics of this layer; thickness, charge, grafting density, molecular conformation and functional groups, all impact the way in which it interacts with opsonin.

3. Active and passive targeting

In general, cellular uptake of nanocarriers is phrased as targeted delivery. This can be subdivided into passive targeting - based on effects such as **enhanced permeability and retention (EPR)** [96, 97], tumor environment and direct local delivery - and active targeting which makes use of the coupling of a tissue/cell specific marker leading to localized accumulation of the nanocarriers [98]. The defective vascular architecture, created due to the rapid vascularization necessary to serve fast-growing cancers, coupled with poor lymphatic drainage allows an enhanced permeation and retention effect (EPR effect) [99, 100].

Considering cellular interaction, passive and active processes might be further specified and sub-divided; paracellular and transcellular route comprising the passive [101], and concentration dependent barrier transport and the endocytotic pathways comprising the active transport. These mechanisms are based on different aspects for uptake like clathrin-mediated, ligand-activated, non-coated vesicular internalization as well as phago- and pinocytosis [102, 103].

Regarding the nanocarrier size and cellular uptake several thresholds have been speculated. Particles of size up to 200 nm are internalized using **clathrin-coated pits** [104] whereas larger objects are taken up via **caveolae membrane invaginations**. Other pathways are still under research and not clarified yet [105]. Particles as large as 500 nm can be taken up by non-phagocytic cells using an energy-dependent process [106].

Panyam *et al.* [107] investigated the uptake and distribution of PLGA nanoparticles in various cell lines. In vascular smooth muscle cells, the nanoparticle internalization was

found to be incorporated through **fluid phase pinocytosis** and in part through clathrin--coated pits [31]. The uptake was concentration and time dependent; efficiency decreased at higher doses, suggesting that the uptake pathway is a saturable process. Following their uptake, nanoparticles were transported to primary endosomes, then to sorting endosomes [31]. A fraction is then sorted out of the cell through recycling endosomes while the remaining fraction is transported to secondary endosomes, which then fuse with lysosomes. In the acidic pH of the endo-lysosomes, charge reversal of the nanoparticles occurs due to transfer of the proton/hydronium ions from the bulk solution to the particle surface [103]. This allows stronger electrostatic interactions leading to localized destabilization of the membrane and escape of the nanoparticles to the cytoplasmic compartment. In another study, the ζ-potential of chitosan-tripolyphosphate nanoparticles was found to be very sensitive to changing pH values, indicating that the surface density of protonated amino groups and the degree of protonation are reversibly responsive to pH changes [108]. On the other hand, polystyrene nanoparticles are unable to escape the endo-lysosomal compartment because they do not exhibit a charge reversal with pH changes [107].

Accordingly, nanoparticles which show transition in their surface charge from anionic at pH 7 to cationic in the acidic endosomal pH (pH 4–5) were found to escape the endosomal compartment whereas the nanoparticles which remain negatively charged at pH 4–5 were retained mostly in the endosomal compartment [31]. Nanoparticles could hence be directed to different cell compartments either by the proper choice of the polymers or surface modification of the nanoparticles with cationic polymers like chitosan [45, 109], PEI [110, 111] or poly (2-dimethyl-amino)ethyl methacrylate [112].

Once the extracellular concentration of nanoparticles decreases, exocytosis begins. Proteins (e.g. albumin) are responsible for inducing nanoparticle exocytosis. While the drop in intracellular nanoparticle levels could lead to lower efficiency of the encapsulated

therapeutic agent, it has to be realized that nanoparticle concentration outside the cell may not fall so rapidly *in vivo*. Thus, there could be a constant presence of nanoparticles next to the cells, which might lead to mass transport equilibrium being reached, resulting in higher intracellular nanoparticle levels [31].

Chitosan is known to be a penetration enhancer in acidic environment towards monostratified and pluristratified epithelia both endowed with and lacking tight junctions [113]. Chitosan nanoparticles are able to be internalized into intestinal, nasal, and ocular epithelial cells [44, 45]. The uptake of chitosan nanoparticles seems to be related to the size and the superficial charge: the higher the superficial positive charge, the stronger is the affinity between the nanoparticles and the negatively charged cell membranes and mucus, respectively [44]. The contact time of the carrier systems with the membrane might increase uptake probability [114, 115]. Nevertheless, opposite results were found as well, where negatively charged and neutral particles showed an increased uptake into the Peyer's patches of mice [116].

In order to promote the internalization into the cells, several cell receptor ligands have been used to take advantage of **receptor-mediated endocytosis**. Among which galactose-, folate- and transferrin-bound cationized polymers have shown to be effective [53, 56, 81, 117]. Recently, chitosan oligomers were substituted with a trisaccharide branch that targets cell-surface lectins to improve the gene delivery to lungs [118]. The results indicated a 10-fold increase in gene expression levels in human bronchial epithelial cell line (16HBE14o-) as well as in human liver hepatocyte (HepG2) cells. Furthermore, *in vitro* and *in vivo* transfection confirmed lectin-mediated uptake [118].

Safety aspects of inhaled nanocarriers

The fast growth of nanoparticle-mediated drug or gene delivery calls for concerns about the potential health and environmental risks related to their use. Such risks include

deposition and clearance of solid nanoparticles, systemic translocation and body distribution as well as direct effects on the central nervous system [119]. Studies showed that nanoparticles can translocate from the respiratory tract via different pathways to other organs/tissues and induce direct adverse responses in remote organs. In particular, such responses may be initiated through the interaction of nanoparticles with subcellular structures following endocytosis by different target cells. Therefore, special attention must be given to such effects, which could have serious consequences in a compromised organism or a compromised organ.

In the field of nanotoxicology, most of the toxicological data are based on our knowledge either from ultrafine nanoparticles (<100 nm in diameter) inhaled during daily life such as carbon black, diesel particulates, silica and titanium oxide nanoparticles or from the widespread production of nanomaterials even for non-medical purposes [120, 121]. Single wall carbon nanotubes also showed some degree of toxicity such as multifocal granulomas and unusual inflammatory responses after inhalation [122, 123]. On the other hand, cationic polystyrene nanospheres induced mitochondrial damage and cell death without inflammation [121], while cerium oxide (CeO_2) nanoparticles generate free radicals that produce significant oxidative stress in the cells as reflected by reduced glutathione and α-tocopherol levels, these toxic effects of CeO_2 nanoparticles are dose and time dependent [124].

On the other hand, in the field of nanomedicine, the toxicological study of nanoscaled drug/gene delivery systems is a critical branch of research as the processing of nanoparticles in biological systems could lead to unpredictable effects. For deep lung delivery there are different aspects which have to be considered; one is the acute toxicity of the drug delivery system on the epithelia; and secondly the interaction of nanoparticles with the alveolar environment. Brzoska et al. [125] investigated the suitability of nanoparticles synthesized from porcine gelatine, human serum albumin and

polyalkylcyanoacrylate as drug and gene carriers for pulmonary administration. The results showed little or no cytotoxicity into bronchial epithelia cells 16HBE14o-cells. Besides, Dailey et al. [126] suggest that biodegradable polymeric nanoparticles of PLGA and diethylaminopropylamine polyvinyl alcohol-grafted-PLGA may not induce the same inflammatory response as non-biodegradable polystyrene particles of comparable size.

Inhalation therapy of nanocarriers

Inhalation therapy, as the name suggests, involves the delivery of drugs to the respiratory tract for either local or systemic effects. The lung's anatomy and its transport function between the external environment and the systemic circulation are perfectly matched. The large alveolar surface area (70-100 m^2) suitable for drug absorption, the low thickness of the epithelial barrier, extensive vascularisation and relatively low proteolytic activity in the alveolar space compared to other routes of administration and the absence of the first pass metabolism favored drug delivery through the pulmonary route.

Nanoparticle delivery to the lungs is an attractive concept; large porous nanoparticles matrices can be retained in the lungs leading to a prolonged drug release, while particles smaller than 260 nm showed reduced uptake by alveolar macrophages [127]. Therefore, successful delivery of inhaled particles depends mostly on particle size, particle density and consequently the mass median aerodynamic diameter. Particles with an aerodynamic diameter of 3 μm are mainly deposited in the alveolar region, beyond this level bronchial deposition starts to increase. On this basis, pulmonary delivery of nanoparticles either via dry powder formulations [128, 129] or nebulised suspensions [130] has gained more attention in recent years for the local treatment of lung diseases [131, 132] and potentially for the systemic delivery of nanosized drug delivery systems [133].

III. Aim of the thesis

In this thesis, the main goal was to develop nanoparticulate carrier system for the pulmonary delivery of nucleotide-based drugs. In particular, we studied the application of PLGA nanoparticles as carrier for the telomerase inhibitor, 2'-O-MethylRNA, for the treatment of lung cancer. In order to improve the binding of the negatively charged oligonucleotide and the nanoparticles, the nanoparticle surfaces were modified with the positively charged polymer, chitosan. Therefore, the main aim can be subdivided into the following objectives:

- Preparation and characterization of chitosan-modified PLGA nanoparticles, in addition to the study of the effect of polymer content and the process parameters on the particle size and surface charge in order to obtain small, positively charged particles with predictive good complexation and uptake behavior.

- Binding to the antisense oligonucleotides, 2'-O-MethylRNA, including characterization of the nanoplexes, their uptake in human cancer cell lines as well as the dependence of this binding and uptake on the surface charge of the particles.

- Investigation of the toxicity aspects of the nanoparticles with different colloidal properties and the factors interfering with the study.

- Application of the nanoplexes as inhalation therapy; selection of the nebulization technique and study of the cellular uptake after air-interface deposition.

REFERENCES

[1] A.K. Singla, A. Garg, D. Aggarwal, Paclitaxel and its formulations. International Journal of Pharmaceutics 235(1-2) (2002) 179-192.

[2] H.S. Yoo, T.G. Park, In vitro and in vivo anti-tumor activities of nanoparticles based on doxorubicin-PLGA conjugates. Polymer Preparation 41 (2000) 992-993.

[3] J. Williams, R. Lansdown, R. Sweitzer, M. Romanowski, R. LaBell, R. Ramaswami, E. Unger, Nanoparticle drug delivery system for intravenous delivery of topoisomerase inhibitors. Journal of Controlled Release 91(1-2) (2003) 167-172.

[4] B. Rosenberg, Noble metal complexes in cancer chemotherapy. Adv. Exp. Med. Biol. 91 (1977) 129-150.

[5] L.M. Schuchter, Exploration of platinum-based dose-intensive chemotherapy strategies with amifostine (Ethyol). Eur. J. Cancer 32A Suppl 4 (1996) S40-42.

[6] C.M. Spencer, D. Faulds, Paclitaxel. A review of its pharmacodynamic and pharmacokinetic properties and therapeutic potential in the treatment of cancer. Drugs 48 (1994) 794-847.

[7] L. Gamelin, O. Capitain, A. Morel, A. Dumont, S. Traore, L.B. Anne, S. Gilles, M. Boisdron-Celle, E. Gamelin, Predictive Factors of Oxaliplatin Neurotoxicity: The Involvement of the Oxalate Outcome Pathway. Clinical Cancer Research 13(21) (2007) 6359-6368.

[8] C. Hebert, K. Norris, J.J. Sauk, Targeting of human squamous carcinomas by SPA470-doxorubicin immunoconjugates. Journal of Drug Targeting 11(2) (2003) 101-107.

[9] A. Funaro, A.L. Horenstein, P. Santoro, C. Cinti, A. Gregorini, F. Malavasi, Monoclonal antibodies and therapy of human cancers. Biotechnology Advances 18(5) (2000) 385-401.

[10] C. Arteaga, Targeting HER1/EGFR: a molecular approach to cancer therapy. Semin. Oncology 30(3 Suppl 7) (2003) 3-14.

[11] G.O. Hellawell, D.J. Ferguson, S.F. Brewster, V.M. Macaulay, Chemosensitization of human prostate cancer using antisense agents targeting the type 1 insulin-like growth factor receptor. BJU Int. 91 (2003) 271-277.

[12] S. Anabousi, M. Laue, C.-M. Lehr, U. Bakowsky, C. Ehrhardt, Assessing transferrin modification of liposomes by atomic force microscopy and transmission electron microscopy. European Journal of Pharmaceutics and Biopharmaceutics 60(2) (2005) 295-303.

[13] L. Brannon-Peppas, J.O. Blanchette, Nanoparticle and targeted systems for cancer therapy. Advanced Drug Delivery Reviews
Intelligent Therapeutics: Biomimetic Systems and Nanotechnology in Drug Delivery 56(11) (2004) 1649-1659.

[14] D.A. Eavarone, X. Yu, R.V. Bellamkonda, Targeted drug delivery to C6 glioma by transferrin-coupled liposomes. J. Biomed. Mater. Res. 51 (2000) 10-14.

[15] A. Signore, M. Chianelli, R. Bei, W. Oyen, A. Modesti, Targeting cytokine/chemokine receptors: a challenge for molecular nuclear medicine. Eur. J. Nucl. Med. Mol. Imaging 30 (2003) 149–156.

[16] J. Liu, C. Kolar, T.A. Lawson, W.H. Gmeiner, Targeted Drug Delivery to Chemoresistant Cells: Folic Acid Derivatization of FdUMP[10] Enhances Cytotoxicity toward 5-FU-Resistant Human Colorectal Tumor Cells. The Journal of Organic Chemistry 66(17) (2001) 5655-5663.

[17] Y. Lu, P.S. Low, Folate-mediated delivery of macromolecular anticancer therapeutic agents. Advanced Drug Delivery Reviews 54(5) (2002) 675-693.

[18] U. Schmidt-Erfurth, H. Diddens, R. Birngruber, T. Hassan, Phyotdynamic targeting of human retinoblastoma cells using covalent low density lipoprotein conjugates. British Journal of Cancer 75 (1997) 54–61.

[19] K. Yanagihara, P.W. Cheng, Lectin enhancement of the lipofection efficiency in human lung carcinoma cells. Biochim. Biophys. Acta 1472 (1999) 25-33.

[20] M. Wirth, A. Fuchs, M. Wolf, B. Ertl, F. Gabor, Lectin-mediated drug targeting: preparation, binding characteristics, and antiproliferative activity of wheat germ agglutinin conjugated doxorubicin on Caco-2 cells. Pharm. Res. 15 (1998) 1031– 1037.

[21] T. Merdan, J. Kopecek, T. Kissel, Prospects for cationic polymers in gene and oligonucleotide therapy against cancer. Advanced Drug Delivery Reviews 54(5) (2002) 715-758.

[22] K.J. Scanlon, Antigenes: siRNA, ribozymes and antisense. Current Pharmaceutical Biotechnology 5(5) (2004) 415-420.

[23] M.C. Woodle, P.Y. Lu, Nanoparticles deliver RNAi therapy. Materials Today 8(8, Supplement 1) (2005) 34-41.

[24] G.B. Morin, The human telomere terminal transferase enzyme is a ribonucleoprotein that synthesizes TTAGGG repeats. Cell 59(3) (1989) 521-529.

[25] J. Feng, W.D. Funk, S.S. Wang, S.L. Weinrich, A.A. Avilion, C.P. Chiu, R.R. Adams, E. Chang, R.C. Allsopp, J. Yu, e. al., The RNA component of human telomerase. Science 269 (1995) 1236-1241.

[26] A. Kilian, D.D. Bowtell, H.E. Abud, G.R. Hime, D.J. Venter, P.K. Keese, E.L. Duncan, R.R. Reddel, R.A. Jefferson, Isolation of a candidate human telomerase catalytic subunit gene, which reveals complex splicing patterns in different cell types. Hum Mol Genet 6 (1997) 2011-2019.

[27] T.M. Nakamura, G.B. Morin, K.B. Chapman, S.L. Weinrich, W.H. Andrews, J. Lingner, C.B. Harley, T.R. Cech, Telomerase catalytic subunit homologs from fission yeast and human. Science 277 (1997) 955-959.

[28] N.W. Kim, M.A. Piatyszek, K.R. Prowse, C.B. Harley, M.D. West, P.L.C. Ho., G.M. Coviello, W.E. Wright, S.L. Weinrich, J.W. Shay, Science 266 (1994) 2011-2015.

[29] B. Herbert, A.E. Pitts, S.I. Baker, S.E. Hamilton, W.E. Wright, J.W. Shay, D.R. Corey, Inhibition of human telomerase in immortal human cells leads to progressive telomere shortening and cell death. Proc. Natl. Acad. Sci. U. S. A. 96 (1999) 14276-14281.

[30] A.E. Pitts, D.R. Corey, Inhibition of human telomerase by 2'-O-methyl-RNA 10.1073/pnas.95.20.11549. Proc. Natl. Acad. Sci. USA 95(20) (1998) 11549-11554.

[31] J. Panyam, V. Labhasetwar, Biodegradable nanoparticles for drug and gene delivery to cells and tissue. Advanced Drug Delivery Reviews
Biomedical Micro- and Nano-technology 55(3) (2003) 329-347.

[32] H. Hwang, I.-S. Kim, I.C. Kwon, Y.-H. Kim, Tumor targetability and antitumor effect of Docetaxel loaded hydrophobically modified glycol chitosan nanoparticles. Journal of Controlled Release 128 (2008) 23-31.

[33] A. Agarwal, S. Saraf, A. Asthana, U. Gupta, V. Gajbhiye, N.K. Jain, Ligand based dendritic systems for tumor targeting. International Journal of Pharmaceutics 350(1-2) (2008) 3-13.

[34] W.W.K. Cheng, T.M. Allen, Targeted delivery of anti-CD19 liposomal doxorubicin in B-cell lymphoma: A comparison of whole monoclonal antibody, Fab' fragments and single chain Fv. Journal of Controlled Release 126(1) (2008) 50-58.

[35] N. Debotton, M. Parnes, J. Kadouche, S. Benita, Overcoming the formulation obstacles towards targeted chemotherapy: In vitro and in vivo evaluation of cytotoxic drug loaded immunonanoparticles. Journal of Controlled Release 127(3) 219-230.

[36] M. Ogris, G. Walker, T. Blessing, R. Kircheis, M. Wolschek, E. Wagner, Tumor-targeted gene therapy: strategies for the preparation of ligand-polyethylene glycol-polyethylenimine/DNA complexes. Journal of Controlled Release 91(1-2) (2003) 173-181.

[37] B. Gopalan, I. Ito, C.D. Branch, C. Stephens, J.A. Roth, R. Ramesh, Nanoparticle Based Systemic Gene Therapy for Lung Cancer: Molecular Mechanisms and Strategies to Suppress Nanoparticle-Mediated Inflammatory Response. Technology in Cancer Research and Treatment 3(6) (2004) 647-658.

[38] G. Kaul, M. Amiji, Tumor-targeted gene delivery using poly(ethyleneglycol)-modified gelatin nanoparticles: in vitro and in vivo studies. Pharm. Res. 22(6) (2005) 951-961.

[39] S.D. Li, L. Huang, Targeted Delivery of Antisense Oligodeoxynucleotide and Small Interference RNA into Lung Cancer Cells. Molecular Pharmaceutics 3(5) (2006) 579-588.

[40] A. Lamprecht, N. Ubrich, H. Yamamoto, U. Schäfer, H. Takeuchi, P. Maincent, Y. Kawashima, C.-M. Lehr, Biodegradable Nanoparticles for Targeted Drug Delivery in Treatment of Inflammatory Bowel Disease. J. Pharm. Exp. Ther. 299(2) (2001) 775 - 781.

[41] W. Zauner, N.A. Farrow, A.M.R. Haines, In vitro uptake of polystyrene microspheres: effect of particle size, cell line and cell density. Journal of Controlled Release 71(1) (2001) 39-51.

[42] S. Prabha, W.-Z. Zhou, J. Panyam, V. Labhasetwar, Size-dependency of nanoparticle-mediated gene transfection: studies with fractionated nanoparticles. International Journal of Pharmaceutics 244(1-2) (2002) 105-115.

[43] M.P. Desai, V. Labhasetwar, G.L. Amidon, R.J. Levy, Gastrointestinal uptake of biodegradable microparticles: effect of particle size. Pharm. Res. 13 (1996) 1838-1845.

[44] M. Huang, E. Khor, L.-Y. Lim, Uptake and cytotoxicity of chitosan molecules and nanoparticles: effects of molecular weight and degree of deacetylation. Pharm. Res. 21(2) (2004) 344-353.

[45] K.A. Janes, P. Calvo, M.J. Alonso, Polysaccharide colloidal particles as delivery systems for macromolecules. Advanced Drug Delivery Reviews 47(1) (2001) 83-97.

[46] C. Kneuer, M. Sameti, U. Bakowsky, T. Schiestel, H. Schirra, H. Schmidt, C.M. Lehr, A Nonviral DNA Delivery System Based on Surface Modified Silica-Nanoparticles Can Efficiently Transfect Cells in Vitro. Bioconjugate Chemistry 11(6) (2000) 926-932.

[47] T. Jung, W. Kamm, A. Breitenbach, K.-D. Hungerer, E. Hundt, T. Kissel, Tetanus toxoid loaded nanoparticles from sulfobutylated poly(vinyl alcohol)-graft-poly(lactide-co-glycolide): Evaluation of antibody response after oral and nasal application in mice. Pharm. Res. 18(3) (2001) 352-360.

[48] A. Vila, A. Sanchez, K. Janes, I. Behrens, T. Kissel, J.L.V. Jato, M.J. Alonso, Low molecular weight chitosan nanoparticles as new carriers for nasal vaccine delivery in mice. European Journal of Pharmaceutics and Biopharmaceutics
Chitosan 57(1) (2004) 123-131.

[49] A. Harada, H. Togawa, K. Kataoka, Physicochemical properties and nuclease resistance of antisense-oligodeoxynucleotides entrapped in the core of polyion complex micelles composed of poly(ethylene glycol)-poly(-Lysine) block copolymers. European Journal of Pharmaceutical Sciences 13(1) (2001) 35-42.

[50] H. Petersen, P.M. Fechner, A.L. Martin, K. Kunath, S. Stolnik, C.J. Roberts, D. Fischer, M.C. Davies, T. Kissel, Polyethylenimine-graft-Poly(ethylene glycol) Copolymers: Influence of Copolymer Block Structure on DNA Complexation and Biological Activities as Gene Delivery System. Bioconjugate Chemistry 13(4) (2002) 845-854.

[51] N. Oku, Y. Yamazaki, M. Matsuura, M. Sugiyama, M. Hasegawa, M. Nango, A novel non-viral gene transfer system, polycation liposomes. Advanced Drug Delivery Reviews 52(3) (2001) 209-218.

[52] C. Oussoren, G. Storm, Liposomes to target the lymphatics by subcutaneous administration. Advanced Drug Delivery Reviews 50(1-2) (2001) 143-156.

[53] M. Hashida, M. Nishikawa, F. Yamashita, Y. Takakura, Cell-specific delivery of genes with glycosylated carriers. Advanced Drug Delivery Reviews 52(3) (2001) 187-196.

[54] K. Shigeru, F. Shintaro, N. Makiya, Y. Fumiyoshi, H. Mitsuru, In Vivo Gene Delivery to the Liver Using Novel Galactosylated Cationic Liposomes. Pharm. Res. 17(3) (2000) 306-313.

[55] V.S. Trubetskoy, J.A. Cannillo, A. Milshtein, G.L. Wolf, V.P. Torchilin, Controlled delivery of Gd-containing liposomes to lymph nodes: surface modification may enhance MRI contrast properties. Magnetic Resonance Imaging 13(1) (1995) 31-37.

[56] Z.M. Qian, H. Li, H. Sun, K. Ho, Targeted Drug Delivery via the Transferrin Receptor-Mediated Endocytosis Pathway. Pharmacological Reviews 54(4) (2002) 561-587.

[57] A. Elouahabi, J.M. Ruysschaert, Formation and intracellular trafficking of lipoplexes and polyplexes. Molecular Therapy 11(3) (2005) 336-347.

[58] A. Vila, A. Sa?nchez, M. Tobi?o, P. Calvo, M.J. Alonso, Design of biodegradable particles for protein delivery. Journal of Controlled Release 78(1-3) (2002) 15-24.

[59] S. Blau, T.T. Jubeh, S.M. Haupt, A. Rubinstein, Drug targeting by surface cationization. Critical Reviews in Therapeutic Drug Carrier Systems 17(5) (2000) 425-465.

[60] M. Chanana, A. Gliozzi, A. Diaspro, I. Chodnevskaja, S. Huewel, V. Moskalenko, K. Ulrichs, H.J. Galla, S. Krol, Interaction of polyelectrolytes and their composites with living cells. Nano Letters 5(12) (2005) 2605-2612.

[61] R. Hardman, A toxicologic review of quantum dots: Toxicity depends on physicochemical and environmental factors. Environmental Health Perspectives 114(2) (2006) 165-172.

[62] P.J.A. Borm, D. Robbins, S. Haubold, T. Kuhlbusch, H. Fissan, K. Donaldson, R. Schins, V. Stone, W. Kreyling, J. Lademann, J. Krutmann, D.B. Warheit, E. Oberdorster, The potential risks of nanomaterials: A review carried out for ECETOC. Particle and Fibre Toxicology 3 (2006).

[63] C.M. Goodman, C.D. McCusker, T. Yilmaz, V.M. Rotello, Toxicity of gold nanoparticles functionalized with cationic and anionic side chains. Bioconjugate Chemistry 15(4) (2004) 897-900.

[64] P.R. Lockman, J.M. Koziara, R.J. Mumper, D. Allen, Nanoparticle surface charges alter blood-brain barrier integrity and permeability. Journal of Drug Targeting 12(9-10) (2004) 635-641.

[65] L. Huang, E. Viroonchatapan, Introduction. in: M. C. H. a. E. W. L. Huang (Ed.), Non-Viral Vectors for Gene Therapy, Academic Press, San Diego, 1999, pp. 3-22.

[66] P.L. Felgner, in: M. C. H. a. E. W. L. Huang (Ed.), Non-Viral Vectors for Gene Therapy, Academic Press, San Diego, 1999, pp. 26-38.

[67] F. Sakurai, R. Inoue, Y. Nishino, A. Okuda, O. Matsumoto, T. Taga, F. Yamashita, Y. Takakura, M. Hashida, Effect of DNA/liposome mixing ratio on the physicochemical characteristics, cellular uptake and intracellular trafficking of plasmid DNA/cationic liposome complexes and subsequent gene expression. Journal of Controlled Release 66 (2000) 255-269.

[68] A. Nemmar, H. Vanbilloen, M.F. Hoylaerts, P.H.M. Hoet, A. Verbruggen, B. Nemery, Passage of intratracheally instilled ultrafine particles from the lung into the systemic circulation in hamster. American Journal of Respiratory and Critical Care Medicine 164 (2001) 1665-1668.

[69] I.A. Khalil, K. Kogure, S. Futaki, S. Hama, H. Akita, M. Ueno, H. Kishida, M. Kudoh, Y. Mishina, K. Kataoka, M. Yamada, H. Harashima, Octaarginine-modified multifunctional envelope-type nanoparticles for gene delivery. Gene Therapy 14 (2007) 682-689.

[70] S. Li, L. Huang, Nonviral gene therapy: Promises and challenges. Gene Therapy 7(1) (2000) 31-34.

[71] H. Lv, S. Zhang, B. Wang, S. Cui, J. Yan, Toxicity of cationic lipids and cationic polymers in gene delivery. Journal of Controlled Release 114(1) (2006) 100-109.

[72] F. Unger, M. Wittmar, T. Kissel, Branched polyesters based on poly[vinyl-3-(dialkylamino)alkylcarbamate-co-vinyl acetate-co-vinyl alcohol]-graft-poly(d,l-lactide-co-glycolide): Effects of polymer structure on cytotoxicity. Biomaterials 28(9) (2007) 1610-1619.

[73] C. Oster, M. Wittmar, F. Unger, L. Barbu-Tudoran, A. Schaper, T. Kissel, Design of Amine-Modified Graft Polyesters for Effective Gene Delivery Using DNA-Loaded Nanoparticles. Pharm. Res. 21(6) (2004) 927-931.

[74] M. Simon, M. Wittmar, T. Kissel, T. Linn, Insulin Containing Nanocomplexes Formed by Self-Assembly from Biodegradable Amine-Modified Poly(Vinyl Alcohol)-Graft-Poly(l-Lactide): Bioavailability and Nasal Tolerability in Rats. Pharm. Res. 22(11) (2005) 1879-1886.

[75] L.A. Dailey, E. Kleemann, M. Wittmar, T. Gessler, T. Schmehl, C. Roberts, W. Seeger, T. Kissel, Surfactant-Free, Biodegradable Nanoparticles for Aerosol Therapy Based on the Branched Polyesters, DEAPA-PVAL-g-PLGA. Pharm. Res. 20(12) (2003) 2011-2020.

[76] J. Haas, M.N.V. Ravi Kumar, G. Borchard, U. Bakowsky, C.-M. Lehr, Preparation and Characterization of Chitosan and Trimethyl-chitosan-modified Poly-(ε-caprolactone) Nanoparticles as DNA Carriers. AAPS PharmSciTech 6(1) (2005) E22-E30.

[77] M. Thanou, B.I. Florea, M. Geldof, H.E. Junginger, G. Borchard, Quaternized chitosan oligomers as novel gene delivery vectors in epithelial cell lines. Biomaterials 23(1) (2002) 153-159.

[78] Y. Ohya, R. Cai, H. Nishizawa, K. Hara, T. Ouchi, Preparation of PEG-grafted chitosan nano-particle for peptide drug carrier. Proc. Intl. Symp. Control. Rel. Bioact. Mater. 26 (1999) 655–656.

[79] T.H. Kim, J.W. Nah, M.-H. Cho, T.G. Park, C.S. Cho, Receptor-mediated gene delivery into antigen presenting cells using mannosylated chitosan/DNA nanoparticles. Journal of Nanoscience and Nanotechnology 6 (2006) 2769-2803.

[80] T.H. Kim, I.K. Park, J.W. Nah, Y.J. Choi, C.S. Cho, Galactosylated chitosan/DNA nanoparticles prepared using water-soluble chitosan as a gene carrier. Biomaterials 25(17) (2004) 3783-3792.

[81] S. Gao, J. Chen, L. Dong, Z. Ding, Y.-h. Yang, J. Zhang, Targeting delivery of oligonucleotide and plasmid DNA to hepatocyte via galactosylated chitosan vector. European Journal of Pharmaceutics and Biopharmaceutics 60(3) (2005) 327-334.

[82] C. Shi, Y. Zhu, X. Ran, M. Wang, Y. Su, T. Cheng, Therapeutic Potential of Chitosan and Its Derivatives in Regenerative Medicine. Journal of Surgical Research 133(2) (2006) 185-192.

[83] L. Illum, Nanoparticulate systems for nasal delivery of drugs: A real improvement over simple systems? Journal of Pharmaceutical Sciences 96(3) (2007) 473-483.

[84] O. Borges, G. Borchard, J.C. Verhoef, A. de Sousa, H.E. Junginger, Preparation of coated nanoparticles for a new mucosal vaccine delivery system. International Journal of Pharmaceutics 299(1-2) (2005) 155-166.

[85] M. Cuna, M. Alonso-Sande, C. Remunan-Lopez, J.P. Pivel, J.L. Lonso-Lebrero, M.J. Alonso, Development of phosphorylated glucomannan-coated chitosan nanoparticles as nanocarriers for protein delivery. Journal of Nanoscience and Nanotechnology 6(9/10) (2006) 2887-2895.

[86] S. Ferrari, G. Pellegrini, F. Mavilio, M. De Luca, Gene therapy approaches for epidermolysis bullosa. Clinics in Dermatology 23(4) (2005) 430-436.

[87] V.P. Torchilin, Multifunctional nanocarriers. Advanced Drug Delivery Reviews 58(14) (2006) 1532-1555.

[88] S.D. Li, L. Huang, Surface-modified LPD nanoparticles for tumor targeting. Ann. N. Y. Acad. Sci. 1082 (2006) 1-8.

[89] S.D. Li, S. Chono, L. Huang, Efficient gene silencing in metastatic tumor by siRNA formulated in surface-modified nanoparticles. Journal of Controlled Release 126(1) (2008) 77-84.

[90] S.-D. Li, S. Chono, L. Huang, Efficient Oncogene Silencing and Metastasis Inhibition via Systemic Delivery of siRNA. Mol Ther 16(5) (2008) 942-946.

[91] I. Brigger, C. Dubernet, P. Couvreur, Nanoparticles in cancer therapy and diagnosis. Advanced Drug Delivery Reviews 54(5) (2002) 631-651.

[92] U. Gaur, S.K. Sahoo, T.K. De, P.C. Ghosh, A. Maitra, P.K. Ghosh, Biodistribution of fluoresceinated dextran using novel nanoparticles evading reticuloendothelial system. International Journal of Pharmaceutics 202(1-2) (2000) 1-10.

[93] G. Storm, S.O. Belliot, T. Daemen, D.D. Lasic, Surface modification of nanoparticles to oppose uptake by the mononuclear phagocyte system. Advanced Drug Delivery Reviews 17(1) (1995) 31-48.

[94] D.E. Owens III, N.A. Peppas, Opsonization, biodistribution, and pharmacokinetics of polymeric nanoparticles. International Journal of Pharmaceutics 307(1) (2006) 93-102.

[95] N. Csaba, A. Sanchez, M.J. Alonso, PLGA: Poloxamer and PLGA: Poloxamine blend nanostructures as carriers for nasal gene delivery. Journal of Controlled Release 113(2) (2006) 164-172.

[96] H. Maeda, J. Wu, T. Sawa, Y. Matsumura, K. Hori, Tumor vascular permeability and the EPR effect in macromolecular therapeutics: a review. Journal of Controlled Release 65(1-2) (2000) 271-284.

[97] Y. Matsumura, H. Maeda, A new concept for macromolecular therapeutics in cancer chemotherapy: Mechanism of tumoritropic accumulation of proteins and the antitumor agent smancs. Cancer Research 46 (1986) 6387-6392.

[98] G.J. Kim, S. Nie, Targeted cancer nanotherapy. Materials Today 8 (2005) 28-33.

[99] B.A. Teicher, Molecular targets and cancer therapeutics: discovery, development and clinical validation. Drug Resistance Updates 3(2) (2000) 67-73.

[100] G.W. Sledge, K.D. Miller, Exploiting the hallmarks of cancer: the future conquest of breast cancer. European Journal of Cancer 39(12) (2003) 1668-1675.

[101] N.N. Salama, N.D. Eddington, A. Fasano, Tight junction modulation and its relationship to drug delivery. Advanced Drug Delivery Reviews 58 (2006) 15-28.

[102] A. Steimer, E. Haltner, C.-M. Lehr, Cell culture models of the respiratory tract relevant to pulmonary drug delivery. J. Aerosol Medicine 18 (2005) 137-182.

[103] P. Watson, A.T. Jones, D.J. Stephens, Intracellular trafficking pathways and drug delivery: Fluorescence imaging of living and fixed cells. Advanced Drug Delivery Reviews 57 (2005) 43-61.

[104] J. Rejman, V. Oberle, I.S. Zuhorn, D. Hoekstra, Size-dependent internalization of particles via the pathways of clathrin-and caveolae-mediated endocytosis. Biochem. Journal 377 (2004) 159-169.

[105] M. Felberbaum-Corti, F.G. Van Der Goot, J. Gruenberg, Sliding doors: Clathrin-coated pits or caveolae? Nat. Cell Biol 5 (2003) 382-384.

[106] T.M. Fahmy, P.M. Fong, A. Goyal, W.M. Saltzman, Targeted for drug delivery. Materials Today 8 (2005) 18-26.

[107] J. Panyam, W.-Z. Zhou, S. Prabha, S.K. Sahoo, V. Labhasetwar, Rapid endo-lysosomal escape of poly(DL-lactide-co-glycolide) nanoparticles: Implications for drug and gene delivery. FASEB Journal 16(10) (2002) 1217-1226.

[108] Q. Gan, T. Wang, C. Cochrane, P. McCarron, Modulation of surface charge, particle size and morphological properties of chitosan-TPP nanoparticles intended for gene delivery. Colloids and Surfaces B: Biointerfaces 44(2-3) (2005) 65-73.

[109] M.N.V. Ravi Kumar, U. Bakowsky, C.M. Lehr, Preparation and characterization of cationic PLGA nanospheres as DNA carriers. Biomaterials 25(10) (2004) 1771-1777.

[110] M. Bivas-Benita, S. Romeijn, H.E. Junginger, G. Borchard, PLGA-PEI nanoparticles for gene delivery to pulmonary epithelium. European Journal of Pharmaceutics and Biopharmaceutics 58(1) (2004) 1-6.

[111] T. Trimaille, C. Pichot, T. Delair, Surface functionalization of poly(D,L-lactic acid) nanoparticles with poly(ethylenimine) and plasmid DNA by the layer-by-layer approach. Colloids and Surfaces A: Physicochemical and Engineering Aspects 221(1-3) (2003) 39-48.

[112] S. Munier, I. Messai, T. Delair, B. Verrier, Y. Ataman-Onal, Cationic PLA nanoparticles for DNA delivery: Comparison of three surface polycations for DNA binding, protection and transfection properties. Colloids and Surfaces B: Biointerfaces 43(3-4) (2005) 163-173.

[113] V. Dodane, M. Amin Khan, J.R. Merwin, Effect of chitosan on epithelial permeability and structure. International Journal of Pharmaceutics 182(1) (1999) 21-32.

[114] M.H. El-Shabouri, Positively charged nanoparticles for improving the oral bioavailability of cyclosporin-A. International Journal of Pharmaceutics 249 (2002) 101-108.

[115] S. Hariharan, V. Bhardwaj, I. Bala, J. Sitterberg, U. Bakowsky, M.N.V. Ravi Kumar, Design of estradiol loaded PLGA nanoparticulate formulations: A potential oral delivery system for hormone therapy. Pharm. Res. 23 (2006) 184-195.

[116] M. Shakweh, M. Besnard, V. Nicolas, E. Fattal, Poly (lactide-co-glycolide) particles of different physicochemical properties and their uptake by peyer's patches in mice. European Journal of Pharmaceutics and Biopharmaceutics 61(1-2) (2005) 1-13.

[117] J. Sudimack, R.J. Lee, Targeted drug delivery via the folate receptor. Advanced Drug Delivery Reviews 41(2) (2000) 147-162.

[118] M.M. Issa, M. Koping-Hoggard, K. Tommeraas, K.M. Varum, B.E. Christensen, S.P. Strand, P. Artursson, Targeted gene delivery with trisaccharide-substituted chitosan oligomers in vitro and after lung administration in vivo. Journal of Controlled Release 115(1) (2006) 103-112.

[119] P. Hoet, I. Bruske-Hohlfeld, O. Salata, Nanoparticles - known and unknown health risks. Journal of Nanobiotechnology 2(1) (2004) 12.

[120] P. Barlow, A. Clouter-Baker, K. Donaldson, J. MacCallum, V. Stone, Carbon black nanoparticles induce type II epithelial cells to release chemotaxins for alveolar macrophages. Particle and Fibre Toxicology 2(1) (2005) 11.

[121] T. Xia, M. Kovochich, J. Brant, M. Hotze, J. Sempf, T. Oberley, C. Sioutas, J.I. Yeh, M.R. Wiesner, A.E. Nel, Comparison of the Abilities of Ambient and Manufactured Nanoparticles To Induce Cellular Toxicity According to an Oxidative Stress Paradigm. Nano Letters 6(8) (2006) 1794-1807.

[122] T. McConville, A. Overhoff, P. Sinswat, M. Vaughn, L. Frei, S. Burgess, L. Talbert, I. Peters, P. Johnston, O. Williams, Targeted High Lung Concentrations of Itraconazole Using Nebulized Dispersions in a Murine Model Pharm. Res. 23(5) (2006) 901-911

[123] G. Oberdorster, A. Maynard, K. Donaldson, V. Castranova, J. Fitzpatrick, K. Ausman, J. Carter, B. Karn, W. Kreyling, D. Lai, S. Olin, N. Monteiro-Riviere, D. Warheit, H. Yang, A.r.f.t.I.R.F.R.S.I.N.T.S.W. Group, Principles for characterizing the potential human health effects from exposure to nanomaterials: elements of a screening strategy. Particle and Fibre Toxicology 2(1) (2005) 8.

[124] W. Lin, Y.-w. Huang, X.-D. Zhou, Y. Ma, Toxicity of Cerium Oxide Nanoparticles in Human Lung Cancer Cells. International Journal of Toxicology 25(6) (2006) 451-457.

[125] M. Brzoska, K. Langer, C. Coester, S. Loitsch, T.O.F. Wagner, C.v. Mallinckrodt, Incorporation of biodegradable nanoparticles into human airway epithelium cells--in vitro study of the suitability as a vehicle for drug or gene delivery in pulmonary diseases. Biochemical and Biophysical Research Communications 318(2) (2004) 562-570.

[126] L.A. Dailey, N. Jekel, L. Fink, T. Gessler, T. Schmehl, M. Wittmar, T. Kissel, W. Seeger, Investigation of the proinflammatory potential of biodegradable nanoparticle drug delivery systems in the lung. Toxicology and Applied Pharmacology 215(1) (2006) 100-108.

[127] N. Tsapis, D. Bennett, B. Jackson, D.A. Weitz, D.A. Edwards, Trojan particles: Large porous carriers of nanoparticles for drug delivery. Proceedings of the National Academy of Sciences 99(19) (2002) 12001-12005.

[128] J.O.H. Sham, Y. Zhang, W.H. Finlay, W.H. Roa, R. Lobenberg, Formulation and characterization of spray-dried powders containing nanoparticles for aerosol delivery to the lung. International Journal of Pharmaceutics 269(2) (2004) 457-467.

[129] A. Grenha, B. Seijo, C. Remunan-Lopez, Microencapsulated chitosan nanoparticles for lung protein delivery. European Journal of Pharmaceutical Sciences 25(4-5) (2005) 427-437.

[130] M.A. Videira, M.F. Botelho, A.C. Santos, L.F. Gouveia, J.J.P. de Lima, A. Almeida, oacute, J. nio, Lymphatic Uptake of Pulmonary Delivered Radiolabelled Solid Lipid Nanoparticles. Journal of Drug Targeting 10(8) (2002) 607-613.

[131] R. Pandey, A. Sharma, A. Zahoor, S. Sharma, G.K. Khuller, B. Prasad, Poly (DL-lactide-co-glycolide) nanoparticle-based inhalable sustained drug delivery system for experimental tuberculosis. Journal of Antimicrobial Chemotherapy 52(6) (2003) 981-986.

[132] R. Pandey, G.K. Khuller, Solid lipid particle-based inhalable sustained drug delivery system against experimental tuberculosis. Tuberculosis 85(4) (2005) 227-234.

[133] L. Ely, W. Roa, W.H. Finlay, R. Lobenberg, Effervescent dry powder for respiratory drug delivery. European Journal of Pharmaceutics and Biopharmaceutics 65(3) (2007) 346-353.

Chapter 2

Chitosan-modified PLGA nanoparticles

Preparation, characterization and effect of the process parameters on their colloidal characteristics*

***This chapter has been published in:**

N. Nafee, S. Taetz, M. Schneider, U. F. Schaefer and C.-M. Lehr. (2007) Chitosan-coated PLGA nanoparticles for DNA/RNA delivery: effect of formulation parameters on the complexation and transfection of antisense oligonuceotides. *Nanomedicine: Nanotechnology , biology, and medicine* 3: 173 – 183.

Abstract

Purpose: Cationically-modified PLGA nanoparticles have recently been introduced as novel carriers for DNA/RNA delivery. The colloidal characteristics of the nanoparticles – particle size and surface charge – are considered the most significant determinants in the cellular uptake and trafficking of the nanoparticles. Therefore, our aim was to prepare chitosan-coated PLGA nanoparticles, and modulate the effect of the formulation parameters to tailor the nanoparticles' size and charge for their special application as carrier for the cellular delivery of nucleotide-based drugs.

Methods: Many formulation parameters including the PVA content, the type and concentration of PLGA, the type and concentration of chitosan and the ratio of the organic to the aqueous phase of the emulsion were studied. In addition, the effect of other process parameters, on the particle size was also studied, such as the emulsification and homogenization time and speed.

Results: The results showed that a wide range of particle sizes (135.95 – 514.3 nm) and surface charges (13.5 – 60.4 mV) can be adjusted in dependence of the process parameters to adapt the carrier system for the envisaged task.

Conclusions: The study proved the efficacy of chitosan-coated PLGA nanoparticles as a flexible and efficient delivery system for antisense oligonucleotides to lung cancer cells.

Background

Biodegradable nanoparticles are an important area of research in the field of drug and gene delivery. One of the most widely used polymers for nanoparticles is the biodegradable and biocompatible poly (D,L-lactide-*co*-glycolide) (PLGA). PLGA nanoparticles have been extensively investigated for sustained [1] and targeted [2] / localized [3] delivery of different agents including anti-cancer drugs [4], plasmid DNA [5], proteins and peptides [6, 7] and low molecular weight compounds [8]. PLGA nanoparticles have hence shown great efficiency as drug delivery vehicles increasing the drug amount crossing various biological barriers such as the Blood rain Barrier [9, 10], gastrointestinal mucosa [11], nasal mucosa [12], ocular tissue [13].

In context of DNA/RNA delivery, the major limitation in the application of these nanoparticles is primarily their negative charge, which limits the interaction with the negatively charged DNA, in addition to the poor transport characteristics of the DNA-encapsulated PLGA nanoparticles through the cell membrane. PLGA nanoparticles with cationic surface modification can overcome these disadvantages and hence readily bind and condense DNA. Several polycations were used to accomplish this cationic surface modification including polyethyleneimine [14], cetyltrimethylamonium bromide [15], poly(2-dimethyl-amino)ethyl methacrylate [16], didodecyl dimethyl ammonium bromide [17] and chitosan [18].

The naturally occurring linear polysaccharide, chitosan, is considered to be a good candidate for gene transfection and expression owing to its biodegradability, biocompatibility, mucoadhesive and permeability enhancing properties [19]. In a recent comparative study, the efficiency of poly (lactide) nanoparticles coated with the cationic polymers; polyethyleneimine, chitosan and poly(2-dimethyl-amino)ethyl methacrylate (pDMAEMA) as DNA carriers was studied. Chitosan-modified nanoparticles were found to be best suited for transfection. Although nanoparticles modified with pDMAEMA

showed the highest transfection efficiency, chitosan-modified nanoparticles were the only carrier that released DNA at pH 7, which is a pre-requisite for the successful delivery [16]. The addition of chitosan to the surface of PLGA nanoparticles was also found to increase the penetration of the encapsulated macromolecules in mucosal surfaces [20]. Moreover, chitosan-modified nanoparticles were found to facilitate gene delivery and expression *in vivo* with increased efficiency and without causing inflammation [21].

The transfection efficiency of the cationically modified particles depends strongly on the particle size, which determines their cellular uptake, and the surface charge, which influences the ability of the particles to efficiently condense plasmid DNA/polynucleotides and to interact with cells. Prabha et al. [22] investigated the gene transfection levels of different size fractions of PLGA nanoparticles and found that the lower size nanoparticle fraction resulted in a 27-fold higher transfection in COS-7 cells and 4-fold higher transfection in HEK293 cells for the same dose of nanoparticles.

Therefore, the ability to control the colloidal characteristics of the nanoparticles, most importantly particle size and surface charge, is central in determining the transfection efficiency. Hence, the aim of our study was to modulate the effect of the formulation parameters to tailor the nanocarriers' size and charge for their special application, to optimize payload, and appropriately address the target system. Accordingly, many formulation parameters including the content of the emulsifier, the type and concentration of PLGA, the type and concentration of chitosan and the ratio of the organic to the aqueous phase of the emulsion were studied. In addition, the effect of other process parameters, on the particle size was also studied, such as the emulsification and homogenization time and speed.

Materials and methods

Materials

Poly(D,L-lactide-*co*-glycolide) 70:30 (Polysciences Europe GmbH, Eppelheim, Germany), poly(D,L-lactide-*co*-glycolide) 50:50 (Sigma Chemical Co., St. Louis, Mo., USA), polyvinyl alcohol Mowiol® 4-88 (Kuraray Specialities Europe GmbH, Frankfurt, Germany), two types of ultrapure chitosan chloride: Protasan® UP CL113 and Protasan® UP CL213 with a molecular weight of < 150 and 150 – 400 kDa, respectively (FMC BioPolymer AS, Oslo, Norway), ethyl acetate (Fluka Chemie GmbH, Buchs, Switzerland) were used as obtained.

Methods

1. Preparation of the nanoparticles

Nanoparticle formulations were prepared by the emulsion-diffusion-evaporation technique [18]. PLGA 70:30 was dissolved in 5 ml ethyl acetate at room temperature. The aqueous phase was prepared by dissolving polyvinyl alcohol (PVA) in MilliQ water. In case of chitosan-modified nanoparticles (cNP), chitosan chloride (Protasan® UP CL113) is added to the aqueous phase. The organic phase was added dropwise to an equal volume of the aqueous phase under stirring using a magnetic stirrer, at 1000 rpm, for 1 h, at room temperature. The emulsion was then homogenized (Ultra-Turrax T25, Janke & Kunkel GmbH & Co-KG, Germany) at 13,500 rpm for 10 min. Nanoparticles were obtained by adding MilliQ water dropwise under gentle stirring to reach a final volume of the suspension of 50 ml. Stirring is continued overnight at room temperature to evaporate the organic solvent. The so-prepared nanoparticle suspension contains 2 mg/ml PLGA, 1 mg/ml PVA and 0.3 mg/ml chitosan and was considered as our reference nanoparticle formulation. In order to investigate the effect of the formulation parameters on the colloidal characteristics of the nanoparticles, other formulations with different

concentrations and/or compositions were prepared following the same procedure and compared to the original particles.

2. Determination of the colloidal characteristics

The mean particle size and size distribution were determined in MilliQ water using the Malvern Zetasizer Nano (Malvern Instruments, Malvern, UK). Measurements were based on the Photon Correlation Spectroscopy (PCS) at 25^{o}C. The surface charge was estimated by measuring the zeta potential based on the electrophoretic mobility (Zetasizer Nano, Malvern Instruments, Malvern, UK). All zeta potential measurements were performed with diluted nanoparticle suspensions (pH 3.5 – 4). Samples were measured in triplicates.

3. ζ-potential – pH titration profile

To measure the zeta potential of the nanoparticles as a function of pH, both chitosan-modified and non-modified nanoparticle suspension were diluted with McIlvaine buffer of different pH-values ranging from 2 to 8. The ζ-potential was measured as previously mentioned.

4. Scanning Probe Microscopy (SPM)

The surface morphology and the shape of the nanoparticles were examined by Scanning Probe Microscopy with a Bioscope^{TM} equipped with a Nanoscope IV^{TM} controller (Digital Instruments, Veeco, Santa Barbara, California, USA). The nanoparticles were investigated under ambient conditions in tapping mode using a scanning probe with a force constant of 40 N/m at resonant frequency of ~170 kHz (Anfatec, Oelsnitz, Germany).

5. Stability of nanoparticles in different buffers and culture media

The complexation procedures with anionic plasmids as well as the transfection studies necessitate the use of certain buffer solutions of different pH values and some culture media of various compositions. These media are expected to have a great influence on the

size and charge of the nanoparticles, especially in the presence of the pH sensitive polymer, chitosan. To determine the effect of the type of buffering solution, three formulations of nanoparticle (F1, F2 and F3) of different sizes and surface charges were applied. The particle size and ζ-potential were measured in MilliQ water and in different solutions including Phosphate Buffer Saline (PBS) pH 7.4, HBSS buffer pH 7.4, HEPES buffer; 4-(2- Hydroxyethyl) piperazine-1-ethanesulfonic acid; 10 mM pH 7.4, sodium chloride solution 10 mM. In addition, the influence of the buffer molarity was verified by measuring the size and ζ-potential of the nanoparticle formulations (F1, F2 and F3) in HEPES buffer pH 7.4 of two different molarities (10 and 25 mM) and in sodium chloride solution (1, 10 and 100 mM).

Results

1. Chitosan-modified versus non-modified PLGA nanoparticles

Chitosan-modified (cNP) and non-modified nanoparticles (ncNP) were prepared with PLGA 70:30 and PVA as stabilizer using the emulsion-diffusion-evaporation technique. Measurements of the particle size showed slight increase in the mean nanoparticle diameter from (271.1 ± 1.03) nm to (278.95 ± 4.95) nm by the addition of chitosan to the aqueous phase. In both cases, the nanoparticles are monodisperse (polydispersity index, P.I., 0.04 – 0.06), spherical and have smooth surfaces as revealed by the SPM micrographs, Figure 1. The pH of the standard nanoparticle suspension was found to be around 4. The addition of chitosan increases the ζ-potential of the particles to 17.1 mV compared to -10 mV for the ncNP in MilliQ water.

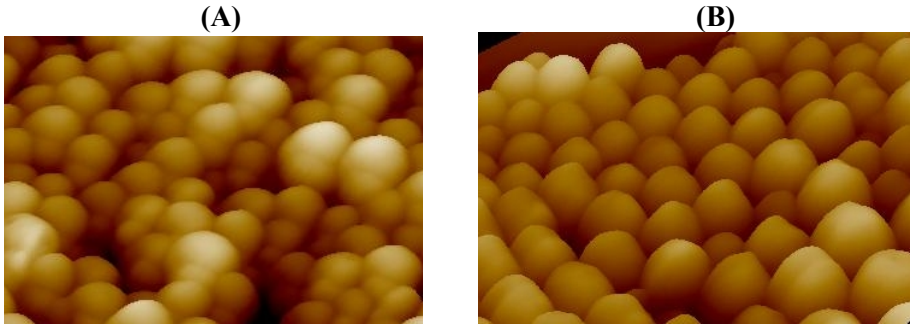

Figure 1: Morphology of non-modified (A) and chitosan-modified (B) PLGA nanoparticles as observed by the SPM

The effect of pH on the surface charge of chitosan-modified and non-modified PLGA nanoparticles was investigated by measuring the ζ-potential versus pH. As shown in Figure 2, the ζ-potential of the non-modified PLGA nanoparticles is almost constant (0.4 – 3.5 mV) at all pH values tested. In comparison, chitosan-modified nanoparticles exhibited a positive potential of 33.6 mV in acidic medium, which decreased by increasing pH values.

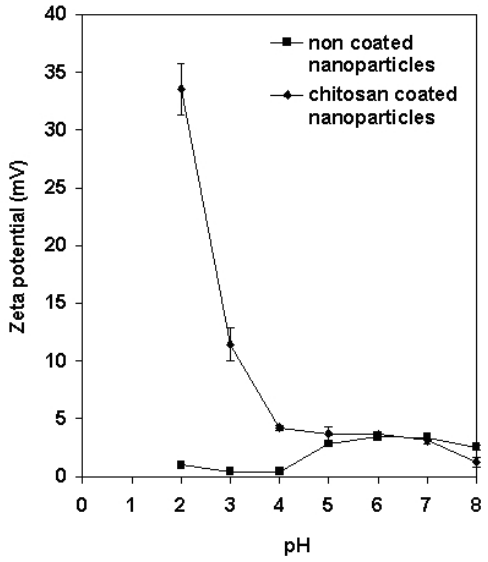

Figure 2: ζ-potential – pH profile for non-modified and chitosan-modified PLGA nanoparticles

In addition to the surface charge of the nanoparticles, the particle size is also considered one of the most important parameters in the mucosal and tissue uptake of the nanoparticles. Smaller nanoparticles are able to penetrate through the sub-mucosal layers while larger size particles were found to be localized in the epithelial lining [23].

Moreover, smaller nanoparticles were found to show significantly higher transfection efficiency as compared to larger nanoparticles [22]. Therefore, our study aimed to produce nanoparticles of relatively small(er) size and more pronounced positive charge on the surface while being able to adjust these parameters deliberately. This necessitates the study of the effect of different formulation variables on the colloidal characteristics of these particles.

2. Factors affecting the colloidal characteristics of the nanoparticles

2.1. Effect of the stabilizer and type of PLGA

The influence of PVA content on the colloidal properties of the chitosan-modified PLGA nanoparticles was studied. Nanoparticles containing various concentrations of PVA ranging from 1 to 5 mg/ml of the nanoparticle suspension were prepared using two different types of PLGA copolymer based on its lactide/glycolide content (PLGA 70:30 and PLGA 50:50). In general, it was observed that increasing the concentration of PVA resulted in a statistically significant decrease in the mean particle size ($p < 0.05$), Figure 3. When the concentration of PVA is increased from 1 to 2 mg/ml, the mean particle diameter was significantly reduced whereas further increase in the PVA concentration lead to smaller reduction in the particle size, Figure 3. Similar results were also reported by Mainardes & Evangelista [24]. The size reduction was significantly more pronounced in case of nanoparticles prepared with PLGA 70:30 than those prepared with PLGA 50:50 ($p < 0.05$), Figure 3. Similarly, measurements of the ζ-potential indicate that nanoparticles containing PLGA 70:30 are characterized by a significantly higher ζ-potential (28.3 – 35.38 mV) compared to those containing PLGA 50:50 (16.4 – 22.9 mV), ($p < 0.05$), Figure 3. The ratio of lactide/glycolide content in the PLGA polymer is known to influence the degradation rate of the polymers [25] as well as their release properties. Therefore, it was interesting to investigate their effect on the colloidal characteristics of the

nanoparticles. Nevertheless, due to the biological requirements and goals we did not test all available ratios of lactide/glycolide units. Only short degradation times were considered and therefore only two types of PLGA copolymers were investigated. No significant correlation was found between increasing PVA concentration and the surface charge of the nanoparticles ($p < 0.05$). Formulations containing different amounts of PVA are all characterized by unimodal size distribution (P.I. 0.08 - 0.15).

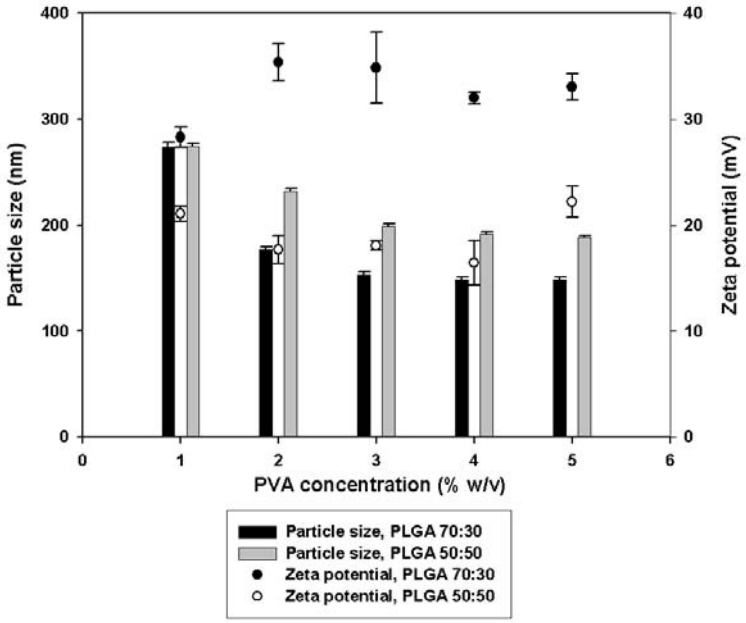

Figure 3: Effect of the concentration of PVA on the particle size and the surface charge of chitosan-modified PLGA nanoparticles (Mean ± S.D.)

2.2. Effect of PLGA concentration

Nanoparticle suspensions containing half and double the concentration of PLGA 70:30 present in the original nanoparticle formulation were prepared. It was observed that by increasing the polymer concentration, nanoparticles of larger sizes were produced, Figure 4. This is in agreement with the findings of Kown et al. [17] and Chorny et al. [8]. However, the change in particle size did not affect the polydispersity of the nanoparticles; mean P.I. of the three formulations is 0.09 ± 0.012. Measurements of the ζ-potential

showed that the surface charge is weakly affected by the variation in the polymer concentration, Figure 4.

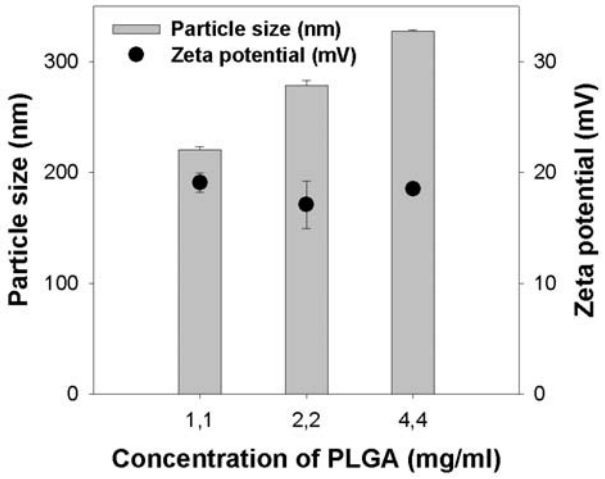

Figure 4: Effect of the concentration of PLGA on the colloidal characteristics of chitosan-modified PLGA nanoparticles (Mean ± S.D.)

2.3. Effect of chitosan

In order to study the effect of chitosan concentration on the colloidal characteristics of the nanoparticles, two non-modified nanoparticle formulations F1 and F2 of two different particle sizes (249.8 and 148.2 nm) were prepared and compared with two formulations of increasing chitosan concentrations from 0.15 – 1.5 mg/ml (all other parameters were unchanged). As observed in Figure 5A, increasing the concentration of chitosan showed a gradual increase in the particle size of the nanoparticles, which become significantly more pronounced for nanoparticles containing more than 0.9 mg/ml chitosan ($p < 0.05$). On the other hand, measurement of the ζ-potential of the different formulations indicates a significant increase in the surface charge with increasing concentration of chitosan ($p < 0.05$). The connecting line between the data points were obtained using $y = y_0 + a(1 - e^{-bx})$, (R^2 = 0.999, 0.996) as a fit function, Figure 5B. However, the small nanoparticles F2 are characterized by a higher surface charge using the same concentration

of chitosan; the ζ-potential of F1 and F2 containing both 0.6 mg/ml chitosan was found to be 33.03 and 46.43 mV, respectively.

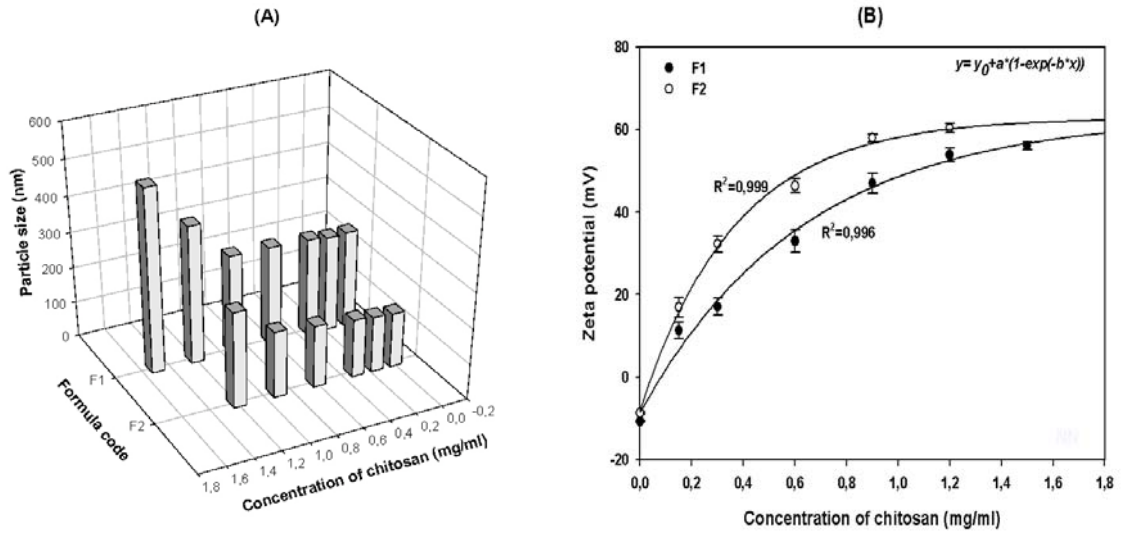

Figure 5: Effect of the concentration of chitosan on (A) the particle size and (B) the surface charge of chitosan-modified PLGA nanoparticles (Mean ± S.D.)

The influence of chitosan properties on the size and surface charge of the nanoparticles was also investigated. Ultrapure chitosan chloride Protasan® UP CL 213 was used to prepare nanoparticles. The polymers are characterized by different molecular weight and viscosity, Table 1. Different molecular weight of the outer polymer might influence the overall charge of the particles.

Table 1: Effect of chitosan properties on the colloidal characteristics of nanoparticles:

Type of chitosan	Chitosan properties		Colloidal characteristics of the nanoparticles		
	Molecular weight [kDa][a]	Viscosity [mPa.s][b]	Mean particle size [nm] ± S.D.[c]	Polydispersity Index (P.I.) ± S.D.[c]	Zeta potential [mV] ± S.D.[c]
Protasan® UP CL113	< 150	< 20	166.05 ± 1.5	0.122 ± 0.02	13.32 ± 0.83
Protasan® UP CL213	150 - 400	20 - 200	167.7 ± 0.5	0.13 ± 0.01	14.4 ± 1.67

[a] Approximate molecular weight (weight average molecular weight).
[b] Standard viscosity ranges (1% solution, 20°C).
[c] S.D. denotes the standard deviation of (n = 3).

The viscosity of chitosan is expected to influence the formation of the nanoparticles which depends on the diffusion and therefore on the viscosity. However, it was noticed that nanoparticles prepared using either type of chitosan have the same mean particle size and surface charge considering the error (Table 1).

2.4. Effect of organic to aqueous phase volume ratio

The ratio between the organic and aqueous phase of the emulsion is of great importance regarding the stability of the emulsion and is expected to influence the size of the dispersed globules. Therefore, the organic to aqueous phase volume ratio was varied between 2:1, 1:1 and 1:2. The results demonstrate a gradual decrease in particle size by changing the ratio from 2:1 to 1:2 (Figure 6A) as well as a corresponding significant increase in surface charge ($p < 0.05$), Figure 6B.

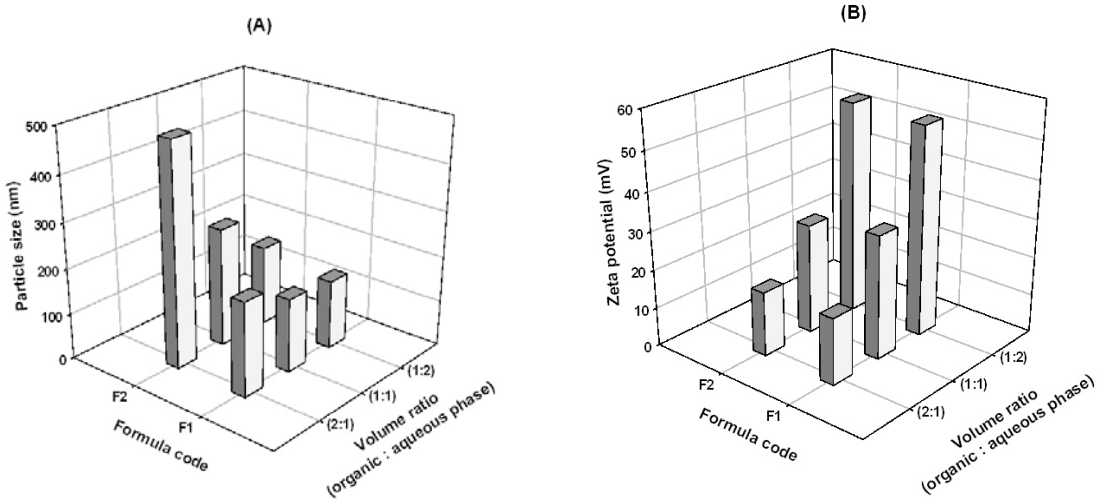

Figure 6: Effect of the organic to aqueous phase volume ratio on (A) the particle size and (B) the surface charge of chitosan-modified PLGA nanoparticles (Mean ± S.D.)

2.5. Effect of process parameters

Attempts to reduce the particle size by increasing the speed of magnetic stirrer or the homogenizer or the number of the homogenization cycles were previously reported [17, 26]. According to Kown et al. [17], an increase in homogenization speed resulted in a

corresponding decrease in the particle size, however, no significant reduction in size was observed by increasing the speed above 12,000 rpm. It can be noticed that the modification of the stirring time of the emulsion, the homogenization speed or time, or sonication resulted in minor reduction in the particle size (Table 2). Further increase in the homogenization time and/or speed was not favorable because the high energy provided lead to particle fusion and aggregation rather than particle size reduction.

Table 2: Effect of different technical parameters on the nanoparticle size

Parameter	Duration	Mean particle size [nm] ± S.D.[a]	Polydispersity Index (P.I.) ± S.D.[a]
Stirring time	1h	277.6 ± 1.3	0.048 ± 0.008
	2h	± 2.08	0.057 ± 0.01
	3h	271.5 ± 2.02	0.047 ± 0.016
Homogenization time	10 min	273.5 ± 1.15	0.036 ± 0.02
	15 min	271.2 ± 3.4	0.049 ± 0.011
Sonication time	1 min	275.7 ± 1.9	0.059 ± 0.01
	6 min	274.6 ± 3.4	0.078 ± 0.009

[a] S.D. denotes the standard deviation of (n = 3).

Based on the aforementioned results chitosan-modified PLGA nanoparticles can be produced over a wide range of size and surface charge. For DNA/RNA delivery purposes, nanoparticles of small size and high surface charge are mandatory. Therefore, we selected a chitosan-modified PLGA nanoparticle formulation characterized by a size of 172.3 ± 4.5 nm and a surface charge of 38.6 ± 1.96 mV to study binding and uptake.

3. Stability of nanoparticles in different buffers

To study the effect of type of buffering solution on the colloidal characteristics of chitosan- modified nanoparticles, three nanoparticle formulations (F1, F2, and F3) of different mean particle size and surface charge density were prepared. The colloidal characteristics of these formulations are represented in Table 3.

Table 3: Colloidal characteristics of chitosan modified nanoparticles in MilliQ water

	F1	F2	F3
Particle size (nm) ± SD	274.0 ± 2.8	154.9 ± 0.9	135.95± 0.8
Polydispersity Index ± SD	0.042 ± 0.019	0.115 ± 0.007	0.233 ± 0.005
ζ-potential (mV) ± SD	13.0 ± 0.3	14.08 ± 2.19	26.25 ± 4.2

Dilutions of the nanoparticle suspensions were prepared in the following solutions; Phosphate Buffer Saline (PBS) pH 7.4, HBSS buffer pH 7.4, HEPES buffer 10 mM pH 7.4, and sodium chloride solution 10 mM. The mean particle size and ζ-potential for formulae F1, F2 and F3 are plotted in Figure 7A & B.

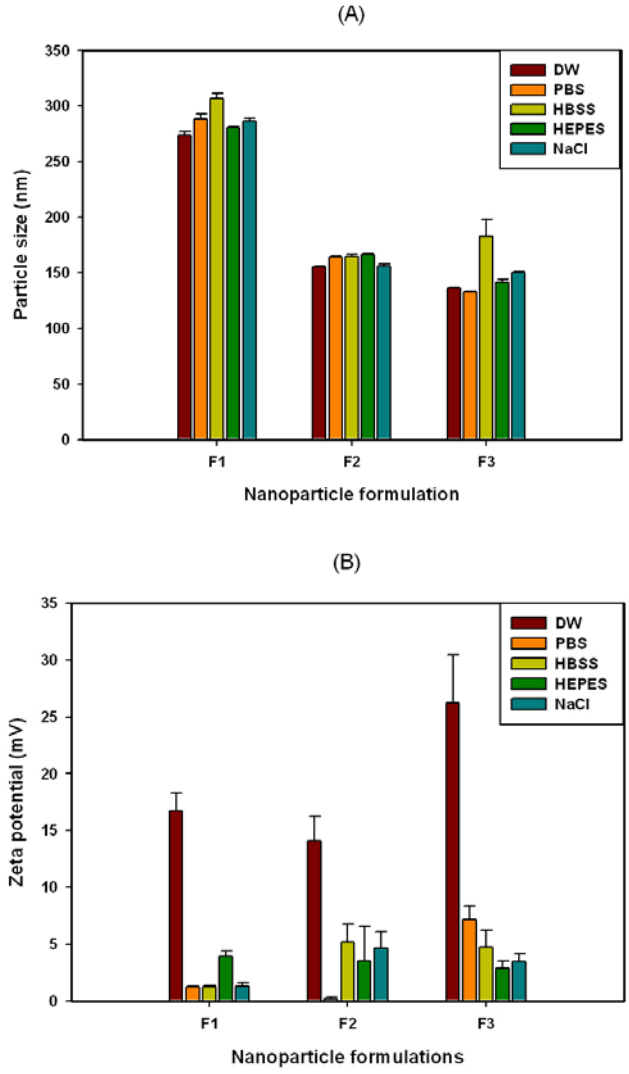

Figure 7: Particle size (A) and ζ-potential (B) of chitosan-modified PLGA nanoparticles in different buffer solutions

The Figure indicates that the nanoparticles exhibit almost the same mean particle size in the different solutions tested. On the other hand, the ζ-potential measurements indicate that the surface charge density is greatly reduced in buffer solutions compared to MilliQ water. It could be expected that the presence of counter ions in the buffer solutions together with the alkaline environment play a significant role in the surface charge density of the nanoparticles.

In order to investigate the effect of molarity of the buffer solution, the particle size and ζ- potential for the three previously mentioned nanoparticle formulations (F1, F2 and F3) were measured in HEPES buffer pH 7.4 of two molarities 10 and 25 mM. Changes in the measured particle size and ζ-potential with the molarity are illustrated in Figure 8 A & B, respectively. The diagrams indicate that the molarity of HEPES buffer has no sharp influence on the colloidal characteristics of the nanoparticles.

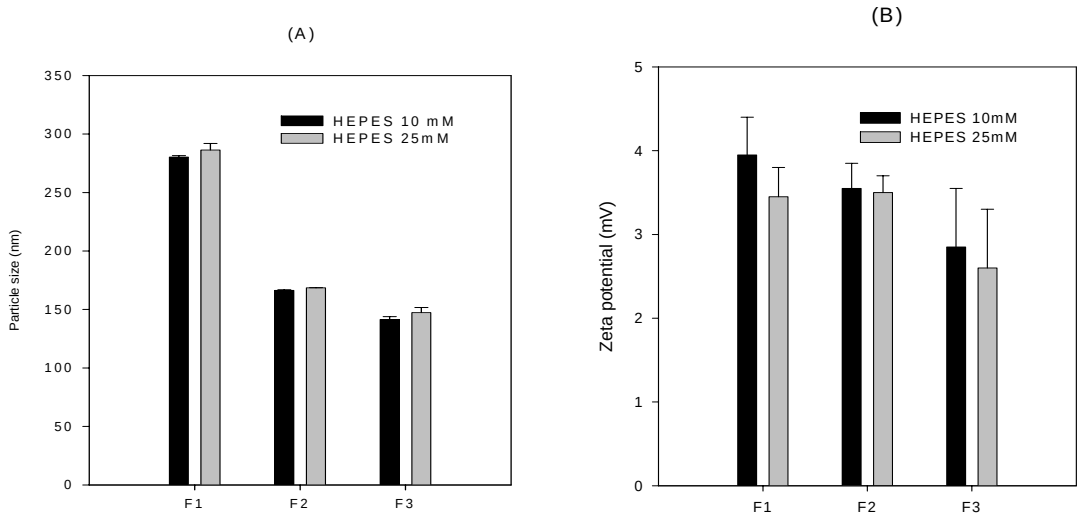

Figure 8: Particle size (A) and ζ-potential (B) of formulae F1, F2 and F3 in HEPES buffer pH 7.4, 10 and 25 mM

The same observation was observed when sodium chloride solution of different molarities (1, 10 and 100 mM) was used during the measurements, Figure 9.

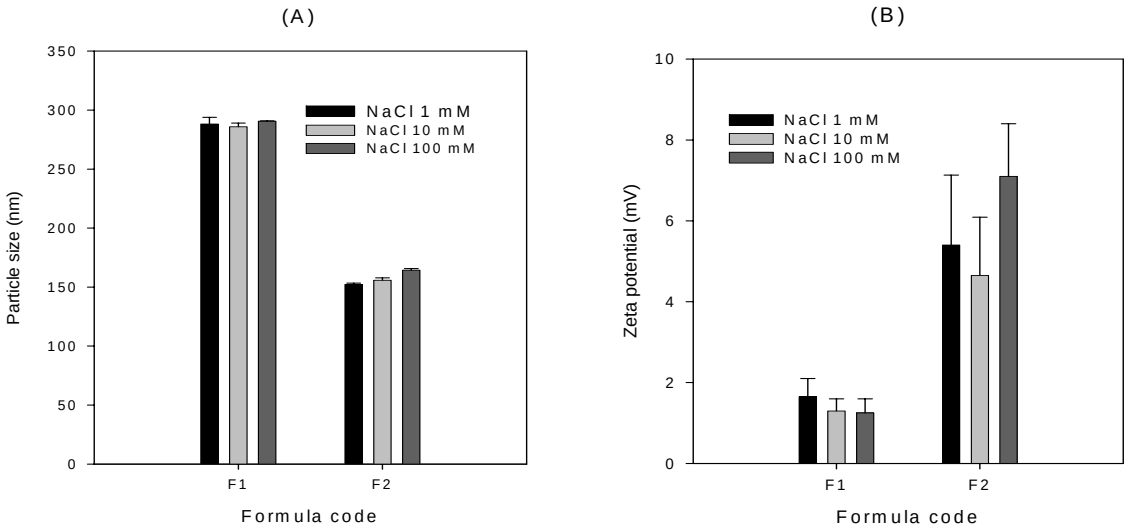

Figure 9: Particle size (A) and ζ-potential (B) of formulae F1 and F2 in NaCl solution 1, 10 and 100 mM

Discussion

Recent studies showed that the adsorption of a cationic hydrophilic polymer on the nanoparticle surface improves not only their transmucosal transport but also their efficiency as gene carriers [16, 27]. In this context, both the size and surface charge of nanoparticles are considered the major determinants for successful gene delivery. PLGA nanoparticles are known to be negatively charged due to the presence of ionized carboxyl groups. The presence of amphiphilic polymers as PVA forms a stable network on the polymer surface. This network shields the surface charge and moves the shear plane outwards from the particle surface, which resulted consequently in a slightly negative ζ-potential [28]. Despite this comparatively weak ζ-potential, the nanoparticles were stabilized by the layers of PVA surrounding the nanoparticles by steric hindrance [18, 29]. PVA has been extensively used as promising stabilizer for PLGA nanoparticles [7, 30]. The mechanism of PVA binding with PLGA has been proposed to be due to the interpenetration of PVA and PLGA molecules during nanoparticle formation. PVA is a copolymer of poly (vinyl acetate) and poly (vinyl alcohol) with considerable block copolymer character. The hydrophobic segments of PVA, the vinyl acetate part, penetrate

into the organic phase and remain entrapped into the polymeric matrix of the nanoparticles. The binding of PVA on the nanoparticle surface is likely to happen when the organic solvent is removed from the interface in which interpenetration of PVA and PLGA molecules takes place [28].

Unlike the non-modified PLGA nanoparticles, chitosan-modified nanoparticles are characterized by a strongly positive ζ-potential. Hence these nanoparticles are stabilized by electrostatic repulsion, which prevents their aggregation. Chitosan is a weak base polysaccharide, consisting of beta-(1,4) linked monomers of D-glucosamine and N-acetyl-D-glucosamine. In acidic medium, the amine groups of the polysaccharide will be positively charged allocating a high surface charge to the nanoparticles [31]. The pH titration profile, Figure 2, depicts a variation in ζ-potential with pH, which reveals that the surface charge of chitosan-modified nanoparticles is strongly dependent on pH. Thus, the ζ-potential titration provided proof of successful cationic surface modification by the addition of chitosan.

The amount of surfactant plays an important role as a stabilizing agent in the emulsification process and in the protection of the droplets. Increasing the concentration of PVA in the aqueous phase resulted in a corresponding increase in the viscosity. This contributes in the formation of a stable emulsion with smaller and uniform droplet size, leading to the formation of smaller sized nanoparticles [28]. However, as revealed from Figure 3, the decrease in particle size with the PVA concentration is not linear and levels off for higher PVA concentrations. Furthermore, the reduction of nanoparticle size is a function of the type of PLGA; PLGA 70:30 formed smaller nanoparticles compared with PLGA 50:50 using the same concentration of PVA. In contrast to the effect of PVA, results showed a significant increase in particle size with higher PLGA concentration, Figure 4. As the polymer concentration increases, the viscosity of the organic solution (dispersed phase) increases, resulting in a poorer dispersability of the PLGA solution into the aqueous

phase. The molecules are expected to coalesce in a more concentrated solution, thereby forming larger particles [24]. The same effect was also noticed by reducing the volume of the inner aqueous phase in relation to the organic phase, Figure 6 A&B. Dissolving the same amount of PVA/chitosan in half the volume of water resulted in a remarkable increase in the viscosity which renders the dispersion of PLGA solution rather difficult and in turn larger nanoparticles were formed. These findings emphasize the great influence of the viscosity on the colloidal characteristics of the nanoparticles.

The addition of chitosan to the aqueous phase during nanoparticles formulation imparts a positive ζ-potential to the nanoparticles, which is a function of chitosan concentration, Figure 5. However, the charge density on the surface remains in dependence of the nanoparticle size according to the free surface area with respect to the chitosan amount. As illustrated in Figure 5B, the smaller particles show a fast increase in surface charge which levels off as the surface is close to saturation, whereas, the same amount of chitosan leads for larger particles to a partially covered surface. Finally, a zeta potential of ~ 58–60 mV seems to indicate the saturation of the nanoparticle surface with the polycation in both cases. This behavior might be easily exploited for modulating the particle surface charge to facilitate both the transport properties as well as the mucoadhesive properties of the nanoparticles.

The relation between the particle size and the surface charge on the nanoparticles is quite of interest. Smaller particles acquire a higher zeta potential compared to larger particles using the same concentration of chitosan, Figure 5B. This reflects the dependency of the zeta potential from the charge density. The smaller the particle size, the larger will be the relative surface area of the nanoparticles available for interaction with chitosan. Hence, using constant chitosan concentration, one can improve the surface charge of the nanoparticles by varying the mean nanoparticle diameter.

In theory, mucoadhesion can be promoted by the positively charged groups on the nanoparticle surface through their electrical interaction with the negatively charged mucus [18]. In addition, the positively charged particle surface may be expected to facilitate adherence to the negatively charged cellular membranes by localized destabilization of the membrane, thus inducing their intracellular uptake into the cytoplasmic compartment [22]. Additionally, nanoparticles carrying positive charge in the acidic solution of endo-lysosomes are more prone to escape into the cytoplasmic compartment for effective release and gene expression [31]. Thus, by varying the surface charge, one could potentially be able to direct the nanoparticles either to lysosomes or to cytoplasm.

Studying the influence of chitosan properties on the colloidal characteristics of the nanoparticles, it was expected that the use of chitosan of a relatively higher molecular weight and higher viscosity would have a more pronounced impact on the particle size and the surface charge of the nanoparticles. However, the effect of chitosan properties was found to be without impact. This might be attributed to the relatively low concentration of chitosan included in the nanoparticle suspension. Therefore, the viscosity is not significantly altered and the particle's size is not influenced. Due to the fact that every monomer may have a charge, the amount of monomers on the surface of the nanoparticles determines the zeta potential and the size of the molecule itself plays a minor role. On the contrary, a remarkable increase in the size and surface charge of the nanoparticles was observed by Gan et al. [31] when higher molecular weight chitosan-tripolyphosphate was used. In the aforementioned study, nanoparticles were produced via tripolyphosphate initiated ionic gelation mechanism, whereas in our study chitosan is thought to form a thin coat around the PLGA nanoparticles as suggested by the linear increase in the surface charge with increasing chitosan concentration previously discussed.

Conclusions

Chitosan-modified PLGA nanoparticles offer a flexible technology platform for DNA/RNA delivery. By varying the formulation parameters, a wide range of particle sizes (135.95 – 514.3 nm) and surface charges (13.5 – 60.4 mV) can be adjusted to adapt the carrier system for the envisaged task.

REFERENCES

[1] A. Sanchez, M. Tobio, L. Gonzalez, A. Fabra, M.J. Alonso, Biodegradable micro- and nanoparticles as long-term delivery vehicles for interferon-alpha. European Journal of Pharmaceutical Sciences 18(3-4) (2003) 221-229.

[2] M. Shakweh, M. Besnard, V. Nicolas, E. Fattal, Poly (lactide-co-glycolide) particles of different physicochemical properties and their uptake by peyer's patches in mice. European Journal of Pharmaceutics and Biopharmaceutics 61(1-2) (2005) 1-13.

[3] C.X. Song, V. Labhasetwar, H. Murphy, X. Qu, W.R. Humphrey, R.J. Shebuski, R.J. Levy, Formulation and characterization of biodegradable nanoparticles for intravascular local drug delivery. Journal of Controlled Release 43(2-3) (1997) 197-212.

[4] L. Brannon-Peppas, J.O. Blanchette, Nanoparticle and targeted systems for cancer therapy. Advanced Drug Delivery Reviews
Intelligent Therapeutics: Biomimetic Systems and Nanotechnology in Drug Delivery 56(11) (2004) 1649-1659.

[5] S. Ribeiro, N. Hussain, A.T. Florence, Release of DNA from dendriplexes encapsulated in PLGA nanoparticles. International Journal of Pharmaceutics
Selected contributions from the 5th European Workshop on Particulate Systems 298(2) (2005) 354-360.

[6] M. Cegnar, A. Premzl, V. Zavasnik-Bergant, J. Kristl, J. Kos, Poly(lactide-co-glycolide) nanoparticles as a carrier system for delivering cysteine protease inhibitor cystatin into tumor cells. Experimental Cell Research 301(2) (2004) 223-231.

[7] J. Panyam, M.M. Dali, S.K. Sahoo, W. Ma, S.S. Chakravarthi, G.L. Amidon, R.J. Levy, V. Labhasetwar, Polymer degradation and in vitro release of a model protein from poly(D,L-lactide-co-glycolide) nano- and microparticles. Journal of Controlled Release 92(1-2) (2003) 173-187.

[8] M. Chorny, I. Fishbein, H.D. Danenberg, G. Golomb, Lipophilic drug loaded nanospheres prepared by nanoprecipitation: effect of formulation variables on size, drug recovery and release kinetics. Journal of Controlled Release 83(3) (2002) 389-400.

[9] L. Costantino, F. Gandolfi, L. Bossy-Nobs, G. Tosi, R. Gurny, F. Rivasi, M. Angela Vandelli, F. Forni, Nanoparticulate drug carriers based on hybrid poly(d,l-lactide-co-glycolide)-dendron structures. Biomaterials 27(26) (2006) 4635-4645.

[10] K. Elkharraz, N. Faisant, C. Guse, F. Siepmann, B. Arica-Yegin, J.M. Oger, R. Gust, A. Goepferich, J.P. Benoit, J. Siepmann, Paclitaxel-loaded microparticles and implants for the treatment of brain cancer: Preparation and physicochemical characterization. International Journal of Pharmaceutics
Local Controlled Drug Delivery to the Brain 314(2) (2006) 127-136.

[11] A. Lamprecht, N. Ubrich, H. Yamamoto, U. Schäfer, H. Takeuchi, P. Maincent, Y. Kawashima, C.-M. Lehr, Biodegradable Nanoparticles for Targeted Drug Delivery in Treatment of Inflammatory Bowel Disease. J. Pharm. Exp. Ther. 299(2) (2001) 775 - 781.

[12] N. Csaba, A. Sanchez, M.J. Alonso, PLGA: Poloxamer and PLGA: Poloxamine blend nanostructures as carriers for nasal gene delivery. Journal of Controlled Release 113(2) (2006) 164-172.

[13] K. Dillen, W. Weyenberg, J. Vandervoort, A. Ludwig, The influence of the use of viscosifying agents as dispersion media on the drug release properties from PLGA nanoparticles. European Journal of Pharmaceutics and Biopharmaceutics 58(3) (2004) 539-549.

[14] T. Trimaille, C. Pichot, T. Delair, Surface functionalization of poly(D,L-lactic acid) nanoparticles with poly(ethylenimine) and plasmid DNA by the layer-by-layer approach. Colloids and Surfaces A: Physicochemical and Engineering Aspects 221(1-3) (2003) 39-48.

[15] M. Singh, M. Ugozzoli, M. Briones, J. Kazzaz, E. Soenawan, D.T. O'Hagan, The effect of CTAB concentration in cationic PLGA microparticles on DNA absorption and in vivo performance. Pharm. Res. 20 (2003) 247 - 251.

[16] S. Munier, I. Messai, T. Delair, B. Verrier, Y. Ataman-Onal, Cationic PLA nanoparticles for DNA delivery: Comparison of three surface polycations for DNA binding, protection and transfection properties. Colloids and Surfaces B: Biointerfaces 43(3-4) (2005) 163-173.

[17] H.-Y. Kwon, J.-Y. Lee, S.-W. Choi, Y. Jang, J.-H. Kim, Preparation of PLGA nanoparticles containing estrogen by emulsification-diffusion method. Colloids and Surfaces A: Physicochemical and Engineering Aspects 182(1-3) (2001) 123-130.

[18] M.N.V. Ravi Kumar, U. Bakowsky, C.M. Lehr, Preparation and characterization of cationic PLGA nanospheres as DNA carriers. Biomaterials 25(10) (2004) 1771-1777.

[19] V. Dodane, M. Amin Khan, J.R. Merwin, Effect of chitosan on epithelial permeability and structure. International Journal of Pharmaceutics 182(1) (1999) 21-32.

[20] K.A. Janes, P. Calvo, M.J. Alonso, Polysaccharide colloidal particles as delivery systems for macromolecules. Advanced Drug Delivery Reviews 47(1) (2001) 83-97.

[21] M.N.V. Ravi Kumar, S.S. Mohapatra, X. Kong, P.K. Jena, U. Bakowsky, C.-M. Lehr, Cationic poly(lactide-co-glycolide) nanoparticles as efficient in vivo gene transfection agents. Journal of Nanoscience and Nanotechnology 4(8) (2004) 1 - 5.

[22] S. Prabha, W.-Z. Zhou, J. Panyam, V. Labhasetwar, Size-dependency of nanoparticle-mediated gene transfection: studies with fractionated nanoparticles. International Journal of Pharmaceutics 244(1-2) (2002) 105-115.

[23] C. Song, V. Labhasetwar, X. Cui, T. Underwood, R.J. Levy, Arterial uptake of biodegradable nanoparticles for intravascular local drug delivery: Results with an acute dog model. Journal of Controlled Release 54(2) (1998) 201-211.

[24] R.M. Mainardes, R.C. Evangelista, PLGA nanoparticles containing praziquantel: effect of formulation variables on size distribution. International Journal of Pharmaceutics 290(1-2) (2005) 137-144.

[25] J.C. Middleton, A.J. Tipton, Synthetic biodegradable polymers as medical devices. Medical Plastics & Biomaterials 5(2) (1998) 30-39.

[26] K. Dillen, J. Vandervoort, A. Ludwig, Factorial design, physicochemical characterisation and activity of ciprofloxacin-loaded PLGA nanoparticles for occular use. Journal of Controlled Release 101 (2005) 369 - 370.

[27] C. Prego, M. Garcia, D. Torres, M.J. Alonso, Transmucosal macromolecular drug delivery. Journal of Controlled Release
Proceedings of the Eight European Symposium on Controlled Drug Delivery 101(1-3) (2005) 151-162.

[28] J. Panyam, W.-Z. Zhou, S. Prabha, S.K. Sahoo, V. Labhasetwar, Rapid endo-lysosomal escape of poly(DL-lactide-co-glycolide) nanoparticles: Implications for drug and gene delivery. FASEB Journal 16(10) (2002) 1217-1226.

[29] M.F. Zambaux, F. Bonneaux, R. Gref, P. Maincent, E. Dellacherie, M.J. Alonso, P. Labrude, C. Vigneron, Influence of experimental parameters on the characteristics of poly(lactic acid) nanoparticles prepared by a double emulsion method. Journal of Controlled Release 50(1-3) (1998) 31-40.

[30] J. Vandervoort, K. Yoncheva, A. Ludwig, Influence of the homogenisation procedure on the physicochemical properties of PLGA nanoparticles. Chemical Pharmaceutical Bulletin 52(11) (2004) 1273 - 1279.

[31] Q. Gan, T. Wang, C. Cochrane, P. McCarron, Modulation of surface charge, particle size and morphological properties of chitosan-TPP nanoparticles intended for gene delivery. Colloids and Surfaces B: Biointerfaces 44(2-3) (2005) 65-73.

Chapter 3

Small- and large-scale purification of chitosan-modified PLGA nanoparticles and quantitative determination of the residual polymers *

*** This chapter is prepared for publication as a journal article:**

N. Nafee, S. Taetz, M. Schneider, U. F. Schaefer and C.-M. Lehr. Small and large scale purification of chitosan-modified PLGA nanoparticles and quantitative determination of residual polymers.

Abstract

Purpose: The potential use of nanoparticles along pulmonary route implies an intensive purification from residual organic solvents, emulsifiers and/or monomers used during the preparation procedure to insure the biological tolerance for the product. The presence of these impurities may alter the physicochemical and release characteristics of the nanoparticles. Additionally, significant amounts of surfactants may disturb the naturally regulated surface tension of the pulmonary lining leading to impaired lung function or inflammation. In this chapter, we aimed to select the most appropriate techniques for purification of the nanoparticles that preserve their colloidal properties.

Methods: Different techniques for the purification of chitosan modified PLGA nanoparticles from residual polymers were investigated. In addition, quantitative estimation of the amount of residual polymers during the preparation process and investigation of the behaviour of the purified nanoparticles versus original nanoparticles with respect to pH were done.

Results: Nanoparticles were efficiently purified (on a small-scale) by centrifugal ultrafiltration using Centrisart I® and by size exclusion chromatography (on a large-scale) using FPLC. The purified particles retained their size and charge along the purification procedure. Quantitative determination of the residual polymers revealed that 2/3 of the emulsifier was bound to the nanoparticles, while the amount of chitosan used was not enough to saturate the nanoparticles surface.

Conclusions: From this study, it can be concluded that the Centrisart I® and the FPLC are promising techniques for small- and large-scale purification of chitosan-modified PLGA nanoparticles, respectively.

Background

The potential use of nanoparticles along pulmonary route implies an intensive purification from residual organic solvents, emulsifiers and/or monomers used during the preparation procedure to insure the biological tolerance for the product. The presence of these impurities may alter the physicochemical and release characteristics of the nanoparticles. Additionally, significant amounts of surfactants may disturb the naturally regulated surface tension of the pulmonary lining, thus leading to impaired lung function or inflammation [1]. In the area of gene delivery, excessive amounts of the stabilizers can also have negative effects on the transfection efficiency of the nanoparticles [2]. Furthermore, in the case of cationically modified PLGA nanoparticles, the presence of residual amounts of the unbound cationic polymer may form undesirable complexes with the negatively charged plasmid resulting in misleading observations. Hence, the investigation of the settlement of a purification procedure with the potential of removing undesirable components, while reserving the colloidal stability of the nanoparticles and providing minimum loss of the particles is a matter of great interest.

A range of approaches have been used for the purification of nanoparticles. Among these techniques, dialysis [3], ultrafiltration [4], gel filtration [5], centrifugation and ultracentrifugation [6] have been investigated. Although dialysis is a simple procedure, it is considered a time-consuming process with a risk of microbial contamination. Besides, molecules of medium size such as the emulsifiers cannot be completely removed with dense dialysis membranes. In addition, dialysis can also result in premature release of nanoparticle payload during the extended purification procedure [7]. The pressure driven processes such as diafiltration, ultrafiltration or microfiltration are of limited efficiency due to the formation of a cake of precipitated particles on the membrane surface. If the adhesion of the particles is stronger than the repulsion, the cake formation is irreversible and membrane permeability decreases dramatically. In addition, gel filtration may cause

irreversible adsorption of the active moieties on the column's stationary phase as well as poor resolution between the large impurities and small nanoparticles [7].

Centrifugation or ultracentrifugation, in combination with washing nanoparticles with an appropriate medium such as deionised water, is the most common approach to remove large quantities of process impurities. However, the impact of the centrifugation force can cause caking and difficulties in the nanoparticle redispersion, whereas insufficient centrifugation force can lead to significant loss of nanoparticles in the supernatant.

Despite the great number of publications that demonstrate the efficacy of polymeric nanoparticles for pulmonary drug/gene delivery, very few of them were concerned about purification from residual unbound polymers. In this chapter we aimed to select the most appropriate small- and large-scale techniques for purification of the nanoparticles that preserve their colloidal properties. In addition, quantitative estimation of the amount of residual polymers during the preparation process and investigation of the behavior of the purified nanoparticles versus original nanoparticles with respect to pH were done.

Materials and Methods

Materials

Poly(D,L-lactide-*co*-glycolide) 70:30 (Polysciences Europe GmbH, Eppelheim, Germany), polyvinyl alcohol; Mowiol® 4-88 (Kuraray Specialities Europe GmbH, Frankfurt, Germany), ultrapure chitosan chloride: Protasan® UP CL113 with a molecular weight of < 150 kDa (FMC BioPolymer AS, Oslo, Norway), Cibacron Brilliant Red 3B-A® (Sigma-Aldrich Co., St Louis, USA) and ethyl acetate (Fluka Chemie GmbH, Buchs, Switzerland). Other chemicals were of analytical grade.

Methods

1. Preparation of nanoparticles

Cationically modified nanoparticles were prepared using the emulsion diffusion evaporation technique previously described [8, 9]. Briefly, solution of PLGA 70:30 in ethyl acetate was added dropwise to 5 ml aqueous solution of PVA and chitosan while stirring at 1000 rpm. The emulsion was stirred for 1h, and then homogenized at 13,500 rpm, for 10 min (Ultra-Turrax® T 25 Mixer, Janke und Kunkel GmbH & Co., Staufen, Germany). Nanoparticles were obtained by adding demineralised water to 50 ml. The suspension was stirred overnight to evaporate the organic solvent.

2. Purification of nanoparticles

Nanoparticles were purified on a ***laboratory scale*** using Centrisart I® (Sartorius AG, Goettingen, Germany), which is a ready to use unit for small volume (up to 2.5 ml) centrifugal ultrafiltration, Figure 1. Centrisart I® consists of an outer centrifuge tube, in which the sample is placed, and a free-sliding inner tube, closed on the underside with an ultrafilter. During centrifugation, the inner tube is pulled down against the sample, so that liquid is forced through the ultrafilter, while particles are simultaneously pulled away from it to the bottom.

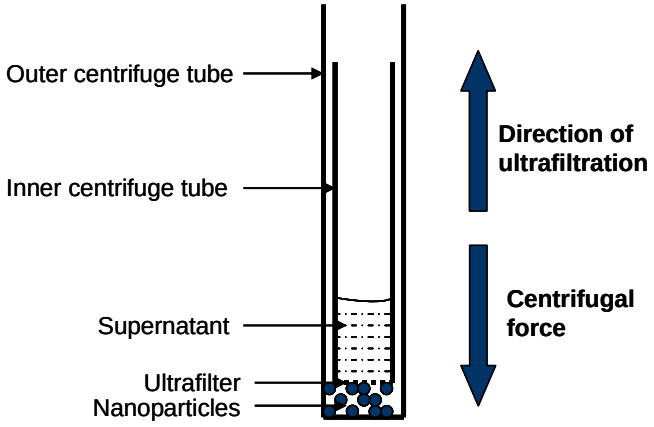

Figure 1: Schematic presentation of Centrisart I® and the forces acting during the separation procedure

The nanoparticles were centrifuged (Universal 30RF, Hettich Centrifuges, Tuttlingen, Germany). After centrifugation of the nanoparticles, supernatant was collected for quantitative determination of unbound PVA and chitosan, while the nanoparticles retained were washed with water and redispersed. This purification cycle was repeated several times. Various parameters were investigated to optimize the purification process in terms of best separation without affecting the nanoparticles integrity or causing their aggregation. The factors studied are molecular weight cut-off (MWCO) of the filter, the Relative Centrifugal Force (RCF) and the Centrifugal time.

Large-scale purification of nanoparticles was carried out by preparative size exclusion chromatography (SEC) using an FPLC® system from Pharmacia Biotech (now Amersham Biosciences; Uppsala, Sweden) equipped with two P-500 pumps, LCC-501 Plus controller, MV-7 injection valve, 50 ml Superloop, C 16/70 column with one AC 16 adaptor, Uvicord SII detector with an interference filter of 206 nm and FRAC-100 fraction collector, Figure 2.

Figure 2: FPLC for large scale purification of nanoparticles

The stationary phase was Sephacryl 1000-SF® from GE Healthcare (Munich, Germany) with a dimension of 65 cm in height and 1.6 cm in diameter. Mobile phase is composed of degased MilliQ-water containing 0.1 mM HCl in a flow rate of 1 ml/min under isocratic conditions. The system was operated by the FPLCdirector™ version 1.3 (Pharmacia Biotech).

Nanoparticles injection volumes were 5 – 7 ml per run. Purified particles were collected and concentrated by ultrafiltration using Vivaspin 20® (Sartorius, Göttingen, Germany) with a MWCO of 300,000 Da at 1000 x g followed by sterile filteration (0.2/0.45 µm, Minisart® sterile cellulose acetate filter, Sartorius).

3. Quantitative determination of PVA concentration

Following small-scale purification with Centrisart I®, samples from the supernatant collected after every centrifugation cycle were analysed for the amount of unbound PVA. The PVA content in the supernatant was determined by a colorimetric method based on the formation of a greenish coloured complex between two adjacent hydroxyl groups of PVA and iodine molecule in the presence of boric acid [10]. Appropriate volumes from the supernatant were diluted to 5 ml with water. The diluted solution was mixed with 3 ml boric acid solution (3.8 % w/v) and 0.6 ml 0.1 M iodine solution (prepared from iodine and potassium iodide), and then the volume was made up to 10 ml with water. The UV absorbance of the final solution was measured by a UV/VIS spectrophotometer at 640 nm using boric acid/iodine solution as a blank solution. A calibration curve was prepared under identical conditions using PVA solution in the concentration range from 0 to 400 µg/ml. The PVA assay was validated for its linearity, accuracy, specificity and reproducibility. In order to investigate the effect of chitosan on the complex formation, another calibration curve was done using a mixture of PVA and chitosan (in the maximum concentration that can be present in the nanoparticle suspension).

4. Quantitative determination of chitosan concentration

The amount of chitosan in the supernatant during the purification procedure was assessed using a colorimetric assay [11], adopted in our laboratory for the specific application. The assay is based on the ionic interaction between the protonated amino groups of chitosan and sulfonic acid groups on the anionic dye, Cibacron Brilliant Red®. In this method, 5 ml of aqueous dye solution (0.15 % w/v) were diluted to 100 ml with 0.1 M glycine hydrochloride buffer. The buffer is prepared by dissolving 7.48 g/L glycine and 5.84 g/L sodium chloride in MilliQ water followed by the addition of 0.1 M HCl to obtain a final pH of 3.2. Samples from the supernatant after each purification step were diluted with glycine buffer to 300 µl. Then, 3 ml of the dye solution were added. The absorbance values were measured at 578 nm using UV/VIS spectrophotometer using a solution of buffer (0.3 ml) and dye (3 ml) as reference solution. A standard curve was done using different dilutions of chitosan. The linearity, accuracy and reproducibility of the assay were verified. In addition, the effect of PVA (which is also present in the supernatant) on the assay was investigated.

5. Effect of the purification process on the colloidal characteristics

The size and ζ–potential of the original nanoparticle suspension was determined using the Malvern Zetasizer Nano (Malvern Instruments, Malvern, UK) in demineralised water. Size measurements were based on the Photon Correlation Spectroscopy (PCS) at 25°C, whereas the ζ–potential was estimated based on the electrophoretic mobility. After each purification step, samples from the nanoparticle suspension were also characterized. A mean of three determinations ± SD was calculated for each sample.

In addition, the particle size and ζ–potential of non-purified and purified nanoparticles were measured at different pH values from 3 to 11 using the automatic titration device MPT-2 (Malvern Instruments, Malvern, UK).

Results and Discussion

1. Characterization of nanoparticles

Chitosan-modified PLGA nanoparticle suspension containing 3 and 0.3 mg/ml PVA and chitosan, respectively, was prepared using the emulsion-diffusion-evaporation technique. The nanoparticles are characterized by a mean particle size of (166.2 ± 1.3) nm, a polydispersity index of 0.164 and a surface charge of (26.7 ± 1.5) mV.

2. Purification of the nanoparticles

Preliminary trials for the purification of nanoparticles based on ultracentrifugation or filtration resulted in either particle aggregation or partial loss of the nanoparticles through the membrane filter, respectively (data not shown). Purification of nanoparticles using the Centrisart I® appeared to be the most promising technique on a laboratory scale. For optimal purification conditions, the effect of different parameters including the MWCO of the ultrafilter, the RCF, and the centrifugation time on the colloidal characteristics of the particles were investigated. Centrisart I® of different MWCO ranging from 5,000 to 300,000 were applied. It was observed that using the smallest MWCO (5,000), no separation could be performed because the polymeric materials were not able to cross the filters into the supernatant; the suspension remained intact. Increasing the MWCO made the separation procedure feasible. In general, higher MWCO is expected to ensure better migration of the large, soluble molecules of chitosan and PVA in the filtrate. Measurement of the particle size indicates that the MWCO does not affect the size of the particles except an increase in the distribution (PI), Figure 3A.

The centrifugal force plays an essential role in the separation process; low centrifugal force usually results in a poor separation whereas high force may cause particle aggregation. To find optimal condition, the effect of increasing the RCF on the particle size was studied. Lower RCF could not allow complete separation of the nanoparticles. On the

other hand, higher RCF (> 3000 ×g) lead to particle aggregation, as shown in Figure 3B by the increased particle size and polydispersity index. Additionally, the centrifugation time was varied between 15 and 60 min at a fixed RCF of 2795 ×g. As depicted in Figure 3C, longer centrifugation time lead to particle aggregation.

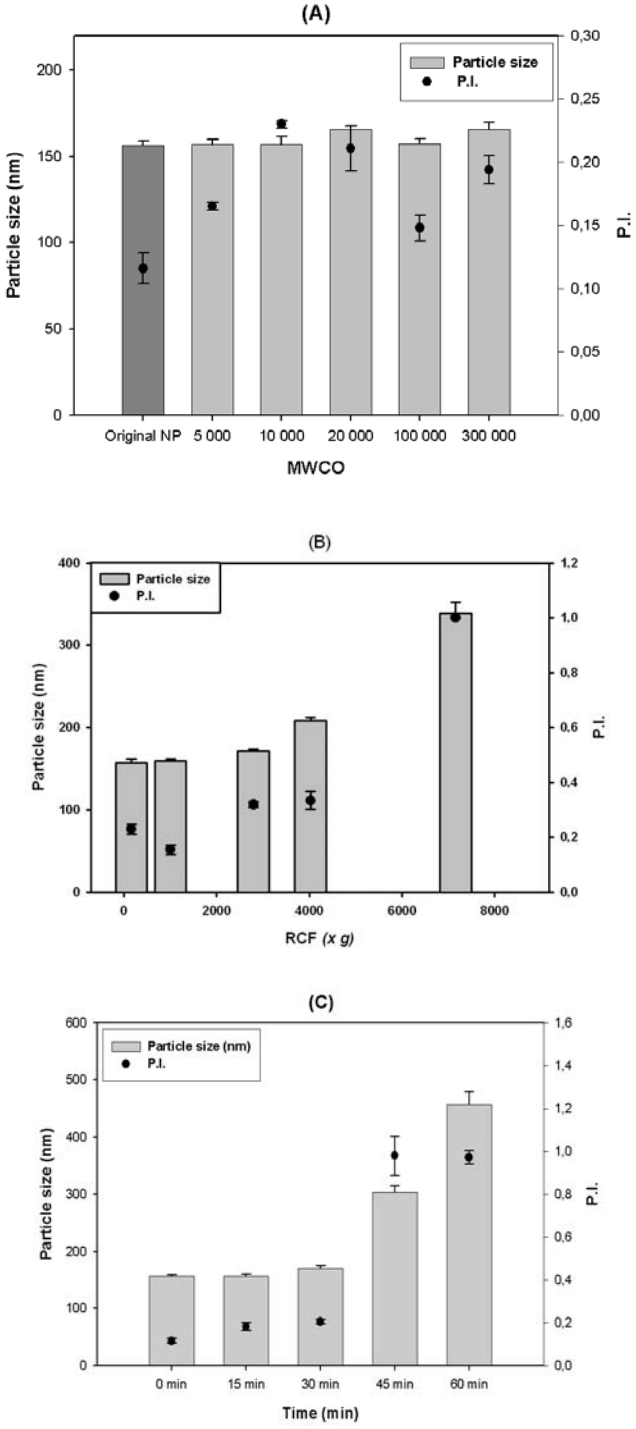

Figure 3: Factors affecting the purification efficiency of chitosan-modified PLGA nanoparticles using the Centrisart I®: (A) MWCO, (B) RCF, and (C) centrifugation time

It should be noted that these parameters are generally dependent on the particle size range of the nanoparticles; larger particles are expected to be separated at comparatively lower RCF and in a shorter time.

Based on these preliminary investigations, optimum purification conditions with respect to the stability/resuspendability of the suspension were identified and applied for the successive studies.

3. Quantitative determination of PVA concentration

The PVA assay used in the present study was adopted from the colorimetric method developed by Finely [12]. The greenish colored complex formed between PVA and iodine in the presence of boric acid was measured spectrophotometrically. The mechanism of this complex formation was discussed by Prichard et al. [13]. Briefly, the green color is found to be due to helical envelopment of iodine molecules by PVA chains stiffened by scattered cyclic groups [13].

Assay validation demonstrated that the reaction is linear in the concentration range of 50 - 250 µg/ml (correlation coefficient r^2 = 0.999). The reproducibility was checked by comparing intraday and interday variation of the absorbance values. Calibration curves made using a mixture of PVA and chitosan demonstrate a shift in the λ_{max} from 640 to 620 nm, Figure 4A; however, the shift in wavelength had a minor effect on the absorbance values due to the broad absorption peak, Figure 4B.

The concentration of unbound PVA was determined by analysing appropriate volumes of the supernatant collected after each centrifugation step. It was noted that the samples analysed showed a λ_{max} of 640 nm, i.e. similar to the calibration curve of PVA alone not that of PVA/chitosan. This might give us already a rough idea that the concentration of unbound chitosan in the supernatant is low and therefore no shift in the λ_{max} was detected. Figure 4C shows the amount of PVA at each purification step. The initial concentration of

unbound PVA in the nanoparticle suspension was found to be around 1 mg/ml. As a consequence, 66.6 % of the PVA were bound to the nanoparticles.

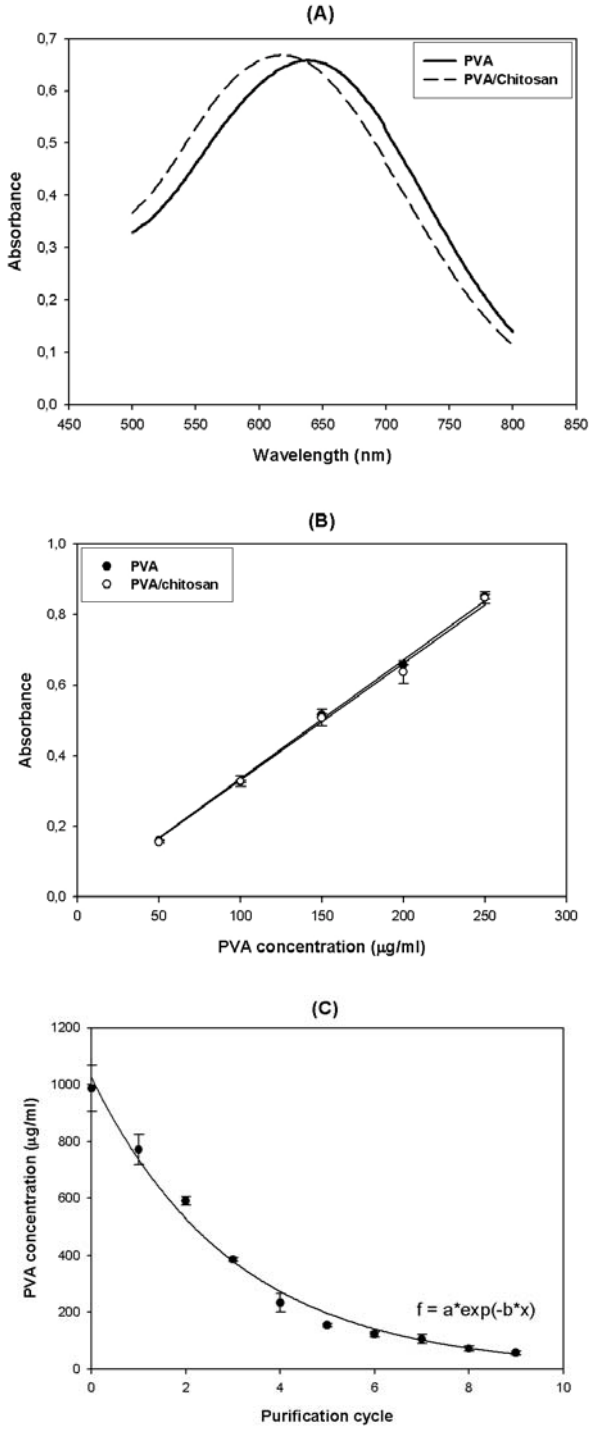

Figure 4: (A) Effect of chitosan on the PVA/iodine reaction, (B) calibration curves using PVA alone and PVA/chitosan solutions, (C) residual amounts of PVA during the purification procedure *(n = 3)*

Successive washing steps reduce the amount of PVA gradually to 50 µg/ml after 10 washing steps. The fit of the data can be done using an exponential relationship as indicated in the following equation:

$$y = a * e^{(-b*x)} \qquad (R^2 = 0.9958)$$

This allows for predictable estimation of the amount of PVA at any point.

4. Quantitative determination of chitosan concentration

Although chitosan nanoparticles and chitosan coated nanoparticles were extensively formulated for drug and gene delivery, no method (to our knowledge) was identified to quantify the actual amount of chitosan on the nanoparticle surface. In this study, we tried to determine the concentration of chitosan through a colorimetric assay developed by Muzzarelli [11].

The linearity of the assay was obtained in the concentration range 120 - 240 µg/ml. A sigmoidal curve was obtained when higher and lower chitosan concentrations were used. The addition of PVA in the same concentration as present in the nanoparticle suspension did not affect the linearity of the assay or alter the λ_{max}, however, relatively higher absorbance values were obtained, Figure 5A, thus slightly increasing the sensitivity. Analysis of the supernatant obtained from nanoparticle purification indicated very weak absorbance values corresponding to unbound chitosan concentration lower than 20 µg/ml, which is beyond the linearity limit of the assay, Figure 5B.

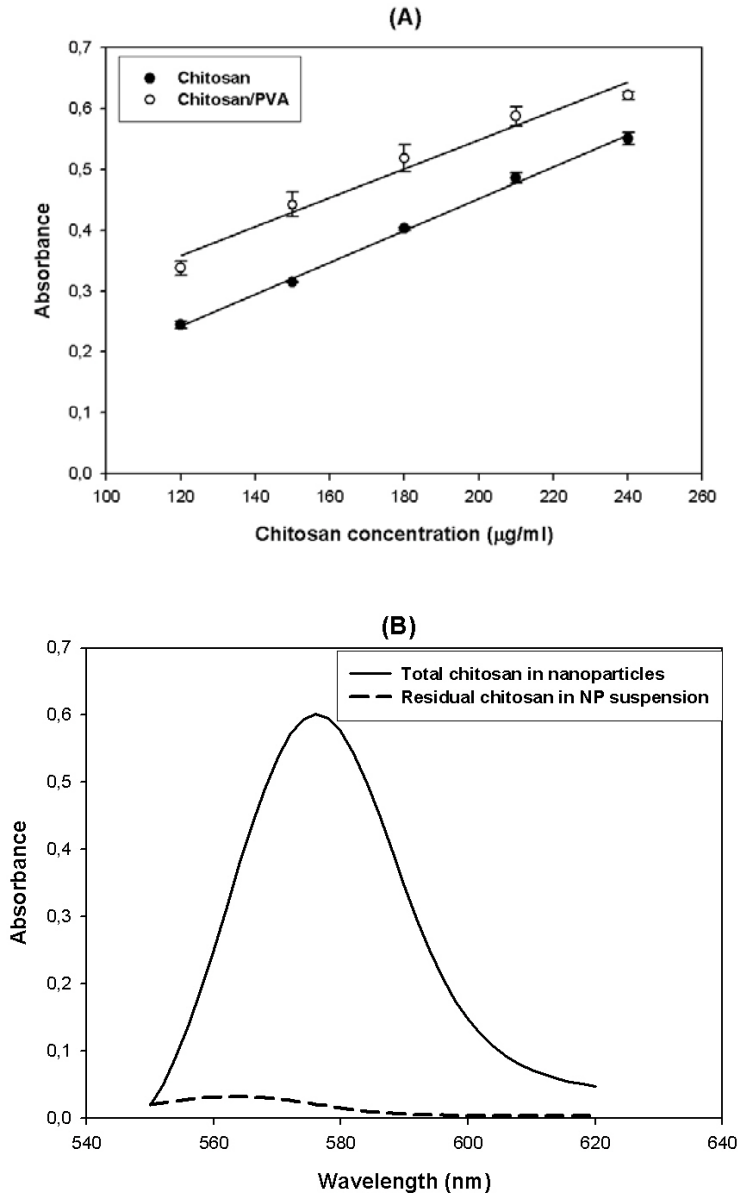

Figure 5: (A) Calibration curves using chitosan alone and chitosan/PVA solutions, (B) quantitative determination of chitosan in the nanoparticle suspension

Hence, although this colorimetric assay was not appropriate to estimate precisely the chitosan concentrations applied, it proved that more than 90% of the chitosan added is actually bound to the nanoparticle surface. Referring to the surface charge measurements as a function of chitosan concentration in our previous study [9], it was observed that the surface charge is directly proportional to the concentration of chitosan added, which means that the concentration of chitosan used here (0.3 mg/ml) is not sufficient to cover the whole particle surface or at least does not form a dense layer around the particles.

5. Effect of the purification procedure on the colloidal stability

Although the removal of unbound polymers is an important issue, the maintenance of the colloidal characteristics of the nanoparticles keeps its significance and remains a big challenge. Therefore, the changes in the mean nanoparticle diameter, the size distribution and surface charge of the nanoparticles were followed along the purification procedure. As shown in Figure 6A, the particles retain their mean diameter along the purification steps. A small increase in the mean size by 13 % was observed at the end of 10 purification steps. Besides, a relative broadening in the size distribution was noticed, Figure 6B.

On the other hand, the ζ- potential was varying with no descriptive trend, Figure 6C, but was always positive as envisaged for successful complexation with genetic material and improved cellular uptake.

The behavior of the purified nanoparticles as a function of pH in comparison to the non purified particles was determined using the autotitration technique in Malvern Zetasizer Nano (Malvern Instruments, Malvern, UK). As shown in Figure 7A, the purified particles are characterized by a slightly smaller mean particle diameter compared to the non purified particles. The effect was much more distinct in the acidic pH values, lower than the pK_a of chitosan, where chitosan is expected to be fully ionized. Similarly, the ζ- potential – pH profile, Figure 7B, indicates more pronounced surface charge of the non-purified particles in the acidic medium compared to the purified particles.

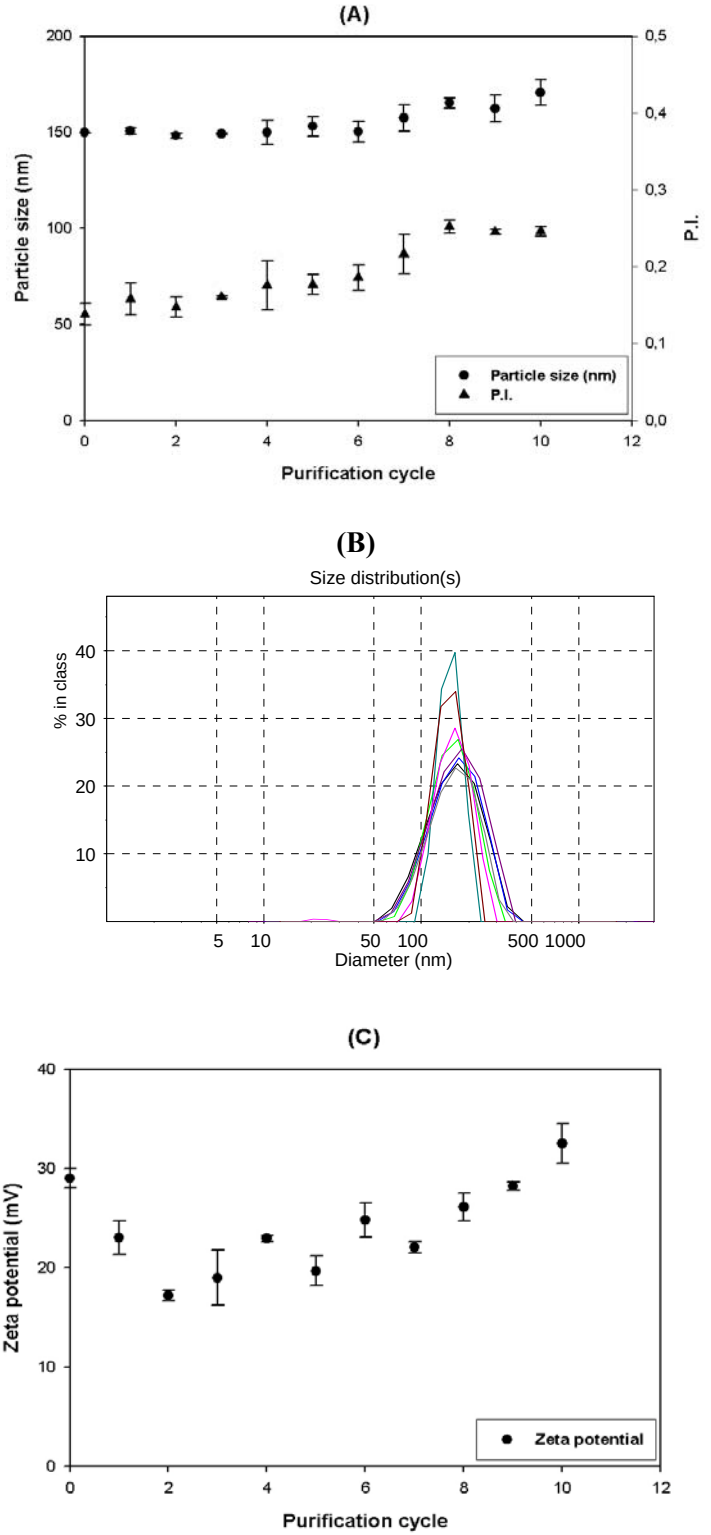

Figure 6: Effect of the purification procedure on (A) particle size, (B) size distribution, and (C) ζ-potential of the nanoparticles

Chitosan molecules in the surrounding medium of the non-purified nanoparticles tend to bind to the nanoparticles surface especially when they are positively charged at lower pH values. This might explain the comparatively larger hydrodynamic nanoparticle size and higher surface charge of the non-purified nanoparticles in the acidic medium. During purification, the loosely bound chitosan molecules are easily detached from the nanoparticle surface. Therefore, the purified nanoparticles are characterized by slightly lower but more stable surface charge at the pH range tested.

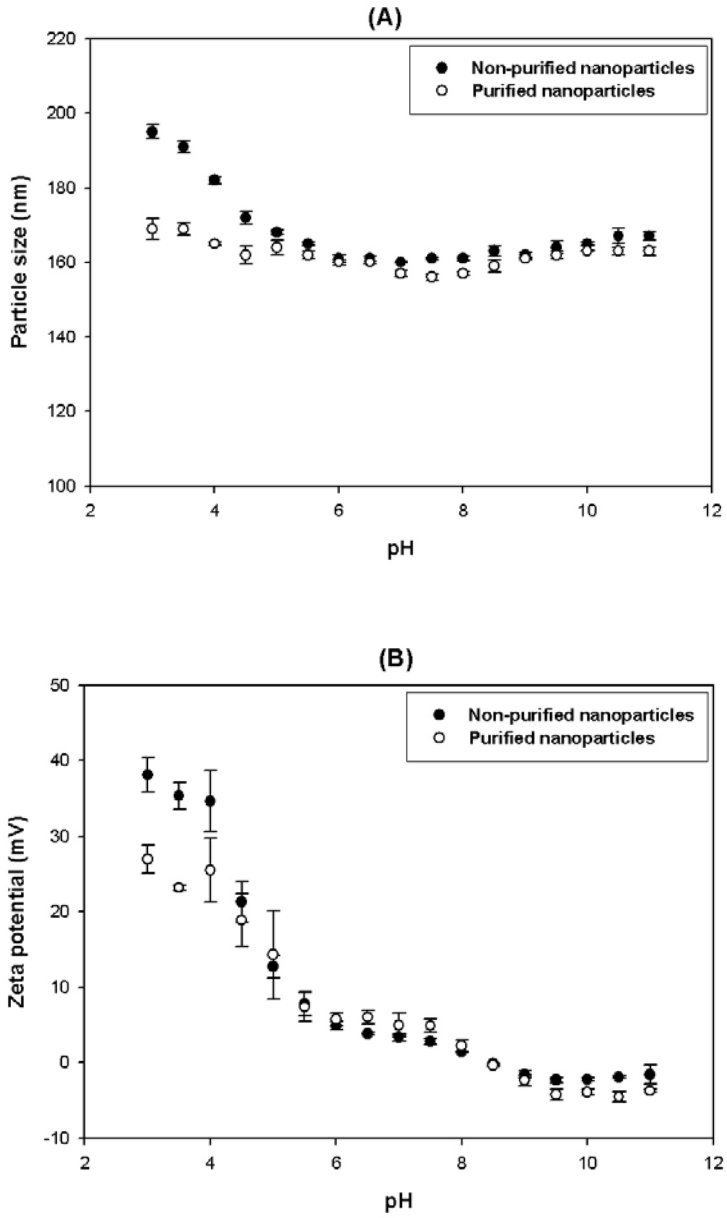

Figure 7: (A) Particle size- , (B) ζ-potential- pH profile of purified and non-purified nanoparticles

6. Large scale purification of nanoparticles

Larger volumes of the nanoparticles were purified based on size exclusion chromatography using FPLC. Nanoparticles prepared with 1 and 2.5% w/v PVA – denoted by cNP-1% and cNP-2.5%, respectively - were purified. As mentioned in the preceding chapter, particles with higher PVA content are smaller in size. Particle size measurements indicate a size of 337 and 184 nm for cNP-1% and cNP-2.5%, respectively. Figure 7A shows the chromatograms of both nanoparticle preparations; smaller particles, cNP-2.5%, were excluded faster (20 min) than larger ones (40 min). In addition, the shoulder belonging to the unbound PVA (~ 80 min) is more pronounced in case of cNP-2.5% indicating a comparatively higher amount of unbound PVA.

On the other side, nanoparticles containing increasing chitosan concentration, 0.3 and 0.6% (cNP-3 and cNP-6) were prepared and were characterized by a surface charge of 21.23 and 33.2 mV, respectively. Their corresponding chromatograms were almost superimposable, Figure 7B.

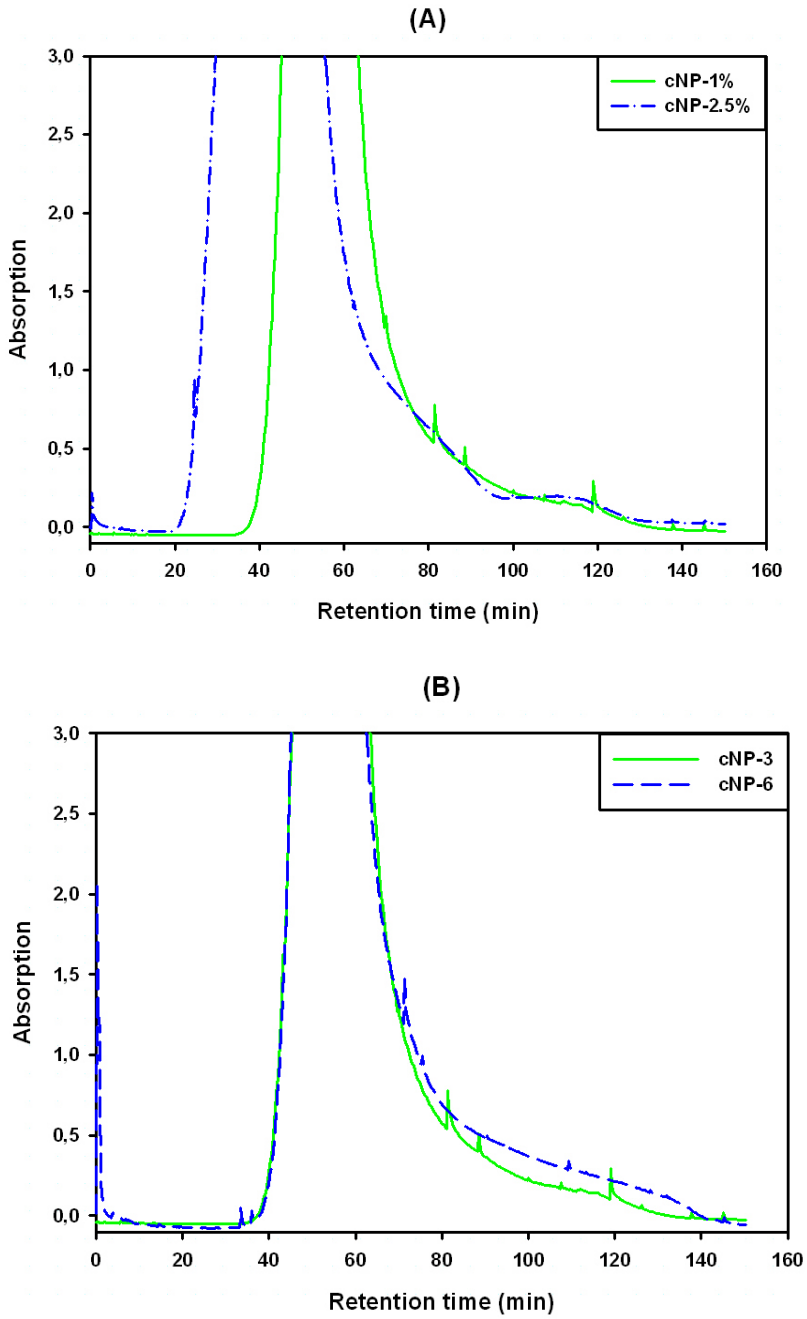

Figure 7: FPLC chromatograms of chitosan-modified PLGA nanoparticles of different (A) particle sizes and (B) ζ-potential

Checking the change in the colloidal properties of the previously mentioned nanoparticles after purification revealed no remarkable change in their size and/or charge as indicated in the histograms, Figure 8 A & B.

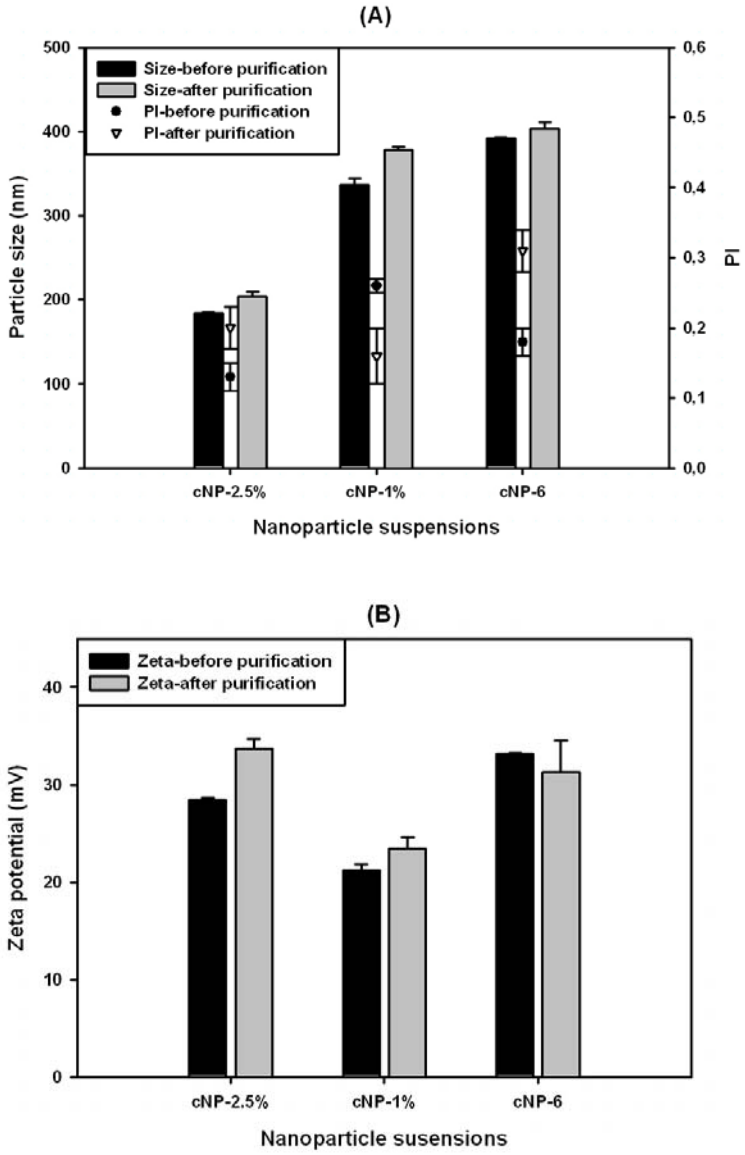

Figure 8: Effect of nanoparticle purification by FPLC on (A) particle size and size distribution, (B) ζ-potential

Conclusions

From this study, it was shown that the centrifugal ultrafiltration technique is a convenient way to remove and estimate quantitatively the residual amounts of unbound polymers from the nanoparticles suspension. The unpurified nanoparticle suspensions investigated contains ~1/3 of the PVA unbound in the surrounding medium, while no excessive chitosan was detected. The purified nanoparticles are successfully recovered with a minimum weight loss and their colloidal stability was maintained. Therefore, it can be concluded that the Centrisart I® and the FPLC are promising techniques for small- and large-scale purification of chitosan-modified PLGA nanoparticles, respectively.

REFERENCES

[1] M. Suzuki, M. Machida, K. Adachi, K. Otabe, T. Sugimoto, M. Hayashi, S. Awazu, Histological study of the effects of of a single intratracheal instillation of surface active agents on lung in rats. J. Toxicol. Sci. 25 (2000) 49-55.

[2] J. Panyam, W.-Z. Zhou, S. Prabha, S.K. Sahoo, V. Labhasetwar, Rapid endo-lysosomal escape of poly(DL-lactide-co-glycolide) nanoparticles: Implications for drug and gene delivery. FASEB Journal 16(10) (2002) 1217-1226.

[3] H.-Y. Kwon, J.-Y. Lee, S.-W. Choi, Y. Jang, J.-H. Kim, Preparation of PLGA nanoparticles containing estrogen by emulsification-diffusion method. Colloids and Surfaces A: Physicochemical and Engineering Aspects 182(1-3) (2001) 123-130.

[4] G. Tishchenko, R. Hilke, W. Albrecht, J. Schauer, K. Luetzow, Z. Pientka, M. Bleha, Ultrafiltration and microfiltration membranes in latex purification by diafiltration with suction. Separation and Purification Technology 30(1) (2003) 57-68.

[5] P. Beck, D. Scherer, K. J., Separation of drug-loaded nanoparticles from free drug by gel filtration. J. Microencapsul. 7(4) (1990) 491 - 496.

[6] S. Prabha, W.-Z. Zhou, J. Panyam, V. Labhasetwar, Size-dependency of nanoparticle-mediated gene transfection: studies with fractionated nanoparticles. International Journal of Pharmaceutics 244(1-2) (2002) 105-115.

[7] G. Dalwadi, H. Benson, Y. Chen, Comparison of Diafiltration and Tangential Flow Filtration for Purification of Nanoparticle Suspensions. Pharm. Res. 22(12) (2005) 2152-2162.

[8] M.N.V. Ravi Kumar, U. Bakowsky, C.M. Lehr, Preparation and characterization of cationic PLGA nanospheres as DNA carriers. Biomaterials 25(10) (2004) 1771-1777.

[9] N. Nafee, S. Taetz, M. Schneider, U.F. Schaefer, C.M. Lehr, Chitosan-coated PLGA nanoparticles for DNA/RNA delivery: effect of the formulation parameters on complexation and transfection of antisense oligonucleotides. Nanomedicine: Nanotechnology, Biology, and Medicine 3(3) (2007) 173-183.

[10] D.P. Joshi, Y.L. Lan-Chun-Fung, J.G. Pritchard, Determination of poly(vinyl alcohol) via its complex with boric acid and iodine. Analytica Chimica Acta 104(1) (1979) 153-160.

[11] R.A. Muzzarelli, Colorimetric determination of chitosan. Anal. Biochem. 260 (1998) 255 - 257.

[12] J.H. Finley, Spectrophotometric determination of polyvinyl alcohol in paper coatings. Anal. Chem. 33(13) (1961) 1925 - 1927.

[13] J.G. Pritchard, D.A. Akintola, Complexation of polyvinyl alcohol with iodine. Talanta 19 (1972) 877 - 888.

Chapter 4

Chitosan-modified PLGA nanoparticles as carrier for antisense oligonucleotides

Influence of surface charge on the binding and uptake of nanoparticles and nanoplexes in different human cancer cell lines*

*** This chapter is prepared for publication as a journal article:**

N. Nafee, K. Friebel, M. Schneider, U. F. Schaefer and C.-M. Lehr. Role of chitosan in improving the uptake of PLGA nanoparticles and their nanoplexes with antisense oligonucleotides in different cell lines.

Abstract

Purpose: In this chapter, we aimed to investigate the role of chitosan and the influence of its concentration on the nanoparticle surface in improving both the binding with antisense oligonucleotides, OMR, and the uptake of NP/OMR nanoplexes in human lung cancer cell lines.

Methods: The uptake of fluorescently labelled PLGA nanoparticles loaded with increasing chitosan concentrations in A549 and Calu-3 cells was studied by flow cytometry and CLSM. The potential of binding of these particles with the antisense oligonucleotides as well as the intracellular uptake the nanoplexes in dependence of the surface charge was investigated.

Results: The surface modification of PLGA nanoparticles significantly increases their potential of binding with OMR and their intracellular uptake. However, further increase in chitosan content was not accompanied by a corresponding improvement in transfection efficiency. The uptake was dependent on the cell type. Furthermore, nanoplexes formed with chitosan solution were not able to be internalized.

Conclusions: Chitosan plays an essential role in improving the binding and uptake of antisense oligonucleotides in human cancer cell lines. Optimum chitosan concentrations on the nanoparticle surface were needed to get the maximum transfection efficiency.

Background

DNA/RNA delivery is gaining growing attention for the treatment of genetic deficiencies and is still a hope for successful future medical treatment [1, 2]. Gene therapy can be defined as the transfer of a genetic material to specific cells in order to have a therapeutic effect. At the present time, major gene delivery systems employ either viral or non-viral vectors [3, 4]. Although viral systems are very efficient for *in vivo* transfection, as well as immunization, their major drawback is their possible toxicity, immunogenicity and inflammatory responses [5, 6]. Non-viral systems based on biocompatible polymers are preferred in terms of safety, stability, relative ease of large scale production and characterization, and the lack of intrinsic immunogenicity [7]. Non-viral vectors include liposomes, complexes of the negatively charged plasmid with cationic polymers and nanoparticles. Even though liposome vesicles prepared from lipids may protect the loaded drugs or proteins from degradation and target them to the site of action [8], they have shown a relatively low encapsulation efficiency, poor storage stability and rapid clearance from the blood [9]. The formation of complexes from cationic polymer with anionic DNA or oligonucleotide solutions was applied by many research groups [10-12]. The simplicity of these self-assembling polyelectrolyte complexes is both an advantage and a drawback. Though such complexes are easy to generate and they can protect DNA from enzymatic degradation, they are always characterized by a broad size distribution and variable shape [12].

Solid, biodegradable nanoparticles have shown their advantage over other carriers by their increased stability and their controlled release ability. Furthermore, the small polydispersity allows better control when used as delivery vehicles. The intracellular delivery of genetic material (RNA, DNA, and oligonucleotides), which is typically negatively charged, requires a positively charged carrier [13]. PLGA nanoparticles are known to be negatively charged due to the presence of ionized carboxyl groups. This

negative charge limits their binding efficiency with these genetic materials and their transport through the cell membrane. PLGA nanoparticles with cationic surface modification can overcome these disadvantages.

Lung cancer is the main cause of cancer-related mortality in western world. A new promising approach for treatment of non-small cell lung cancer (NSCLC) is based on the inhibition of telomerase in cancer cells. Telomerase, a ribonucleoprotein that adds telomeric repeats to the end of the telomeres [14] and therefore prevents telomere shortening occurring during replication of the cell cycle. Telomerase activity has been detected in most human cancers and cancer cell lines as well as in stem cells and regenerative tissues, but not in most normal somatic cells [15]. Telomerase activity is required for continuous cell proliferation and allows cells to overcome senescence. Therefore, activation of telomerase is considered to be one of the key mechanisms leading to immortalization of tumor cells and tumor progression. The antisense oligonucleotide 2´-O-methyl-RNA (OMR) with a phosphorothioate backbone is a potent and sequence-selective inhibitor of telomerase. 2´-O-methyl-RNA binds to the complementary hTR template sequence with high affinity acting as a competitive enzyme inhibitor of telomerase [16].

In this chapter, we investigated the potential of fluorescently-labeled nanoparticles containing increasing concentrations of chitosan to be taken up by human cancer cell lines A549 and Calu-3 cells. In addition, the efficiency of these chitosan-modified PLGA nanoparticles as carrier for nucleotide-based drugs was studied. Their binding with the 13mer antisense oligonucleotide, OMR, as well as the intracellular uptake of cNP/OMR polyplexes in dependence of the surface charge was demonstrated.

Materials and methods

Materials

Poly(D,L-lactide-*co*-glycolide) 70:30 (Polysciences Europe GmbH, Eppelheim, Germany), polyvinyl alcohol Mowiol® 4-88 (Kuraray Specialities Europe GmbH, Frankfurt, Germany), different types of ultrapure chitosan: the chloride salts; Protasan® UP CL113 and Protasan® UP CL213, and the glutamate salts; Protasan® UP CG113 and Protasan® UP CG213 with different properties (see Table 1) (FMC BioPolymer AS, Oslo, Norway), 5-Fluoresceinamin (FA) and 1-ethyl-3-(3-Dimethylaminopropyl)-carbodiimide hydrochloride (DMAP) were obtained from Sigma (Sigma Chemical Co., St. Louis, MO, USA), ethyl acetate (Fluka Chemie GmbH, Buchs, Switzerland) were used as obtained. The antisense oligonucleotide 2'-O-Methyl-RNA (OMR) with a phosphorothioate (ps) backbone (5' -2' -O- methyl [C(ps)A(ps)GUUAGGGUU(ps)A(ps)G]-3') was obtained from (Biomers.net GmbH, Ulm, Germany). For the uptake studies, the carboxyfluoresceinamine labeled derivative 5'-FAM-OMR was used.

Table 1: Properties of different types of chitosan:

Type of chitosan	Chitosan properties	
	Molecular weight [kDa]*	**Viscosity [mPa.s]†**
Protasan® UP CL113	< 150	< 20
Protasan® UP CL213	150 – 400	20 – 200
Protasan® UP G113	< 200	< 20
Protasan® UP G213	200-600	20 – 200

Methods

1. Fluorescent labeling of PLGA

Fluoresceineamine-bound PLGA (FA-PLGA) was prepared based upon the method described by Horisawa et al. [17] and Weiss et al. [18]. Briefly, PLGA (3.07 g) and FA (0.0583 g) were dissolved entirely in 30 ml of acetonitrile with 0.0408 g of DMAP and incubated at room temperature for 24 h under light protection and gentle stirring. The resulting FA-PLGA was precipitated by the addition of purified water and separated by centrifugation. The polymer was rinsed from excessive reagents (repeated dissolvation in acetone and precipitation with ethanol) and then lyophilized (Alpha 2-4 LSC, Martin Christ Gefriertrocknungsanlagen GmbH, Osterode, GE).

2. Preparation of the nanoparticles

PLGA nanoparticles (NP-0) and chitosan-modified PLGA nanoparticles containing increasing concentration of chitosan 0.3 – 1.2 %w/v (denoted by NP-3 - NP-12, respectively) were prepared by the emulsion-diffusion-evaporation technique as described in the previous chapters. Fluorescently labeled nanoparticles of the same formulations mentioned above were prepared using the fluorescinamine-labeled PLGA polymer (FA-PLGA); these particles are denoted by the abbreviations FA-NP-0 to FA-NP-12 (Table 2).

3. Loading of nanoparticles with oligonucleotides; formation of nanoplexes

In order to study the ability of the different nanoparticles as a carrier for gene delivery, nanoparticles were loaded with the antisense oligonucleotide, 2'-O-Methyl RNA. Predetermined volumes of the nanoparticle suspensions were mixed with an aqueous

solution of the oligonucleotide at room temperature and vortexed for 30 s followed by incubation on an orbital shaker at room temperature. The factors affecting the binding conditions including the incubation medium, the incubation time and the OMR:NP weight ratio were investigated. The binding conditions were optimized to ensure maximum binding ability of the oligonucleotide to the nanoparticles.

4. Characterization of nanoplexes

The colloidal characteristics of different plain nanoparticles, the FA-nanoparticles as well as the NP/OMR nanoplexes were determined using the Malvern Zetasizer Nano (Malvern Instruments, Malvern, UK). The effect of the change in OMR:NP ratio, the incubation medium and the incubation time on the size and surface charge of the nanoparticles was studied. The morphology of the nanoplexes was examined by Scanning Force Microscopy with a Bioscope™ equipped with a Nanoscope IV™ controller (Digital Instruments, Veeco, Santa Barbara, California, USA). The nanoparticles were investigated under ambient conditions in tapping mode using a scanning probe with a force constant of 40 N/m at resonant frequency of ~170 kHz (Anfatec, Oelsnitz, Germany).

5. Binding and uptake to A549 cells

5.1. Cell cultures and treatments

A549 cells (CCL-185; ATCC, Manassas, VA, USA) were cultivated in RPMI with L-glutamine (PAA Laboratories GmbH, Pasching, Austria) supplemented with 10% fetal calf serum (FCS). One day prior to experiments, A549 cells were detached using trypsin-EDTA and seeded at a density of 100,000 cell/ml, in 24-well or 96-well plates 0.5 or 0.2 ml/well, respectively.

Calu-3 cells (HTB- 55; ATCC) were cultivated in Minimum Essential Medium (MEM) with Earl's Salts and L- glutamine (PAA Laboratories GmbH) supplemented with 10% FCS, 1% MEM non- essential amino acid (NEAA) solution and 1 mM sodium pyruvate (all from Sigma- Aldrich Chemie GmbH, Steinheim, Germany).

Cells were kept in an incubator set to 37°C, 5% CO_2 and 95% humidity. On the day of experiment, cells were washed with PBS and medium was changed.

5.2. Experimental design

The binding and intracellular uptake of 5'-FAM-2OMR (4 μM) to A549 cells were studied by flow cytometry (FACS) and confocal laser scanning microscopy (CLSM), respectively. For comparison, binding and uptake of the fluorescently labeled nanoparticles (FA-NP-0 to FA-NP-12) were investigated. Non-treated cells, cells treated with fluorescently labeled oligonucleotides in addition to cells treated with nanoparticles only were used as control. Nanoplexes of 5'-FAM-2OMR prepared with different nanoparticle formulations were incubated with A549 cells for 6h, after which the nanoplexes were replaced with fresh medium and the cells were incubated till the next day where the green fluorescence of the oligonucleotides was measured. The effect of OMR:NP ratio was investigated by using two ratios (1:50 and 1:100). Besides, the binding and uptake of nanoplexes formed with chitosan solutions of different properties (CL113, CL213, CG113 and CG213) were studied. Chitosan concentration in these solutions was equivalent to that used during the preparation of nanoparticles.

5.3. Flow cytometry

A549 cells were seeded in 6-well plates at a density of 100,000 cells per well and grown for 1 day. Nanoplexes prepared as mentioned above were diluted with RPMI cell culture medium containing 10% FCS. After incubation with the cells, the suspensions were removed and replaced with normal cell culture medium. Analysis by flow cytometry was

performed the next day with a FACSCalibur flow cytometer from Becton Dickinson (BD) Biosciences (Heidelberg, Germany) using the software CellQuest™ Pro Version 4.02 (BD Biosciences). For this purpose cells were detached by incubation with trypsin/EDTA, washed with PBS and resuspended in sheath fluid (BD Biosciences). Green fluorescence was excited at 488 nm and measured after passing a 530/30 nm band pass filter. During each run 15,000 cells were counted. Nanoplex uptake was evaluated after gating and definition of a fluorescence threshold with non-treated cells.

5.4. Cellular uptake of NP/OMR nanoplexes

A549 cells were seeded on LabTec chamber slides (Nunc GmbH, Wiesbaden, Germany) at a density of 12,500 cells/ml. Nanoplexes prepared as mentioned above were incubated with the cells. After 6h of incubation, the medium was replaced by normal cell culture medium. The cells were stained after 24 h then examined by CLSM.

Cell membranes were stained with the red fluorescent rhodamine labeled ricinus communis agglutinin I (RRCA; excitation maximum 552 nm, emission maximum 577 nm; Vector Laboratories Peterborough, England). Cells were washed once with PBS and afterwards incubated with 25 µg/ml of RRCA in PBS for 15 min in the incubator. After two washing steps with PBS the cells were fixed with 4% paraformaldehyde in PBS for 10 min at room temperature. The nuclei were then stained with 4',6-Diamidino-2-phenylindole dihydrochloride (DAPI, Em_{max}: 461 nm, Exc.: 374 nm; Fluka Chemie GmbH, Buchs, Switzerland).

Fluorescence imaging was performed using a BioRad MRC-1024 confocal laser scanning microscope equipped with an argon/krypton laser. The objective used was an oil immersion objective 100x NA=1.3. The excitation was performed using $\lambda = 488$ nm and the fluorescence signal was collected after a band pass filter (522/35). A step motor was used to perform 3D sections through the cells. The green fluorescent particles were located

with respect to the red stained cell membrane and the blue stained nuclei. Data evaluation and 3D reconstruction was done using volocity software (Improvision, Tübingen, Germany).

Results

1. Characterization of nanoparticles

Nanoparticles (both plain and fluorescently-labeled) containing increasing concentrations of chitosan were characterized in term of particle size, size distribution and surface charge. The colloidal characteristics of these particles are summarized in Table 2.

2. Formation and characterization of nanoplexes

In order to investigate the behavior of the nanoplexes during cellular uptake experiments, binding was carried out in various incubation media including MilliQ water, sodium chloride (NaCl) 10 mM, phosphate buffer saline (PBS) pH 7.4 and Hank's balanced salt solution (HBSS) pH 7.4. The colloidal characteristics of the OMR-loaded nanoparticles were compared to the unloaded nanoparticles (NP-3). As shown in Figure 1A, dynamic light scattering did not show a noticeable increase in size of the nanoparticles due to oligonucleotide adsorption. In addition, changing the incubation medium did not result in a corresponding change in the size of the nanoparticles. On the other hand, binding of the OMR to particles was confirmed by the surface charge measurements, Figure 1B. OMR-loaded particles are characterized by lower ζ-potential values (in MilliQ water and sodium chloride solution) in comparison to unloaded particles, whereas in PBS and HBSS buffers pH 7.4, a weak ζ-potential was recorded with either non-loaded or OMR-loaded nanoparticles.

Table 2: Colloidal characteristics of PLGA nanoparticles modified with different concentrations of chitosan:

Chitosan content (%w/v)	Plain nanoparticles				Fluorescently labeled nanoparticles			
	Code	Particle size (nm)	PI	ζ-potential (mV)	Code	Particle size (nm)	PI	ζ-potential (mV)
0	NP-0	145.7 ± 1.6	0.05 ± 0.02	-19.2 ± 0.1	FA-NP-0	156.3 ± 4.9	0.037 ± 0.015	3.2 ± 0.3
0.3	NP-3	203.1 ± 1.7	0.16 ± 0.01	30.5 ± 1.24	FA-NP-3	177.7 ± 3.1	0.07 ± 0.021	22.3 ± 2.7
0.6	NP-6	228.1 ± 3.3	0.18 ± 0.02	39.2 ± 2.1	FA-NP-6	174.9 ± 2.1	0.113 ± 0.014	33.7 ± 0.6
0.9	NP-9	250.8 ± 0.9	0.22 ± 0.01	52.6 ± 0.76	FA-NP-9	198.2 ± 2.0	0.127 ± 0.018	39.1 ± 0.7
1.2	NP-12	250.3 ± 3.17	0.20 ± 0.01	55.9 ± 0.14	FA-NP-12	201.7 ± 3.7	0.148 ± 0.012	46.2 ± 4.0

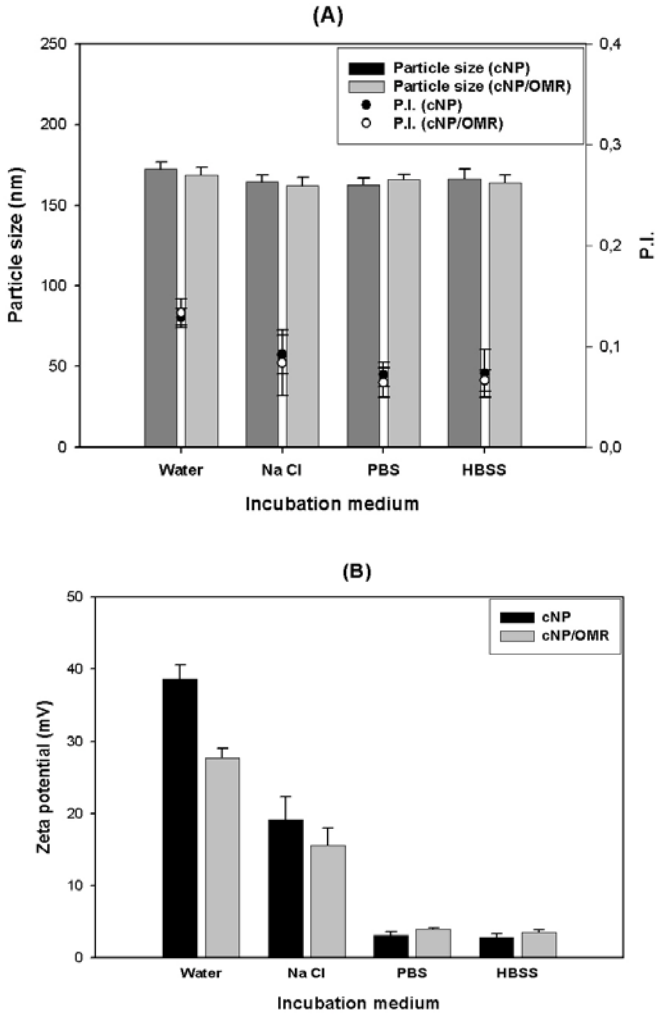

Figure 1: Effect of the incubation medium on the binding of OMR to cNP (A) particle size and size distribution, (B) ζ-potential

Our binding experiments reflected that the addition of oligonucleotides to the nanoparticles caused a reduction in the surface charge especially in MilliQ water and sodium chloride solution 10 mM indicating electrostatic binding of the negatively charged oligonucleotides to the positively charged nanoparticles.

This effect was more pronounced when MilliQ water was used as incubation medium than in sodium chloride reflecting the ionic strength of the medium which in turns affects the surface charge and hence the binding efficiency of the OMR to the nanoparticles. The pH of the incubation medium also plays an important role in the OMR binding to the

nanoparticles. The electrostatic forces involved in the binding process are relatively weak at pH 7.4 as deduced from the low ζ-potential of the nanoparticles in PBS and HBSS buffers. Thus, less OMR molecules is expected to be attracted to the surface at this pH.

The incubation time (t_{inc} =15 – 60 min), referring to the duration of mixing of the nanoparticles with OMR in MilliQ water, was tested with the OMR:NP-3 weight ratio (1:50) and was found to have no effect on the size and ζ-potential, Figure 2A & B.

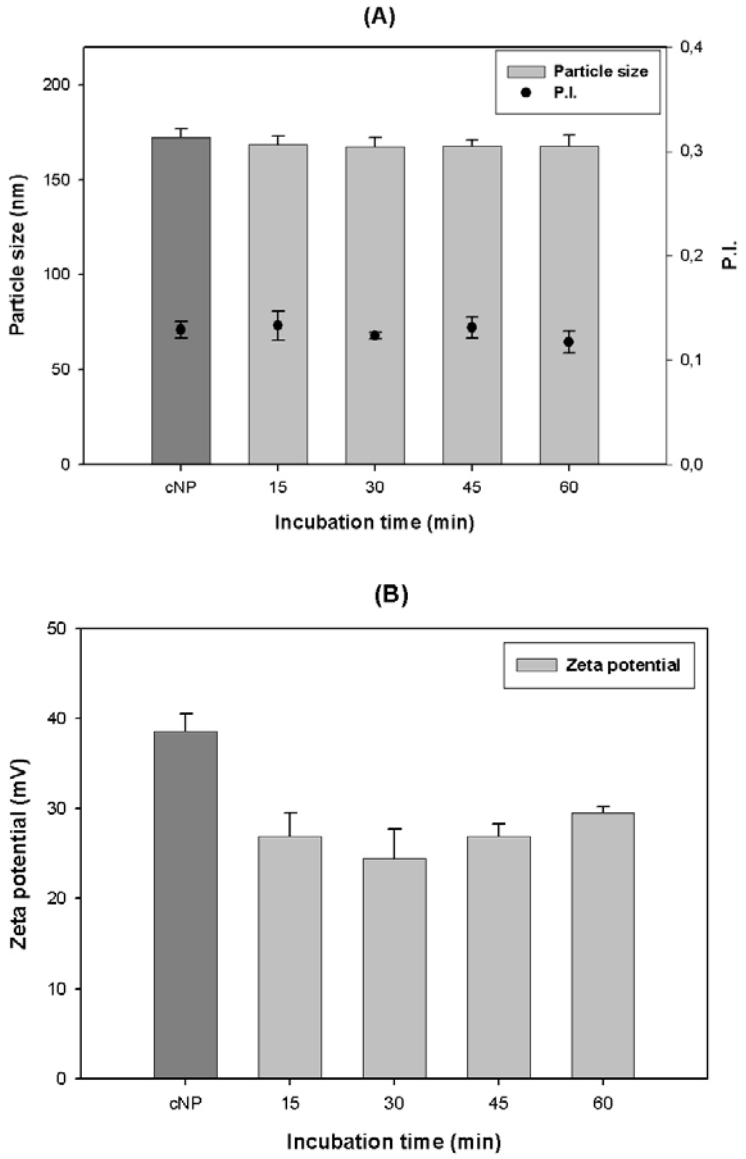

Figure 2: Effect of the incubation time on the binding of OMR to cNP (A) particle size and size distribution, (B) ζ-potential (the properties of pure nanoparticles, cNP, are represented by the dark bars for comparison)

The binding was investigated as a function of the weight ratio between the NP and OMR. Besides, the influence of increasing the surface charge on the nanoparticles on the extent of binding was also studied. For the different nanoparticle formulations (NP-0 – NP-12), various OMR:NP weight ratios (ranging from 1:100 to 1:1) were mixed in MilliQ water and incubated for 15 min. The size of the nanoplexes formed, their size distribution and surface charge were measured. Figure 3A demonstrates the change of the nanoplex size by gradual increase in the concentration of OMR. In general, all NP preparations showed the same tendency; at lower OMR ratios, a considerable increase in the size was noticed which is negligible in case of PLGA NPs (NP-0). Increasing OMR concentration lead to the formation of more compact nanoplexes with a size almost comparable to the plain NPs. Interestingly, at the OMR:NP ratio 1:10, a distinct increase in size and PI of chitosan-modified PLGA NPs were observed revealing certain sort of agglomeration, Figure 3 A&B.

In addition, increasing the oligonucleotide concentration resulted in gradual reduction of the surface charge, Figure 3C, indicating surface binding or loading of the negatively charged OMR on the nanoparticle surface. In the area between the OMR:NP ratio 1:10 and 1:1, the surface charge is crossing the zero point which might explain the agglomerate formation around this area. Equal weight concentration of the OMR and NPs lead to complete saturation of the NP surface with the oligonucleotides and a net negative ζ-potential of -20 mV was recorded for all NP preparations tested.

The morphology of NP-3 as well as their nanoplexes with OMR (OMR:NP ratio 1:50) was examined by the SFM, Figure 4 A&B, respectively. They showed no changes in the surface morphology of the particles and were in the size range found by PCS.

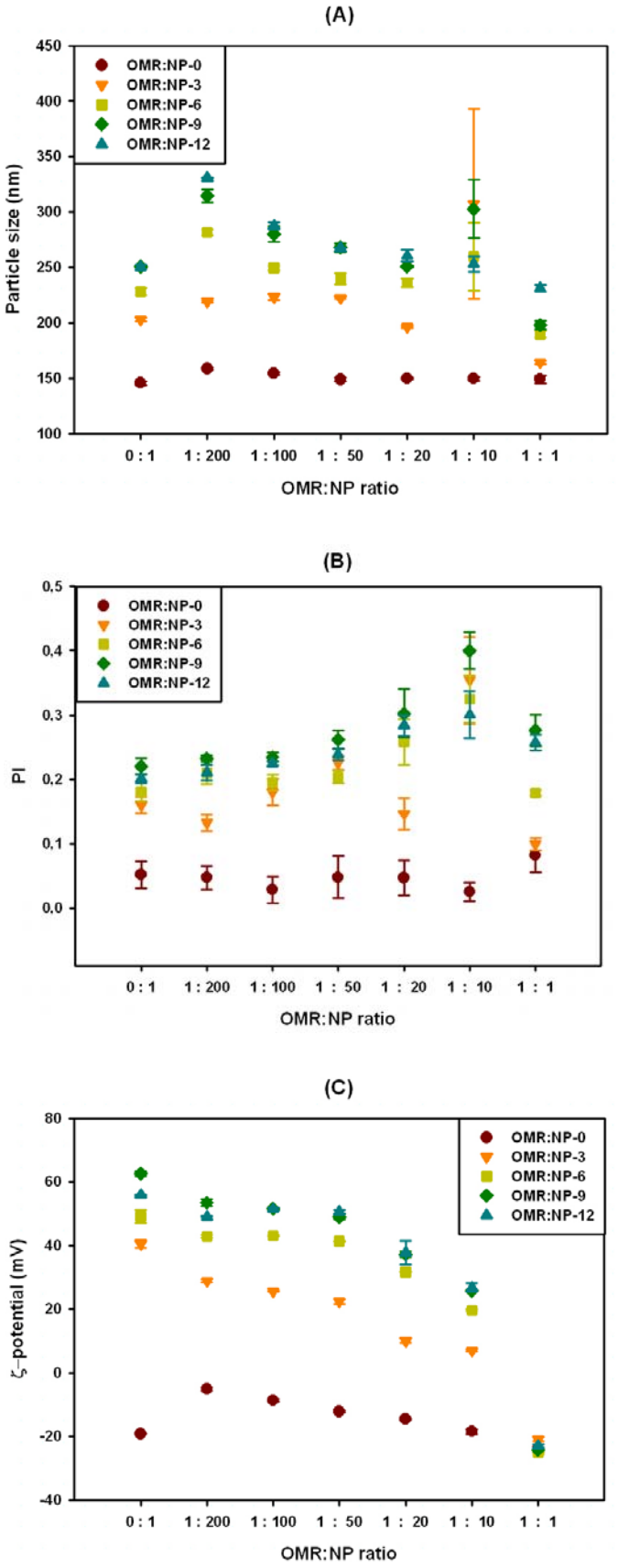

Figure 3: Effect of the OMR concentration on the binding of OMR to cNP (A) particle size, (B) size distribution, and (C) ζ-potential

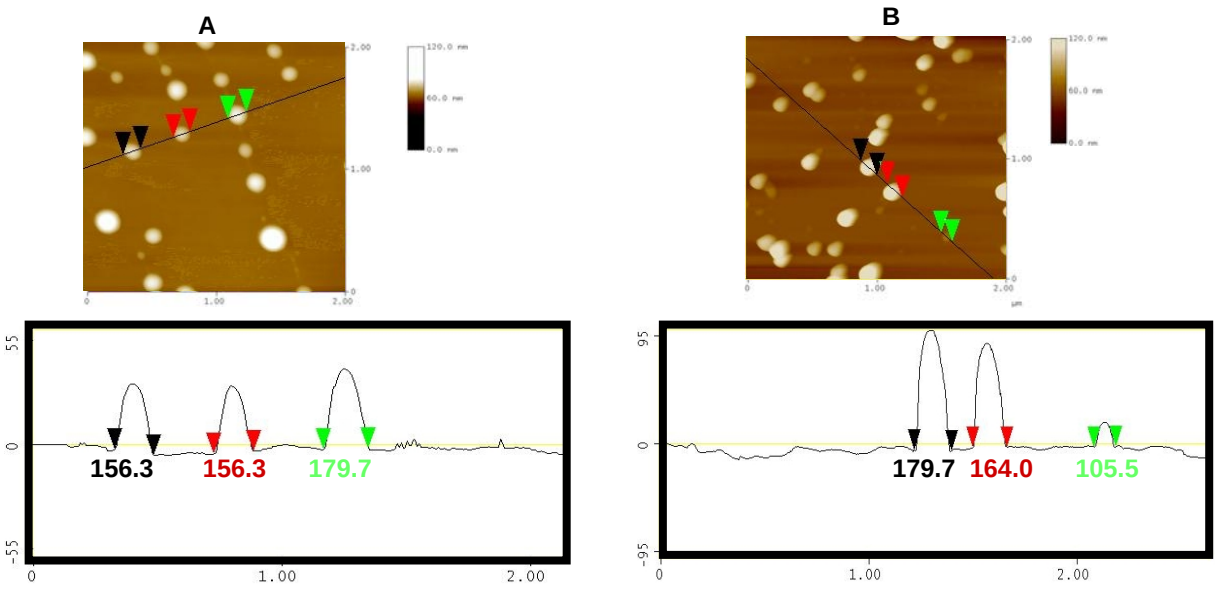

Figure 4: Morphology and section analysis of (A) cNP, (B) cNP/OMR nanoplexes as observed by the SFM

3. Uptake of fluorescently labeled nanoparticles in different cell lines

The ability of the nanoparticles to be taken up intracellularly and in a significant amount is a prerequisite for their use as carrier for nucleotide-based drugs. Besides, the influence of chitosan on the NP surface on their uptake is worth to be investigated. Accordingly, fluorescently labeled NPs (FA-NP-0 - FA-NP-12) were incubated with A549 and Calu-3 cells for 6 h, the uptake was tested next day by CLSM.

Flow cytometry, Figure 5, showed the binding of different fluorescent nanoparticles to A549 cells. A remarkable shift in fluorescence peak was observed in case of FA-NP-3 compared to the control. Interestingly, further increase in the chitosan content on the NP surface was not accompanied by an increase in cell binding, on the contrary, the peaks were shifted backwards to get very weak fluorescence with FA-NP-12.

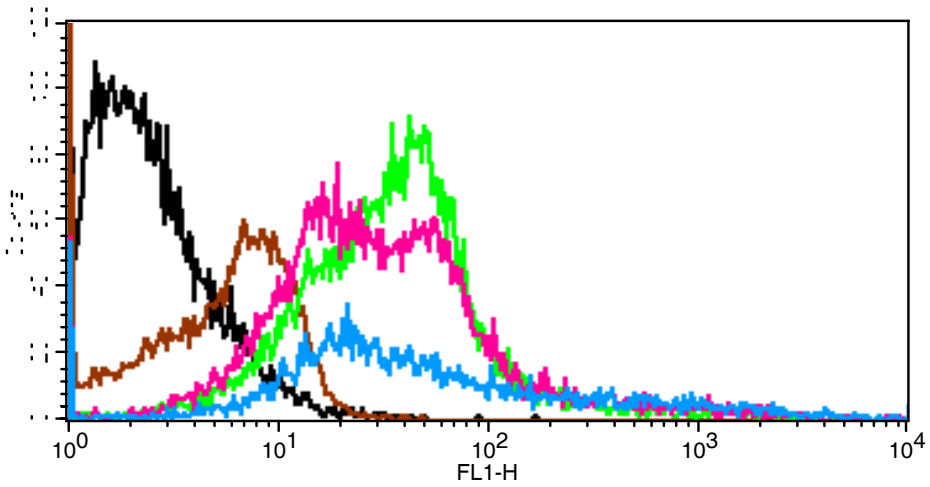

Figure 5: Binding of fluorescently labeled nanoparticles to A549 cells by flow cytometry: control; black, FA-NP-3; green, FA-NP-6; pink, FA-NP-9; cyan, and FA-NP-12; brown

The results of the uptake studies (CLSM) were in accordance with the FACS experiments. Figure 6 demonstrates an overview of the A549 cell monolayer where the membranes were stained with RRCA - an adsorbing red dye bound to a lectin - and the nuclei stained in blue with DAPI. A significant green fluorescence was observed in A549 cells incubated with FA-NP-3 compared to the control (non-treated cells) and those incubated with FA-NP-0. Further increase in chitosan content, FA-NP-6 and FA-NP-9, also showed cellular uptake but relatively lower than FA-NP-3. On the other hand, FA-NP-12 containing highest content of chitosan were very poorly internalized.

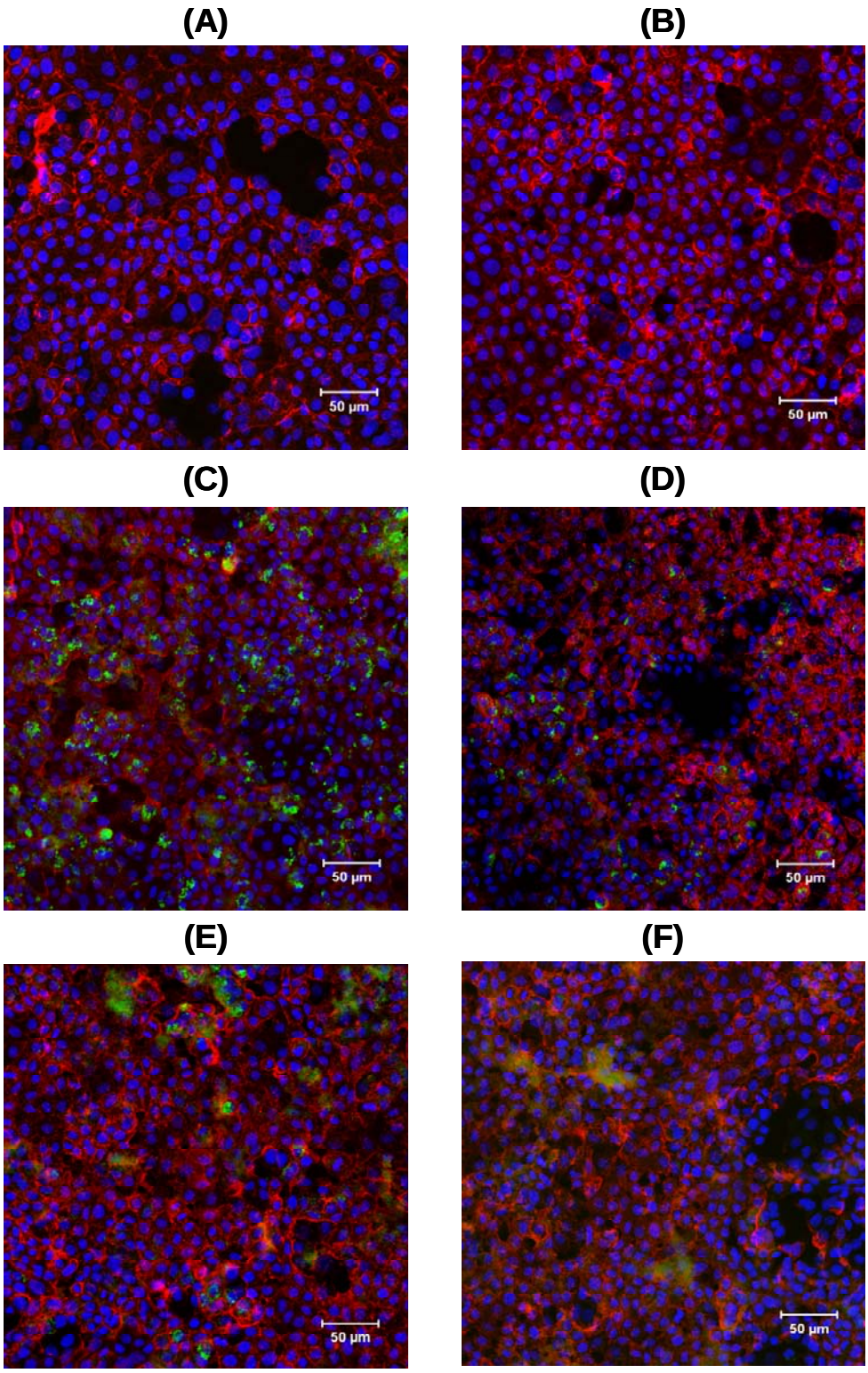

Figure 6: Uptake of fluorescently labeled nanoparticles in A549 cells – An overview: (A) control, (B) FA-NP-0, (C) FA-NP-3, (D) FA-NP-6, (E) FA-NP-9 and (F) FA-NP-12

A better parameter for comparison is to calculate the transfection efficiency of every NP formulation. The number of transfected cells relative to the total number of cells was

used as a measure of the transfection efficiency in different areas (~ 10 areas) of the sample. As a comparative measure, the transfection efficiency was categorized into 4 groups as indicated in the following Table 3.

Table 3: degree of transfection

Transfection efficiency	Symbol
< 20 %	+
20 – 40 %	++
40 – 60 %	+++
> 60 %	++++

While no uptake of fluorescent PLGA NPs was observed, around 50% of the cells were transfected with FA-NP-3, indicating the essential role of surface modification of NP with chitosan in improving the intracellular uptake of the particles. However, the efficiency decreased gradually with higher amounts of chitosan to be < 10 % in case of FA-NP-12.

Table 4: Transfection efficiency of different NP formulations in A549 cells

Nanoparticles	Degree of transfection
FA-NP-0	**0**
FA-NP-3	+++
FA-NP-6	++
FA-NP-9	+
FA-NP-12	+

Internalization of FA-NPs was proved by making sections in the z-direction of the cells. Figure 7 depicts the xy-plane of the cells after incubation with the fluorescent nanoparticles out of a 3-dimensional stack. In addition, cuts along the xz- and the yz-direction are shown. These cross sections allow determining the location of the particles relative to apical cell surface labeled with RRCA and the nuclei labeled with DAPI. On the enlarged and focused xz-section the green fluorescence of all NP preparations can be clearly seen inside the cell, mainly in the cytoplasm and appeared to be point-shaped

indicating that the particles are entrapped in intracellular vesicles. Besides, in case of FA-NP-12, some agglomerates were observed on the cell surface. Agglomeration of NP induced by higher concentration of chitosan might be the reason behind the reduced cellular uptake of the particles.

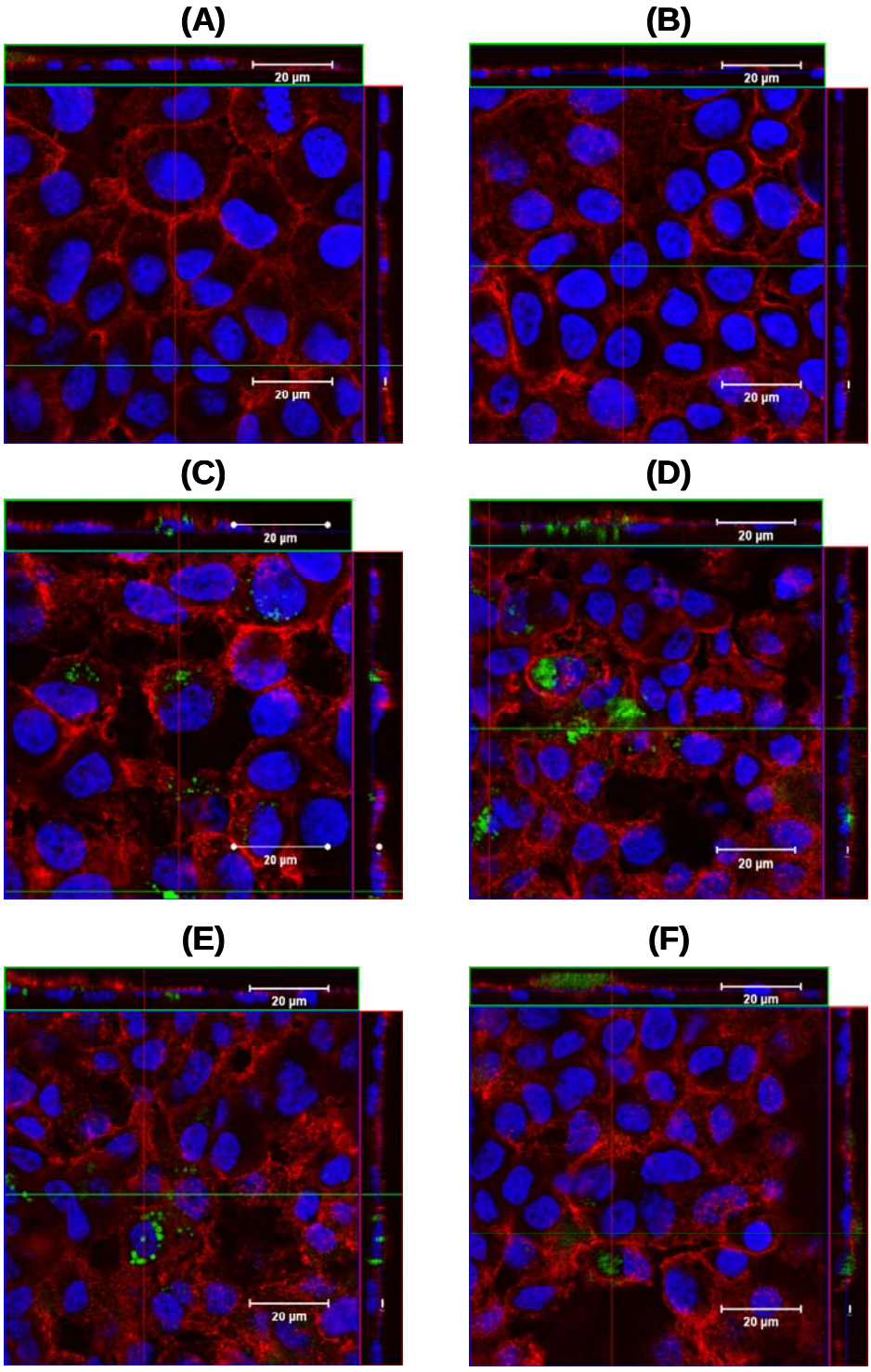

Figure 7: Uptake of fluorescently labeled nanoparticles in A549 cells – Z-sections: (A) control, (B) FA-NP-0, (C) FA-NP-3, (D) FA-NP-6, (E) FA-NP-9 and (F) FA-NP-12

Incubation of FA-NPs with Calu-3 cells resulted in a relatively weak uptake. This was demonstrated by the negligible increase in fluorescence detected by flow cytometry (data not shown), in addition to the very weak intracellular uptake illustrated by the CLSM images. In case of Calu-3 cells the transfection efficiency of all NPs was < 20 %, Figure 8.

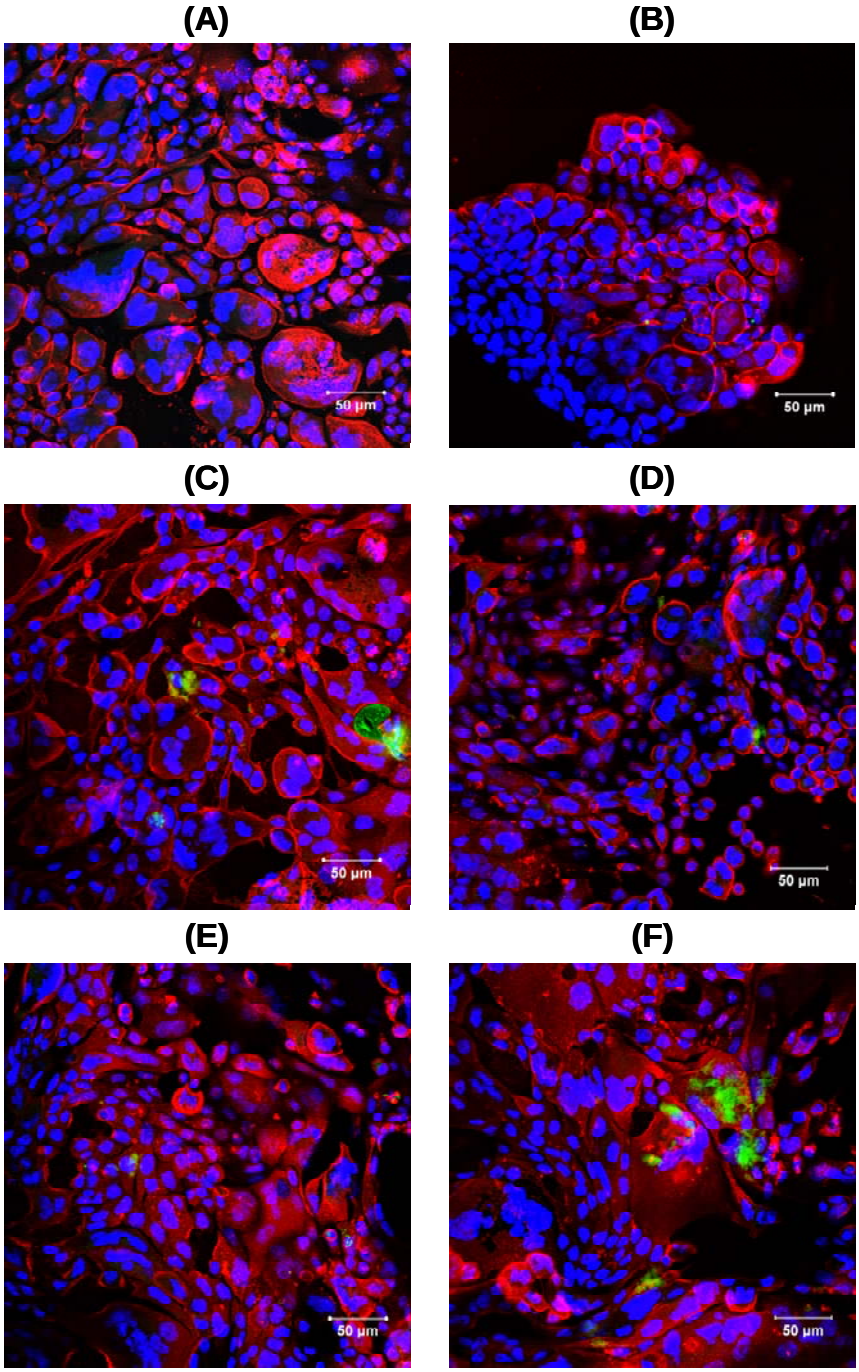

Figure 8: Uptake of fluorescently labeled nanoparticles in Calu-3 cells - An overview: (A) control, (B) FA-NP-0, (C) FA-NP-3, (D) FA-NP-6, (E) FA-NP-9 and (F) FA-NP-12

Besides, no distinct effect of the chitosan content on the uptake was observed. Calu-3 cells are known by their slow rate of division and growth compared to A549 cells; this might explain their relative weak transfection efficiency. A higher level of transfection would be expected if cells were allowed to grow for longer duration. On the other hand, transfected A549 cells replicate very fast and the number of transfected cells can be significantly increased during the 24 h prior to fixation.

Despite the low level of transfection, transfected particles appear as spots in the cytoplasm, while no particles were observed in the cores, as observed in the Z-sections of the cells, Figure 9 and the zoomed cells, Figure 10.

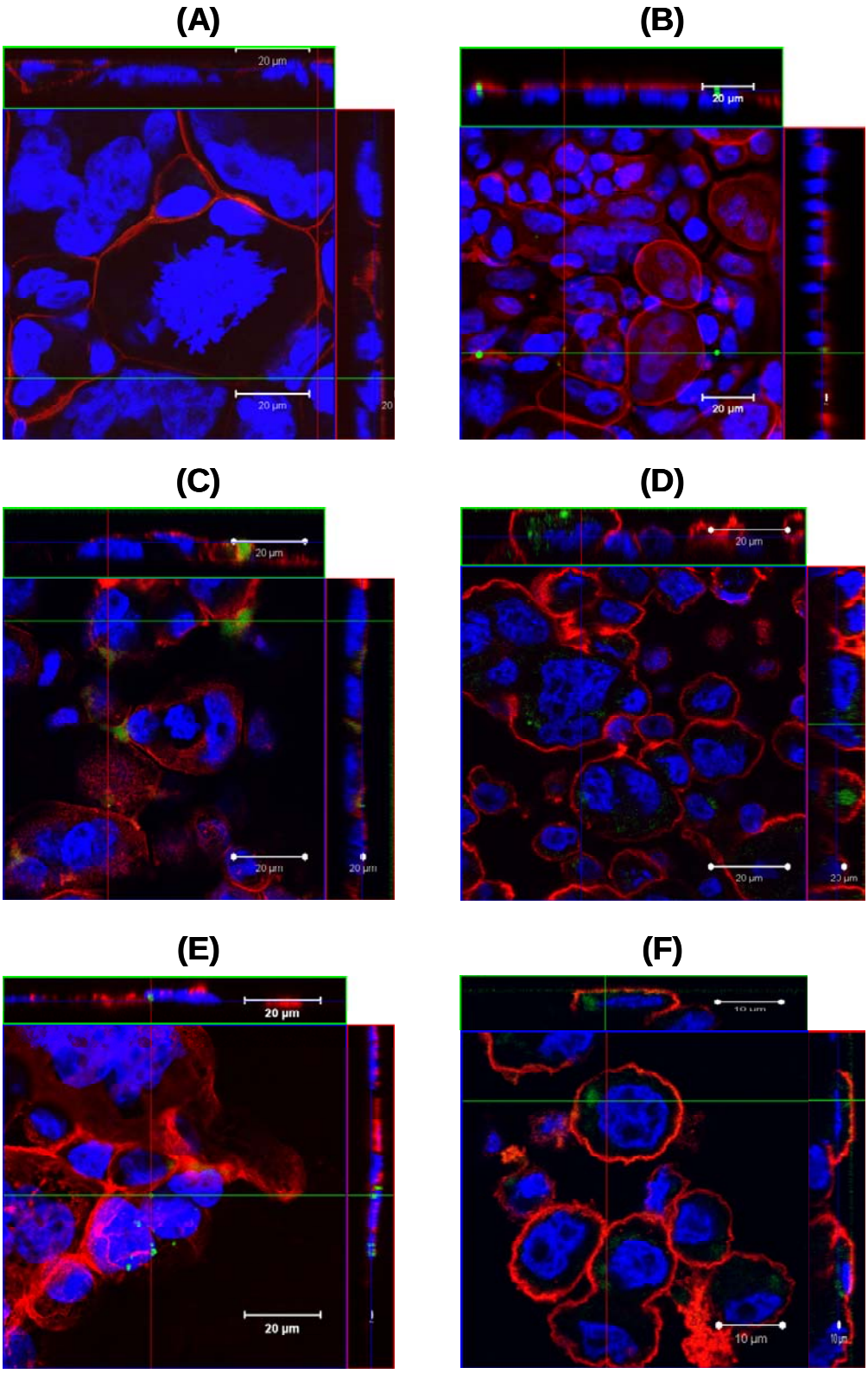

Figure 9: **Uptake of fluorescently labeled nanoparticles in Calu-3 cells-Z-sections: (A) control, (B) FA-NP-0, (C) FA-NP-3, (D) FA-NP-6, (E) FA-NP-9 and (F) FA-NP-12**

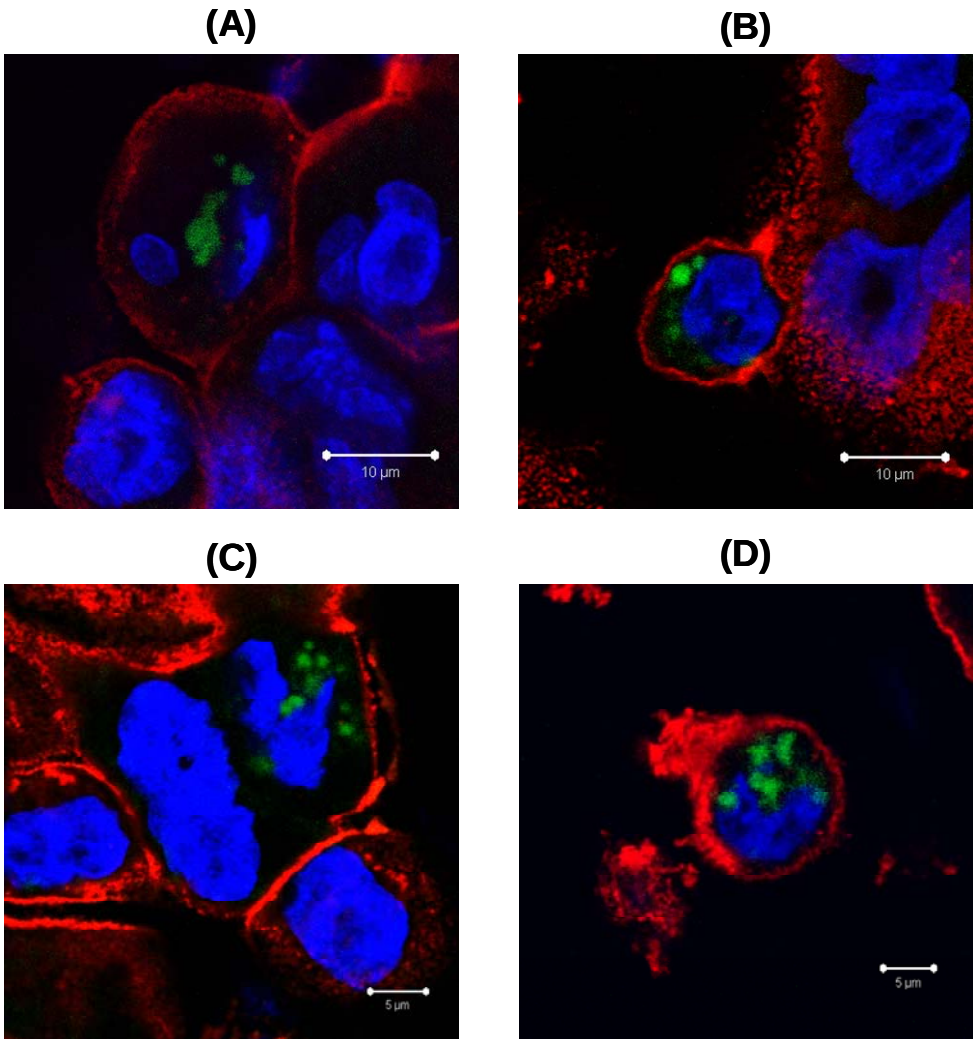

Figure 10: Colocalization study of fluorescently labeled nanoparticles in Calu-3 cells: (A) FA-NP-3, (B) FA-NP-6, (C) FA-NP-9, and (D) FA-NP-12

4. Binding and uptake of nanoplexes

Our main goal was essentially the application of chitosan-modified PLGA nanoparticles as carrier to enhance the intracellular uptake of the antisense oligonucleotides. Therefore, after improving the preparation of nanoparticles and the formation of nanoplexes, it is quite important to check the efficacy of these nanoplexes to be taken up by the cells as good as the plain FA-NPs. For this purpose, the intracellular uptake of OMR nanoplexes in A549 cells was studied as previously described by CLSM.

A549 cells were selected to continue our uptake studies as Calu-3 cells showed weak/slow uptake of FA-NPs in general.

FAM-OMR nanoplexes with non-labeled NP formulations (NP-0 – NP-12) were prepared in the OMR:NP weight ratio 1:50 and incubated with the cells for 6 h. Figure 11 represents an overview of the uptake of the nanoplexes 24 h after incubation with A549 cells. OMR/NP-0 nanoplexes were poorly taken up, Figure 11B, whereas OMR/NP-3 were efficiently internalized as noticed by the huge amount of fluorescent spots in the cells, Figure 11C. In correlation with uptake results of FA-NPs, the uptake of OMR nanoplexes with NP-6 – NP-12 was lower compared to OMR/NP-3 nanoplexes indicating that increasing chitosan content in the nanoparticles above certain limit is not correlated with a consequent improvement in cellular uptake. As shown in Figure 11F, agglomerates of OMR/NP-12 nanoplexes on the cell surface can be observed, which might explain their poor internalization as in case of FA-NP-12.

For the different OMR/NP nanoplexes tested, the transfection efficiency was maximum for NP-3 (~ 75 %), followed by NP-6 & NP-9 (30 – 40 %), and then NP-0 & NP-12 (< 10 %), Table 5.

Table 5: Tranfection efficiency of OMR/NP nanoplexes in A549 cells

Nanoplexes	Degree of transfection
OMR/NP-0	+
OMR/NP-3	++++
OMR/NP-6	++
OMR/NP-9	++
OMR/NP-12	+

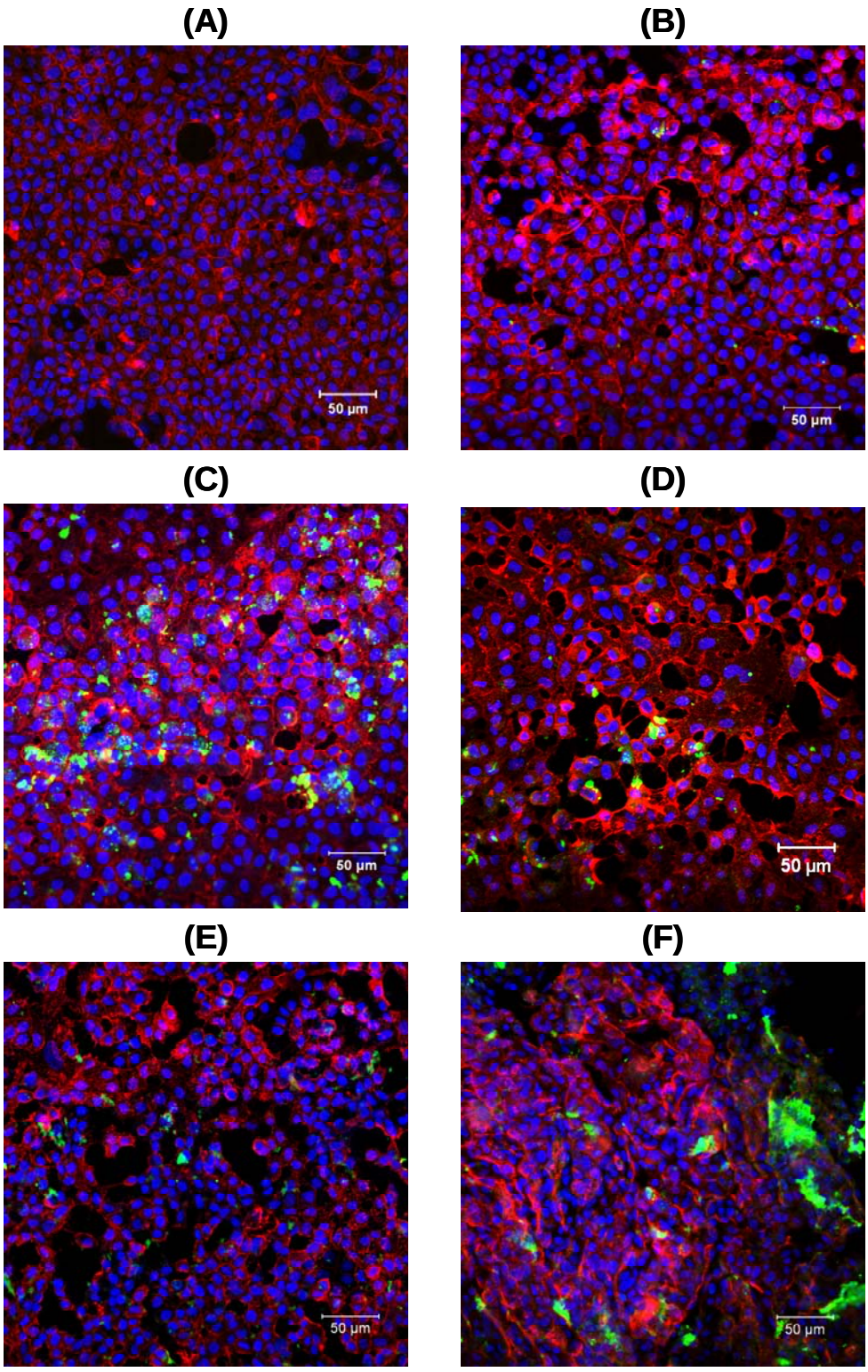

Figure 11: Uptake of OMR nanoplexes with different nanoparticles in A549 cells - An overview: (A) control, (B) OMR/NP-0, (C) OMR/NP-3, (D) OMR/NP-6, (E) OMR/NP-9 and (F) OMR/NP-12

Independent of the magnitude, OMR nanoplexes with all nanoparticle formulations were successfully internalized in A549 cells and localized in the cytoplasm as clearly illustrated in the z-stacks, Figure 12. This hence proves the potential of our nanoparticles as carrier for OMR oligonucleotides.

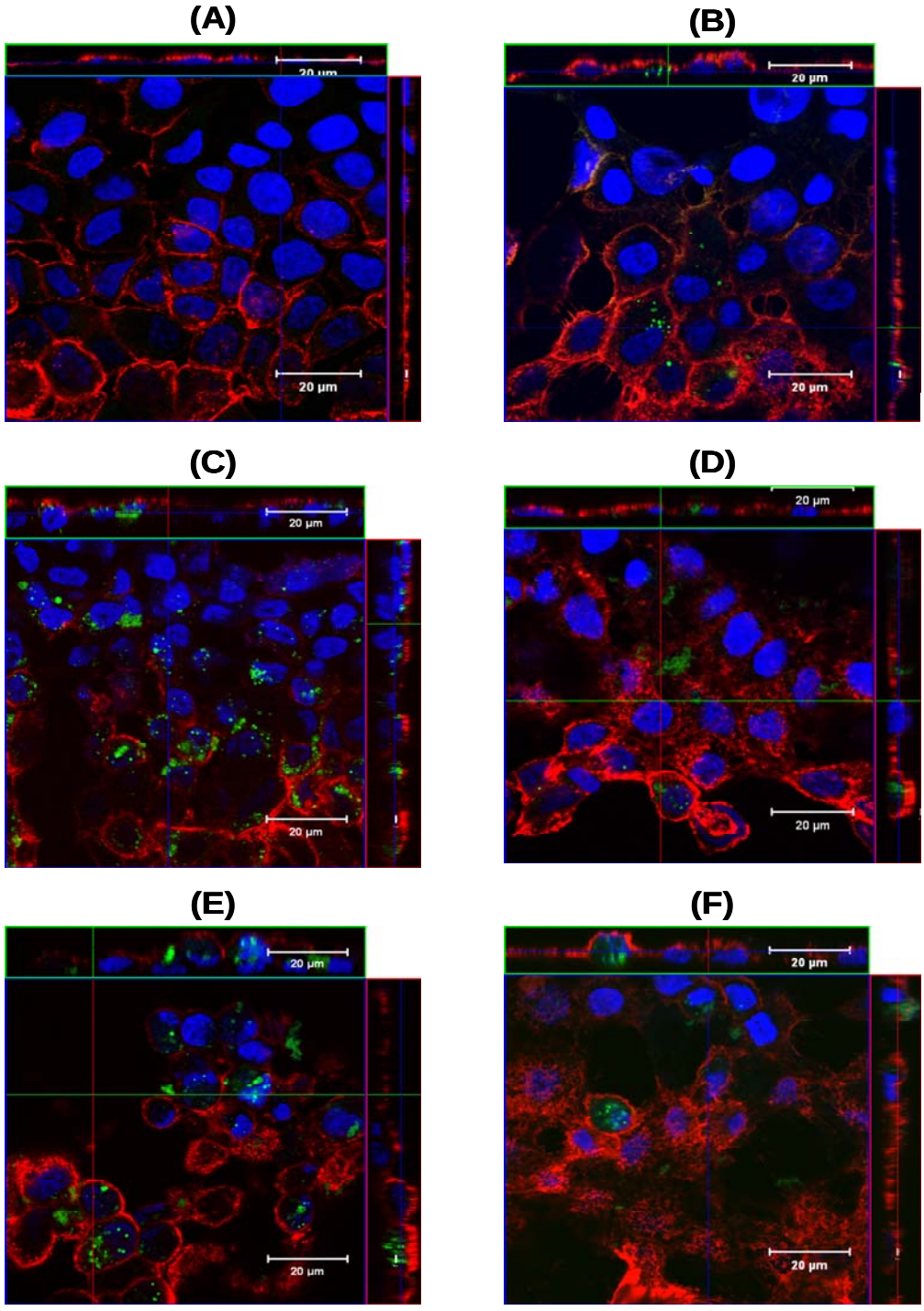

Figure 12: Uptake of FAM-OMR nanoplexes with different nanoparticles in A549 cells-Z-sections: (A) control, (B) OMR/NP-0, (C) OMR/NP-3, (D) OMR/NP-6, (E) OMR/NP-9 and (F) OMR/NP-12

5. Self-assembled nanoplexes of OMR with chitosan solution

Owing to the significant improvement in intracellular uptake due to surface modification of nanoparticles using chitosan, it was necessary to investigate the potential of chitosan solution alone as carrier for OMR and the impact of chitosan properties on this uptake. Self assembled complexes of FAM-OMR with chitosan were prepared by simple mixing of the solutions and charge interaction. Four types of chitosan salts (refer to Table 1) with different viscosities and/or molecular weights were applied. FACS analysis revealed the association of OMR nanoplexes with chitosan solution to A549 cells, Figure 13. The dot plots showed a noticeable shift in fluorescence to the upper right quadrant by 60-63% for the different chitosan types.

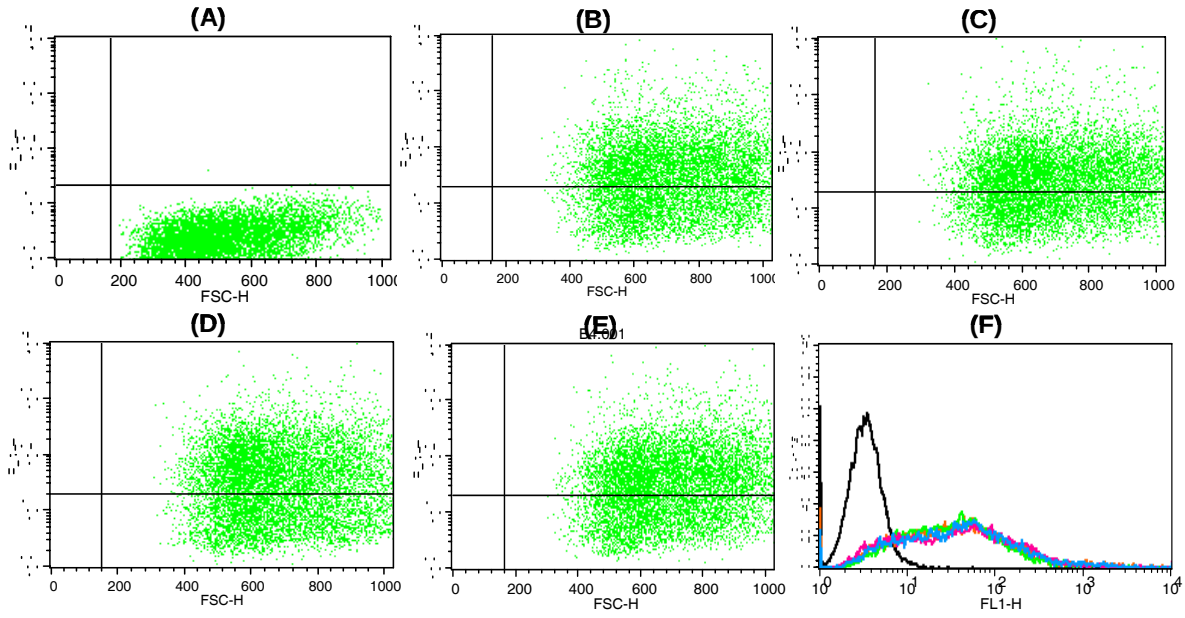

Figure 13: Binding of OMR/chitosan nanoplexes to A549 cells by flow cytometry; (A) control: non-treated cells, (B) cells treated with OMR/CL113, (C) cells treated with OMR/CL213, (D) cells treated with OMR/CG113, (E) cells treated with OMR/CG213, (F) histogram showing fluorescence peaks of FAM-OMR nanoplexes with different chitosan solutions compared to the control

The uptake of these nanoplexes in A549 cells was visualized by CLSM, Figure 14. The images showed significant amount of fluorescent nanoplexes agglomerated as patches on the outer surface of the cell membrane as indicated by the overlap of the green labeled

nanoplexes and red fluorescence of the membrane giving bright yellow areas, indicating strong interaction with the cell membrane. The internalization of these self-assembled nanoplexes was thus prohibited by the preferential interaction between chitosan and the cell membrane.

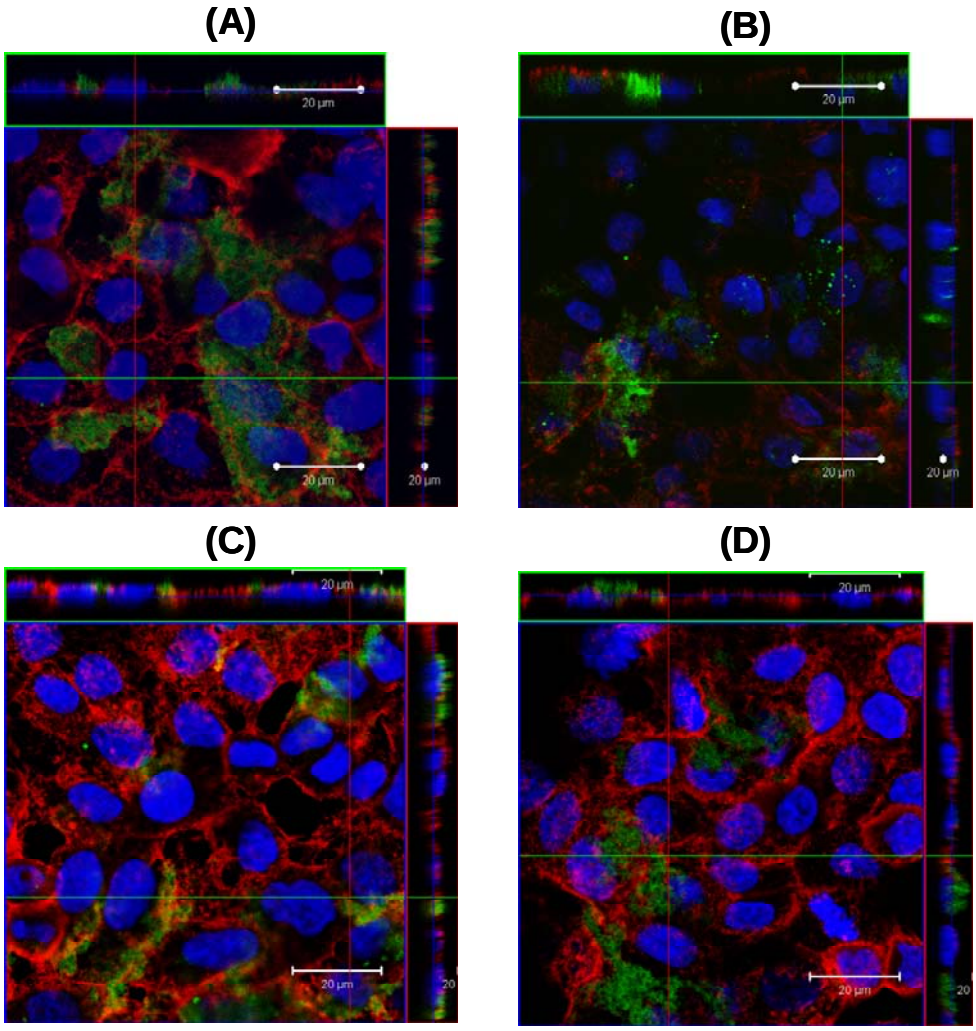

Figure 14: Uptake of FAM-OMR complexes with chitosan solutions of different types: (A) CL113, (B) CL213, (C) CG113, (D) CG213, in A549 cells

6. Effect of OMR:NP ratio on the uptake of nanoplexes

Based on the previous observation, nanoplexes of the FAM labeled oligonucleotides with NP-3 were prepared in two OMR:NP ratio (1:50 and 1:100). Their binding was found to increase by increasing the OMR:NP ratio, Figure 15.

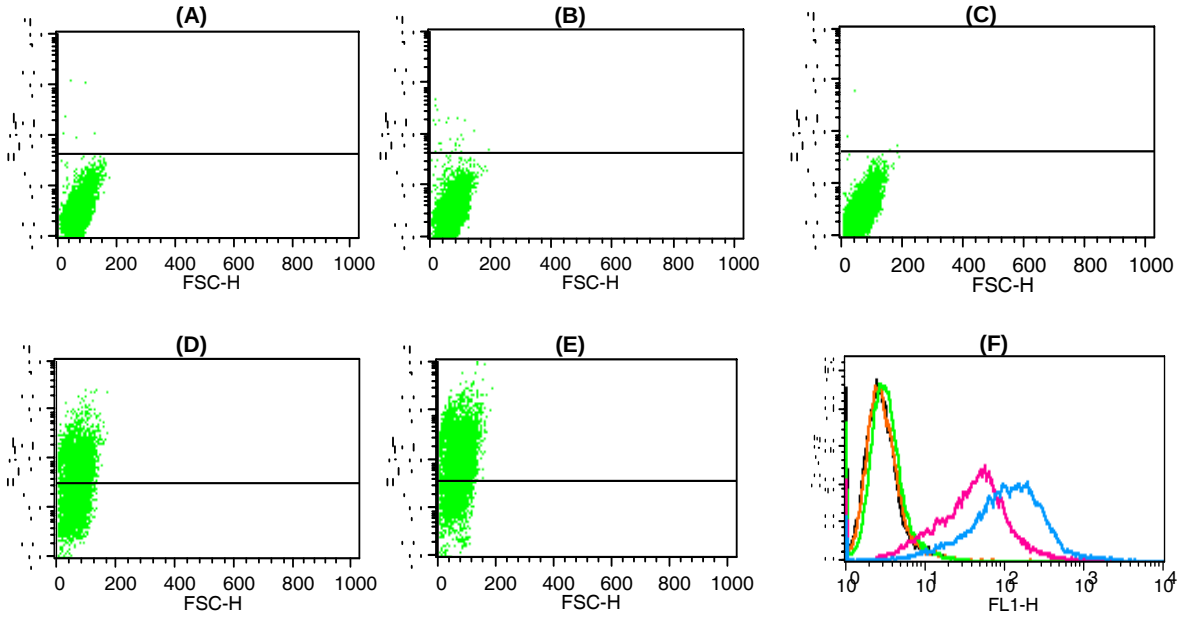

Figure 15: Binding of FAM-OMR to cNP in 2 ratios to A549 cells by flow cytometry: (A) control: non treated cells, (B) control: cells treated with OMR solution, (C) control: cells treated with NP-3, (D) OMR : NP (1:50), (E) OMR : NP (1:100), (F) fluorescence histogram of controls A-C; black, red, green, OMR : NP (1:50); pink, OMR : NP (1:100); blue

In order to investigate the impact of the surface charge of nanoplexes on the transfection efficiency, nanoplexes of FAM-OMR with NP-6, NP-9 & NP-12 were further prepared in the OMR:NP weight ratio 1:15. At this ratio the overall ζ-potential was estimated to be approximately similar to that of OMR/NP-3 nanoplexes (ratio 1:50, described by maximum cellular uptake). Uptake studies in A549 cells were carried out as previously described and the transfection efficiency was determined, Table 6. Reducing the surface charge resulted in a considerable increase in the transfection efficiency in case of OMR/NP-9 and -12 nanoplexes, which was not observed in OMR/NP-6 nanoplexes. However, in general, none of these nanoplexes reached the transfection efficiency of

OMR/NP-3 (1:50), indicating that the surface charge cannot be considered the only parameter controlling the cellular uptake.

Table 6: Transfection efficiency of OMR/NPs in different OMR:NP ratios:

Nanoplexes	OMR:NP 1:50	OMR:NP 1:15
OMR/NP-6	++	++
OMR/NP-9	++	+++
OMR/NP-12	+	++

Discussion

Our study revealed that chitosan-modified PLGA nanoparticles can be prepared in a tunable way allowing flexible surface charge modification. Measurement of the colloidal characteristics gives evidence of the adsorption of OMR molecules on the nanoparticle surface in a saturable way till charge reversal occur at equal OMR:NP weight ratios.

Our main goal is to use these particles as carrier for nucleotide based drugs and deliver them intracellularly for the treatment of lung cancer. Therefore, trafficking the uptake of the nanoparticles in pulmonary cell lines is an essential concern. In addition, the impact of the colloidal characteristics namely the surface charge on the binding and uptake of these particles as well as their corresponding nanoplexes with the antisense oligonucleotides in A549 cells was studied. The use of fluorescently labeled PLGA polymer was favorable over including a certain fluorescent dye in the nanoparticles by simple encapsulation. Fixing the fluorescinamine to the polymer by a covalent linkage was expected to guarantee more stable fluorescent nanoparticles and minimize the leakage of the fluorescent dye along the uptake studies. Detailed investigations concerning the fluorescently labeled PLGA nanoparticles were previously fully described [18].

The surface modification of PLGA nanoparticles with chitosan did not only improve the binding potential with OMR but also greatly enhance the uptake of nanoplexes as revealed by the significant increase in transfection efficiency from < 10% to ~70 % for OMR/NP-0 and OMR/NP-3 nanoplexes, respectively. Epithelial cells usually exhibit net negative surface charge due to the presence of negatively charged extracellular plasma membrane protein moieties [19]. This may account in part for the higher translocation rates of positively charged nanoparticles, NP-3, as compared with negatively charged particles, NP-0, in our study. The relevance of the surface charge of different types of particles on their cellular uptake was previously studied; nevertheless, these data were still missing for chitosan-modified PLGA nanoparticles. Lorenz et al. studied the uptake of polystyrene particles characterized by increasing densities of amino groups on the surface in different cell lines [20]. The results revealed improved uptake in Hela cells (as an adherent cell line), Jukat cells (as a model of T cells) and KG1a cells (as a model of CD34+ hematopoetic stem cells) by increasing the density of amino groups, whereas no correlation was found in case of mesenchymal stem cells. The superior uptake of positively charged nanoparticles over negatively charged ones was demonstrated by many authors for other types of particles. Recently, trafficking of polystyrene nanoparticles (PNP; 20 and 100 nm; carboxylate, sulfate, or aldehyde-sulfate modified [negatively charged] and amidine-modified [positively charged]) across rat alveolar epithelial cell monolayers was investigated. In case of positively charged PNPs, trafficking was 20–40 times faster than highly negatively charged PNP of comparable size [21]. Similarly, des Rieux et al. [22] reported that cationic (amine coating) polystyrene particles translocate across intestinal epithelial cell monolayers significantly faster than anionic (carboxylate coating) polystyrene particles. In another study, Geiser et al [23] demonstrated the uptake of polystyrene particles (78, 200, and 1000 nm; uncharged, amine-modified, or carboxylate-

modified) by porcine lung macrophages, but uptake rates of differently charged particles were not determined.

Investigating the influence of chitosan content on the NP surface on the cellular uptake, a linear relationship was expected, however, it has been observed that there is an optimum chitosan concentration required for maximum transfection efficiency in A549 cells. Interestingly, the uptake behavior of the nanoplexes prepared with the different NP formulations was in accordance with the uptake of fluorescently labeled plain nanoparticles. Further increase in chitosan content might negatively affect the uptake either due to preferential adsorption to the cellular membrane or due to increased agglomeration of the nanoparticles as shown in the confocal images. The latter could be attributed to increased interaction of the positively charged NPs with serum proteins, divalent ions and the mulicomponents in the culture medium, which becomes more obvious in case of highly positive NPs. Nanoparticle surface interaction with serum proteins was investigated by many authors [24]. Chithrani et al. [25] in a study with gold nanoparticles (14, 50, and 75 nm), showed that uptake into HeLa cells reaches a plateau, mediated in part by nonspecific adsorption of serum proteins to particles. Besides, the finding that no steady increase in uptake of particles with higher surface charge suggests that this uptake should not only be attributed to surface charge but also to other surface properties; [22] suggested that the enhanced uptake of amine-coated polystyrene particles over carboxylate-coated would be referred to the increased hydrophobicity of the former, assuming that hydrophobicity might lead to different binding and uptake mechanisms. From our part to further investigate the role of charge, we assumed that the net surface charge (20 - 30 mV) is the one giving maximum uptake. Therefore, OMR/NP nanoplexes were prepared using nanoparticles of higher surface charges (NP-6, NP-9, and NP-12) but with lower OMR:NP ratio (1:15) instead of (1:50) in case of NP-3. The uptake behavior of these nanoplexes was studied in A549 cells. Although the uptake was relatively improved the transfection efficiency with

these nanoplexes did not reach the value of OMR/NP-3 (1:50) even at the same level of surface charge. This further reinforces the evidence that although charge plays an important role it cannot be the only parameter managing the cellular uptake.

Colocalization studies revealed that the nanoparticles were localized mainly in the cytoplasm, while the nuclei were devoid of nanoparticles. Similar behavior was previously reported for polystyrene nanoparticles in rat alveolar epithelial cells [21] and gold nanoparticles in Hela cells [25] and alveolar macrophages [26]. However, mechanisms by which nanoparticles interact with the lung alveolar epithelium and their cellular fate once internalized, are currently not well understood and require further investigation.

Coming to the question, if chitosan plays this important role in uptake when added to the NP surface, why not to use simply chitosan solution to deliver OMR as was always the case in many previous researches [27-29]. Despite the ability of chitosan polymer to easily create self-assembled complexes with the negatively charged oligonucleotides, we have found out that these nanoplexes were mostly retained associated with cellular membrane and not internalized as revealed by the FACS analysis and CLSM images. This proves the superior efficacy of chitosan-modified PLGA NP over both plain PLGA NPs and chitosan solution as carrier for nucleotide based drugs.

No clear impact of the chitosan properties on the uptake was observed. Similarly, Huang et al. showed that the uptake of chitosan molecules was independent of the molecular weight and degree of deacetylation [30].

The superior behavior of NP-3 in term of uptake leads us to select this formulation for our future investigations such as cytotoxicity and nebulization studies.

Conclusions

In this chapter, the potential of chitosan-modified PLGA nanoparticles to form nanoplexes with the antisense oligonucleotides, 2'-O-Methyl-RNA, and deliver them to

A549 cells was demonstrated. Surface modification of the nanoparticles with chitosan significantly improves the transfection of nanoplexes in the cells. However, increasing chitosan concentration doesn't lead to a corresponding improvement in uptake. This delivery system can be suggested as promising carrier for antisense oligonucleotides.

REFERENCES

[1] L.P. Brewster, E.M. Brey, H.P. Greisler, Cardiovascular gene delivery: The good road is awaiting. Advanced Drug Delivery Reviews
Gene Delivery for Tissue Engineering 58(4) (2006) 604-629.

[2] M.D. Kofron, C.T. Laurencin, Bone tissue engineering by gene delivery. Advanced Drug Delivery Reviews
Gene Delivery for Tissue Engineering 58(4) (2006) 555-576.

[3] Y. Qian, R.B. Mugiira, X. Zhou, A modified viral satellite DNA-based gene silencing vector is effective in association with heterologous begomoviruses. Virus Research 118(1-2) (2006) 136-142.

[4] L. Sen, S.S. Gambhir, H. Furukawa, D.B. Stout, A. Linh Lam, H. Laks, G. Cui, Noninvasive Imaging of ex Vivo Intracoronarily Delivered Nonviral Therapeutic Transgene Expression in Heart. Molecular Therapy 12(1) (2005) 49-57.

[5] S. Hama, H. Akita, R. Ito, H. Mizuguchi, T. Hayakawa, H. Harashima, Quantitative Comparison of Intracellular Trafficking and Nuclear Transcription between Adenoviral and Lipoplex Systems. Molecular Therapy 13(4) (2006) 786-794.

[6] M.J. Lim, S.-H. Min, J.-J. Lee, I.C. Kim, J.T. Kim, D.C. Lee, N.-S. Kim, S. Jeong, M.N. Kim, K.D. Kim, Targeted Therapy of DNA Tumor Virus-Associated Cancers Using Virus-Activated Transcription Factors. Molecular Therapy 13(5) (2006) 899-909.

[7] S. Li, L. Huang, Nonviral gene therapy: Promises and challenges. Gene Therapy 7(1) (2000) 31-34.

[8] C. Zhang, N. Tang, X. Liu, W. Liang, W. Xu, V.P. Torchilin, siRNA-containing liposomes modified with polyarginine effectively silence the targeted gene. Journal of Controlled Release 112(2) (2006) 229-239.

[9] T. Ishida, M. Harada, X.Y. Wang, M. Ichihara, K. Irimura, H. Kiwada, Accelerated blood clearance of PEGylated liposomes following preceding liposome injection: Effects of lipid dose and PEG surface-density and chain length of the first-dose liposomes. Journal of Controlled Release 105(3) (2005) 305-317.

[10] T.H. Kim, S.I. Kim, T. Akaike, C.S. Cho, Synergistic effect of poly(ethylenimine) on the transfection efficiency of galactosylated chitosan/DNA complexes. Journal of Controlled Release 105(3) (2005) 354-366.

[11] M.R. Park, K.O. Han, I.K. Han, M.H. Cho, J.W. Nah, Y.J. Choi, C.S. Cho, Degradable polyethylenimine-alt-poly(ethylene glycol) copolymers as novel gene carriers. Journal of Controlled Release 105(3) (2005) 367-380.

[12] M. Köping-Höggard, K.M. Varum, M. Issa, S. Danielsen, B.E. Christensen, B.T. Stokke, P. Artursson, Improved chitosan-mediated gene delivery based on easily dissociated chitosan polyplexes of highly defined chitosan oligomers. Gene Therapy 11(19) (2004) 1441-1452.

[13] A. Elouahabi, J.M. Ruysschaert, Formation and intracellular trafficking of lipoplexes and polyplexes. Molecular Therapy 11(3) (2005) 336-347.

[14] G.B. Morin, The human telomere terminal transferase enzyme is a ribonucleoprotein that synthesizes TTAGGG repeats. Cell 59(3) (1989) 521-529.

[15] N.W. Kim, M.A. Piatyszek, K.R. Prowse, C.B. Harley, M.D. West, P.L.C. Ho, G.M. Coviello, W.E. Wright, S.L. Weinrich, J.W. Shay, Science 266 (1994) 2011-2015.

[16] A.E. Pitts, D.R. Corey, Inhibition of human telomerase by 2'-O-methyl-RNA 10.1073/pnas.95.20.11549. Proc. Natl. Acad. Sci. USA 95(20) (1998) 11549-11554.

[17] E. Horisawa, K. Kubota, I. Tuboi, K. Sato, H. Yamamoto, H. Takeuchi, Y. Kawashima, Size-dependency of DL-Lactide/Glycolide copolymer particulates for intra-articular delivery system on phagocytosis in rat synovium. Pharm. Res. 19 (2002) 132-139.

[18] B. Weiss, U.F. Schaefer, J. Zapp, A. Lamprecht, A. Stallmach, C.-M. Lehr, Nanoparticles made of fluorescently-labelled poly(L-lactide-co-glycolide): preparation, stability and biocompatibility. Journal of Nanoscience and Nanotechnology 6 (2006) 3048-3056.

[19] Y. Rojanasakul, L. Wang, M. Bhat, D. Glover, C. Malanga, J. Ma, The transport barrier of epithelia: a comparative study on membrane permeability and charge selectivity in the rabbit. Pharm. Res. 9 (1992) 1029-1034.

[20] M.R. Lorenz, V. Holzapfel, A. Musyanovych, K. Nothelfer, P. Walther, H. Frank, K. Landfester, H. Schrezenmeier, V. Mailänder, Uptake of functionalized, fluorescent-labeled polymeric particles in different cell lines and stem cells. Biomaterials 27(14) (2006) 2820-2828.

[21] N.R. Yacobi, L. DeMaio, J. Xie, S.F. Hamm-Alvarez, Z. Borok, K.-J. Kim, E.D. Crandall, Polystyrene nanoparticle trafficking across alveolar epithelium. Nanomedicine: Nanotechnology, Biology and Medicine 4(2) (2008) 139-145.

[22] A. des Rieux, E.G.E. Ragnarsson, E. Gullberg, V. Préat, Y.-J. Schneider, P. Artursson, Transport of nanoparticles across an in vitro model of the human intestinal follicle associated epithelium. European Journal of Pharmaceutical Sciences 25(4-5) (2005) 455-465.

[23] M. Geiser, B. Rothen-Rutishauser, N. Kapp, S. Schürch, W. Kreyling, H. Schulz, M. Semmler, V. Im Hof, J. Heyder, P. Gehr, Ultrafine particles cross cellular membranes by nonphagocytic mechanisms in lungs and in cultured cells. Environmental Health Perspectives 113 (2005) 1555-1560.

[24] C. Schulze, A. Kroll, C.-M. Lehr, U.F. SchÃ¤fer, K. Becker, J.r. Schnekenburger, C. Schulze Isfort, R. Landsiedel, W. Wohlleben, Not ready to use - overcoming pitfalls when dispersing nanoparticles in physiological media. Nanotoxicology 2(2) (2008) 51-61.

[25] B.D. Chithrani, A.A. Ghazani, W.C.W. Chan, Determining the Size and Shape Dependence of Gold Nanoparticle Uptake into Mammalian Cells. Nano Letters 6(4) (2006) 662-668.

[26] S. Takenaka, E. Karg, W.G. Kreyling, B. Lentner, W. Mueller, M. Behnke-Semmler, L. Jennen, A. Walch, B. Michalke, P. Schramel, J. Heyder, H. Schulz, Distribution Pattern of Inhaled Ultrafine Gold Particles in the Rat Lung. Inhalation Toxicology 18(10) (2006) 733-740.

[27] M.M. Issa, M. Koping-Hoggard, P. Artursson, Chitosan and the mucosal delivery of biotechnology drugs. Drug Discovery Today: Technologies 2(1) (2005) 1-6.

[28] M. Thanou, B.I. Florea, M. Geldof, H.E. Junginger, G. Borchard, Quaternized chitosan oligomers as novel gene delivery vectors in epithelial cell lines. Biomaterials 23(1) (2002) 153-159.

[29] S. Mansouri, P. Lavigne, K. Corsi, M. Benderdour, E. Beaumont, J.C. Fernandes, Chitosan-DNA nanoparticles as non-viral vectors in gene therapy: strategies to improve transfection efficacy. European Journal of Pharmaceutics and Biopharmaceutics 57(1) (2004) 1-8.

[30] M. Huang, E. Khor, L.-Y. Lim, Uptake and cytotoxicity of chitosan molecules and nanoparticles: effects of molecular weight and degree of deacetylation. Pharm. Res. 21(2) (2004) 344-353.

Chapter 5

Cytotoxicity of chitosan-modified PLGA nanoparticles

Relevance of the colloidal stability on the toxicity results*

***This chapter has been submitted for publication as a journal article:**

N. Nafee, M. Schneider, U.F. Schäfer, and C.-M. Lehr. Relevance of the colloidal stability of chitosan-modified PLGA nanoparticles on their cytotoxicity profile. *International Journal of Pharmaceutics*. (submitted article)

Abstract

Purpose: The application of nanoparticles for cellular delivery of nucleotide-based drugs necessitates an in depth study of their biocompatibility. However, complete characterization of the particles under the physiological conditions relevant for toxicity studies is still lacking. Our goal is therefore to evaluate the possible toxicity aspects of chitosan-modified PLGA nanoparticles on different cell lines and relate them to the parameters involved in colloidal stability of the nanoparticles.

Methods: The impact of different factors such as nanoparticle concentration, exposure time, chitosan content in the particles and pH fluctuations on the viability of different cell lines - COS-1, A549 and Calu-3 cells - were investigated. Meanwhile, the colloidal stability of the particles in cell culture media was checked by measuring their size and charge as well as visualizing the particles by scanning force microscopy (SFM).

Results: Cytotoxicity of chitosan-modified PLGA nanoparticles is a function of the cell line. Nevertheless, the toxicity is suggested to be underestimated due to the colloidal instability in culture media, reduction in effective nanoparticle concentration on the nanosize range, in addition to adsorption of medium components to the nanoparticle surface. Slight shift of the surrounding pH allows ionization of chitosan and increase in surface charge of the nanoparticles, which as a consequence lead to more pronounced loss of membrane integrity of the cells.

Conclusions: In this chapter, we highlight the key factors predetermining the toxicity of nanoparticles as a function of their colloidal state during the assay procedures and their possible interaction with the culture media.

Background

In the last decade, an increasing number of investigations concerning the use of nanoscale structures for drug and gene delivery purposes have been observed [1, 2]. Despite the significant scientific interests and promising potential of nanomedicines in numerous applications, the safety aspects of nanoparticulate systems remain a growing concern and a good local and systemic tolerance need to be ensured. Especially in the field of nanomedicine where the surface area-to-volume ratio significantly increases, the toxicity could differ from a similar bulk material [3]. On the other hand, the large-scale production of nanoparticles even for non-medical purposes or as side products for combustion can lead to numerous negative effects on the environment. Hence, a new subdiscipline of nanotechnology called nanotoxicology has emerged [4].

Poly(D,L-lactide-co-glycolide) (PLGA) is a biodegradable, synthetic polymer frequently used in drug/gene delivery [5]. The slight negative surface charge of PLGA nanoparticles (PLGA NP) tends to limit their interaction with the negatively charged plasmids and their intracellular uptake. Therefore, the surface of PLGA NP was modified using cationic polymers such as chitosan [6, 7] retrieved from biological sources. Chitosan has been shown to be relatively safe [8, 9]. Moreover, chitosan is approved as a food additive in Japan, Italy and Finland and as a wound dressing in the USA [10] and is widely used in drug delivery owing to its biocompatibility, mucoadhesive and permeability enhancing properties [11]. Nowadays, chitosan gained a great interest as non-viral transfection reagent [12]. Many chitosan derivatives such as trimethyl chitosan [13, 14], thiolated chitosan [15] and hydrophobically modified chitosan [16, 17] have been recently reported as improved gene carrier systems [18]. However, this derivatization was sometimes found to influence the safety of the polymer. For instance, Kean et al. [19] observed a general increase in cytotoxicity of chitosan with increasing degree of trimethylation. On the other hand, thiolation did not significantly alter the toxicity of

chitosan [20]. Besides, the cytotoxicity of chitosan nanoparticles was attenuated by decreasing the degree of deacetylation but was less affected by a lowering in molecular weight when evaluated against A549 cells [21]. Other studies also revealed a size-dependent toxicity [22, 23].

The degree of toxicity of polymeric nanomedicines is strongly influenced by the biological conditions of the local environment, which influence the rate of degradation or release of polymeric nanomedicines. Many cationic polymers have been found to be toxic and it has been suggested that this toxicity is due to interactions with the plasma membrane and/ or with negatively charged cell components and proteins [24, 25]. On this basis, the physicochemical properties such as size distribution and surface charge and the presence of functional groups on the particle surface are considered key factors in judging the cytotoxicity. However, a complete understanding of the size, shape, composition and aggregation-dependent interactions of nanostructures with biological systems is currently still lacking.

Therefore, the aim of our study was not only the regular *in vitro* testing of the toxicity of chitosan-modified PLGA nanoparticles but also a deeper understanding of the factors responsible for the observed cytotoxicity assays results. In this context we investigated the influence of the surface modification of PLGA-NP with chitosan, with emphasis on the importance of the colloidal stability of the particles along the study. Three different cell lines were used within the study; COS-1 cells, human alveolar cancer cells A549, and human bronchial epithelial cells Calu-3; COS-1 and A549 cells represent fast growing cell lines whereas Calu-3 cells were selected for their ability to form tight monolayer and to produce mucus allowing to investigate the toxic effect on a different biological hierarchy level. The safety of the particles was checked at different biological endpoints, including membrane integrity, mitochondrial activity, ATP release and integrity of the cell monolayer. The impact of pH changes, which are expected in the body, on the surface

charge and subsequently on cytotoxicity was investigated. In addition, surface interaction of serum proteins and the multiple components in the cell culture medium with nanoparticle surface and their influence on toxicity and colloidal stability of the particles was verified. Scanning force microscopy was applied to visualize and evidence these surface interactions.

Materials and methods

Materials

Poly(D,L-lactide-*co*-glycolide) 70:30 (Polysciences Europe GmbH, Eppelheim, Germany), polyvinyl alcohol Mowiol® 4-88 (Kuraray Specialities Europe GmbH, Frankfurt, Germany), ultrapure chitosan chloride: Protasan® UP CL113 (molecular weight of 50-150 kDa and a degree of deacetylation between 75 and 90%) from NovaMatrix (FMC BioPolymer AS, Oslo, Norway), ethyl acetate (Fluka Chemie GmbH, Buchs, Switzerland) were used as obtained.

Methods

1. Preparation of nanoparticles

Chitosan-modified PLGA nanoparticles were prepared by an emulsion-diffusion-evaporation technique as we previously described [6, 7]. In brief, 5 ml of PLGA dissolved in ethyl acetate (20 mg/ml) were added dropwise to 5 ml of an aqueous solution of the stabilizer PVA (2.5% w/v) and the cationic polymer chitosan under magnetic stirring. The emulsion was stirred at 1000 rpm for 1 hour. Afterwards, it was homogenized using an UltraTurrax T25 (Janke & Kunkel GmbH & Co-KG, Staufen, Germany) at 13 500 rpm for 10 minutes. The homogenized emulsion was diluted to a volume of 50 ml under constant stirring with MilliQ-water to form the nanoparticles. Remaining ethyl acetate was

evaporated by continuous stirring overnight at room temperature. The concentration of chitosan in the aqueous phase was varied to obtain nanoparticles with different surface charges, Table I. The abbreviations stated in the table will be used throughout the document as reference to the different particle preparations.

2. Measurement of colloidal characteristics

Nanoparticles were characterized with respect to mean diameter, size distribution revealed by the polydispersity index (PI) and ζ-potential using the ZetaSizer Nano ZS (Malvern Instruments Ltd, Worcestershire, UK). In general, the colloidal properties were determined in MilliQ-water. To check the colloidal stability nanoparticle suspensions were also diluted (0.9 mg/ml) and investigated in the biological media applied in the study. All measurements were performed in triplicates.

3. Cell cultures and treatments

COS -1 cells (CCL-185; ATCC, Manassas, VA, USA), passage No 10-20, were cultivated in DMEM supplemented with 10% fetal calf serum (FCS), 4500 mg/L glucose, Glutamax^{TM} and 1 mM sodium pyruvate (all from Sigma- Aldrich Chemie GmbH, Steinheim, Germany). Cells were seeded in 96-well plates at a density of 20,000 cells/well and allowed to attach for 24 h.

A549 cells (CCL-185; ATCC, Manassas, VA, USA) were cultivated in RPMI with L-glutamine (PAA Laboratories GmbH, Pasching, Austria) supplemented with 10% FCS. One day prior to experiments, A549 cells were detached using trypsin-EDTA and seeded at a density of 100,000 cells/ml, in 24-well or 96-well plates 0.5 or 0.2 ml/well, respectively.

Calu-3 cells (HTB- 55; ATCC, Manassas, VA, USA) were cultivated in Minimum Essential Medium (MEM) with Earl's Salts and L- glutamine (PAA Laboratories GmbH, Pasching Austria) supplemented with 10% FCS, 1% MEM non- essential amino acid

(NEAA) solution and 1 mM sodium pyruvate (all from Sigma- Aldrich Chemie GmbH, Steinheim, Germany).

All cells were kept in an incubator set to 37°C, 5% CO_2 and 95% humidity. On the day of experiment, cells were washed with PBS and medium was changed.

4. Biological endpoints

- **MTT assay**

MTT reduction (cleavage of the yellow tetrazolium salt to purple formazan crystals by metabolically active cells) was used to quantify cell viability. Cells were incubated with nanoparticle samples in different concentrations, for different time periods as will be described later. In addition, cells grown in culture medium only were considered as high control (100% cell viability) and others incubated with Triton X-100 (2% w/v) were used as low control (0% cell viability). Substance control, composed of nanoparticle suspension with the assay reagents only, showed no interference of the particles with the assay conditions. Afterwards, cells were washed with PBS and allowed to grow in the culture medium. On the next day, MTT solutions (3,4,5 dimethylthiazol-yl)-2,5- diphenyl tetrazolium, 5 mg/ml in PBS pH 7.4 were added. Following incubation for 3 h, the precipitated formazan was dissolved using acidified isopropanol for 0.5-1 h and quantified by measuring the absorbance at 550 nm in a multiwell plate reader (Tecan Deutschland GmbH, Crailsheim, Germany). Samples were applied in quadruplicates. Cell viability (%) was calculated by the following equation:

$$\%\ \text{cell viability} = \frac{(\text{Abs}^{550}_{\text{exp}} - \text{Abs}^{550}_{\text{low conrol}})}{(\text{Abs}^{550}_{\text{high conrol}} - \text{Abs}^{550}_{\text{low conrol}})} \cdot 100$$

Means and relative standard deviations (RSD) were calculated.

- **LDH assay**

LDH assay is based on the measurement of lactate dehydrogenase (LDH) activity released from the cytosol of dead or plasma membrane damaged cells into the culture supernatant. LDH assay was performed on the same plates applied for MTT assay. After incubation of cells with the samples, the supernatants (100 µl) were transferred to 96-well plate for LDH assay whereas the original plates were used for MTT assay. Equal volume of the reaction mixture was added per well. Absorbance was measured at 492 nm and the cytotoxicity (%) was calculated relative to Triton X-100 as high control (100% cytotoxicity), and cells in culture medium as low control (0% cytotoxicity) as follows:

$$\%\,\text{cytotoxicity} = \frac{(\text{Abs}^{492}_{\text{exp.}} - \text{Abs}^{492}_{\text{low conrol}})}{(\text{Abs}^{492}_{\text{high conrol}} - \text{Abs}^{492}_{\text{low conrol}})} \cdot 100$$

Interaction of the samples with the assay procedure (substance control) was also checked and not detectable.

- **ATP (Vialight® Plus) assay**

In this assay, ATP (adenosine triphosphate) was used to assess the functional integrity of living cells, since all cells require ATP to remain alive. Any form of cell injury results in a rapid decrease in cytoplasmic ATP levels which can be detected utilizing the luciferase enzyme to catalyse the formation of light from ATP and luciferin. The emitted light intensity is linearly related to the ATP concentration. After incubation of A549 cells with the nanoparticle samples, 50 µl/well cell lysis reagent® were added for 10 min. Equal volumes of cell lysate and ATP monitoring reagent Plus® (100 µl) were incubated in white walled luminometer plate for 2 min at room temperature then the bioluminescence was measured.

$$\%Cellviability = \frac{Lum_{\text{exp}} - Lum_{lowcontrol}}{Lum_{highcontrol} - Lum_{lowcontrol}}.100$$

Substance control was done in parallel.

- **Measurement of transepithelial resistance (TEER)**

Measurements of the TEER values are usually used as an indicator for the integrity of the tight junctions in the cell monolayer. A decrease in the TEER values reveals certain loss in the integrity of the tight junctions which might interpret a sort of toxicity. Calu-3 cells were seeded on tissue culture treated polyester membrane inserts for 12-well plate at a seeding density of 200,000 cells/ml. Culture medium was changed every second day and the resistance across the insert membrane was measured using EVOM voltohmmeter (World Precision Instruments Inc., Sarasota, FL, USA) connected to a pair of chopstick electrodes. When the resistance readings were between 1000-1500 Ω (typically between 8-10 days), nanoparticle samples, NP-3, were applied in different concentrations to the apical chamber and TEER measured at 2 and 4h. Thereafter, nanoparticles were removed and replaced with culture medium. The reversibility of the effect was checked by measuring TEER after 24 h. The resistance of the empty filter was also determined and subtracted from all other values and the data were expressed as percentage of the initial (baseline) value. The other cell lines, A549 and COS-1 cells, are lacking the tight junctions and therefore are characterized by very low TEER values. Therefore, these cell lines were excluded from this study.

5. Scanning Force Microscopy (SFM)

In order to investigate the surface morphology of the nanoparticles in the culture media, different nanoparticles containing increasing amounts of chitosan were examined by Scanning Force Microscopy with a Bioscope™ equipped with a Nanoscope IV™ controller (Digital Instruments, Veeco, Santa Barbara, CA, USA). Dried samples (nanoparticles/culture media) were investigated under ambient conditions in tapping mode using a scanning probe with a force constant of 40 N/m at resonant frequency of ~170 kHz (Anfatec, Oelsnitz, Germany).

Results

Chitosan-modified PLGA nanoparticles prepared by the emulsion-diffusion-evaporation technique were characterized by a homogeneous size distribution and positive surface charge in MilliQ water. Increasing chitosan content gradually increases the surface charge from 21 – 58 mV, NP-3 – NP-9, as well as the width of the size distribution as can be seen from the increasing P.I. values, Table 1.

Table 1: Colloidal properties of different nanoparticles

	NP-0	NP-3	NP-6	NP-9
Chitosan (% w/v)	0	0.3	0.6	0.9
Particle size (nm)	148.2 (2.3)*	163.6 (2.9)	186.2 (5.5)	247.4 (5.64)
PI	0.03 (0.01)	0.14 (0.01)	0.17 (0.01)	0.19 (0.01)
ζ-potential (mV)	-8.62 (0.2)	32.3 (1.96)	46.4 (1.65)	58.0 (1.01)

* Values between brackets denote the standard deviations (n = 3)

- **Parameters investigated**

In order to understand the possible effects of the nanoparticles on the biological activity of the cells, several variables were investigated including:

- Concentration of nanoparticles: different concentrations of the nanoparticle suspension (NP-3), Table I, ranging from 0.1 – 2.5 mg/ml were incubated with two different cell types, COS-1 & A549 for 6 h, then MTT and LDH assays were performed.
- Contact time: immediate and long term toxicity of the particles (NP-3), Table I, were studied by incubating the particles with A549 cells for 2, 4, 6, 8 & 24 h after which the cell viability was determined.
- Surface charge of the nanoparticles: different nanoparticle suspensions containing increasing concentrations of chitosan and accordingly carrying higher surface

charges were prepared (Table I). The effect of the surface charge on the cytotoxicity of the particles was studied on COS-1, A549 and Calu-3 cell lines.

- pH of the culture medium: RPMI mixed with HEPES buffer 100 mM of two different pH values 4.7 & 7.4 were applied during the incubation of the particles with A549 cells. The experimental pH of these mixtures was 6.5 and 7.4, respectively. The possible effects on cell proliferation (MTT-assay) and/or membrane integrity (LDH-assay) were investigated.
- Presence of FCS in the culture medium: FCS was suggested to affect the colloidal stability of the nanoparticles, therefore, nanoparticle samples in serum-free media as well as media supplemented with serum were applied and the viability of A549 cells was determined.
- Assay procedure: cytotoxicity of nanoparticles with increasing chitosan content was assessed by three different assays (MTT, LDH and ATP-assays). The cell viability was compared.

1. Nanoparticle concentration

Our previous studies demonstrated the efficacy of chitosan-modified PLGA nanoparticles, NP-3, to be taken up by A549 cells within 6h incubation [7, 26]. The effects of these particles on different cell lines were investigated by testing membrane integrity via the LDH release and metabolic activity via mitochondrial enzymes. The viability of the cells after incubation with nanoparticles, NP-3, of increasing concentrations (0.1 – 2.5 mg/ml) for 6 h was found to be clearly dependent on the cell type; the viability of COS-1 cells was remarkably decreased with increasing NP concentration to reach ~35% with the highest NP concentration, Figure 1A. On the other hand, 80 – 90% of A549 remained metabolically active after incubation with NP in the whole concentration range investigated. Cell morphology observed by optical microscopy also showed normal

proliferation rate indicating that the cytotoxicity of the nanoparticles was quite low. The effect of NP on the membrane integrity (LDH assay) was negligible and independent of the NP concentration with both cell lines (within the experimental error), Figure 1B.

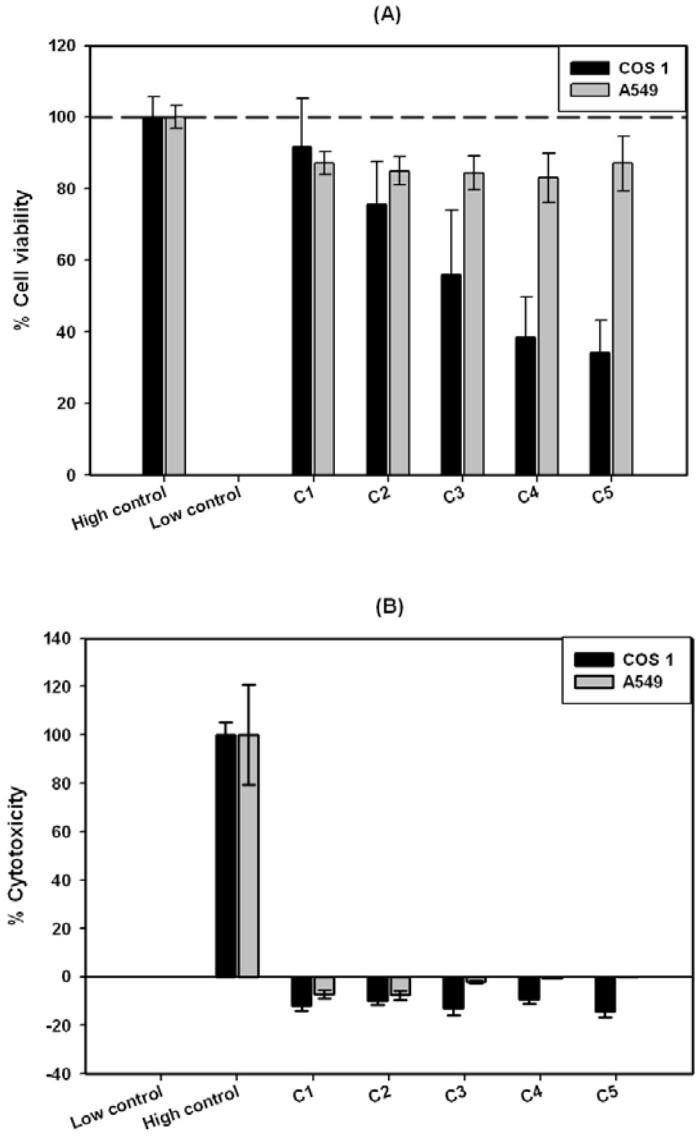

Figure 1: (A) MTT assay, (B) LDH assay of chitosan-modified PLGA nanoparticles at different concentrations in COS-1 and A549 cells

2. Contact time

PLGA nanoparticles are known to be slowly biodegraded; therefore, testing long-term toxicity is as interesting as short-term toxicity. Incubation of nanoparticles with COS-1

cells showed a remarkable toxicity on short-time incubation periods. Therefore, a less sensitive cell line was selected for long-term toxicity investigation. A549 cells were incubated with the nanoparticles (0.9 mg/ml) for different time periods ranging from 2 to 24 h. As shown in Figure 2, the survival rate was comparable to the control during the first 6h, and then started to decrease to ~ 85% after 24 h.

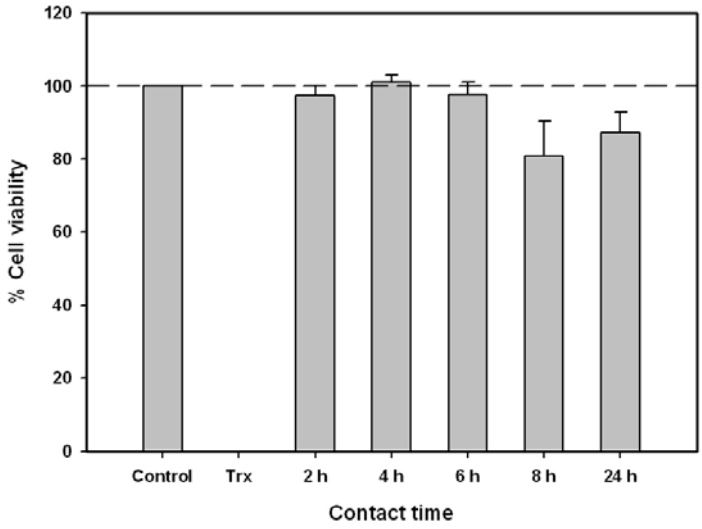

Figure 2: MTT assay for chitosan-modified PLGA nanoparticles at different contact times with A549 cells

3. Chitosan content on the nanoparticles

Cationic polymers are known to exhibit cytotoxic effects [24], however, chitosan can be considered as one of the safe polymers. For this reason, it was interesting to study the effect of different nanoparticles (NP-3 – NP-9) prepared with increasing chitosan concentrations (0.3 - 0.9 mg/ml) - thus characterized by higher surface charge – on the viability of different cell lines. The survival rate, estimated by the MTT-test, was dependent on the cell type and was in the ranking order: Calu-3 > A549 > COS-1 cells, Figure 3A. Around 90% of A549 and Calu-3 cells were metabolically active after incubation with NP-9 compared to only 40 % in case of COS-1 cells.

Particle size measurement of the nanoparticles in different culture media indicate uniform distribution of PLGA nanoparticles, NP-0, in water, RPMI and MEM, Figure 3B. In contrast, agglomerates were observed when chitosan-modified particles, NP-3 – NP-9, were measured in culture media, Figure 3C-E. Agglomeration was more pronounced in MEM than in RPMI. Besides, increasing chitosan concentration increases the tendency toward agglomeration. This agglomeration is thought to reduce the effective concentration of the particles in the nanosize range, which in turns correlates with the reduced toxic effect of NP with higher chitosan content on A549 and Calu-3 cells.

(A)

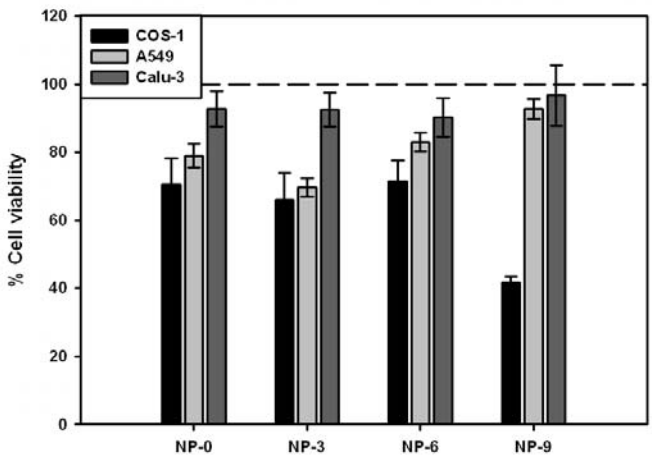

(B)

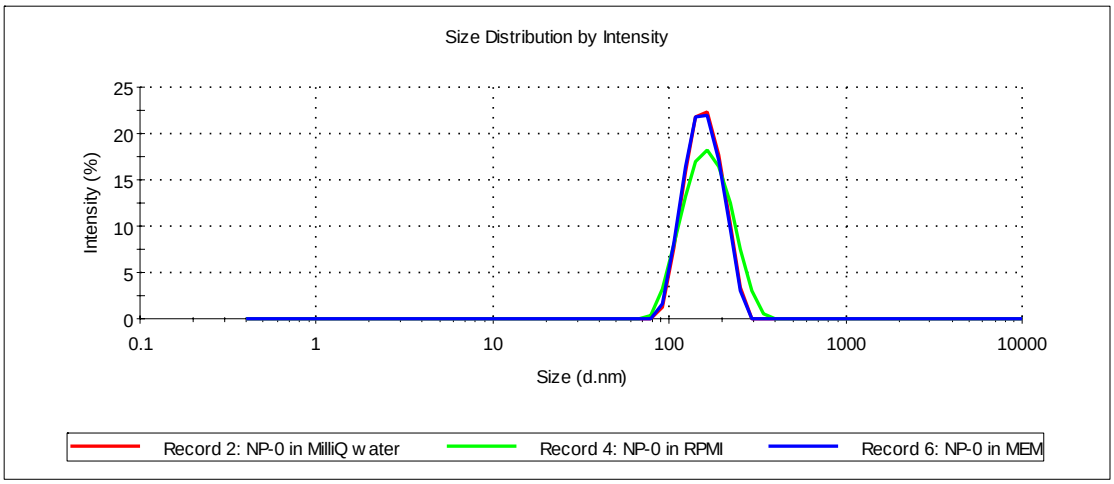

(C)

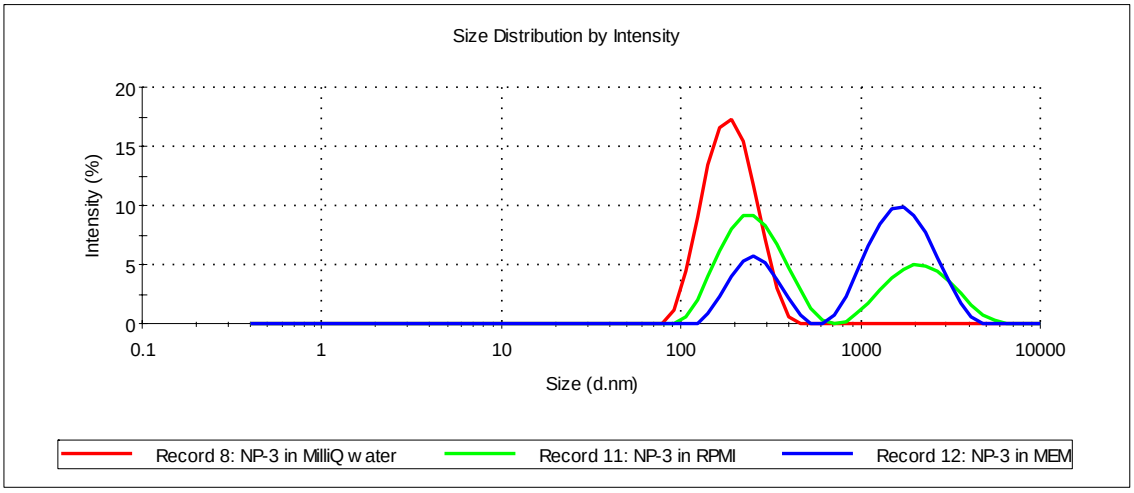

(D)

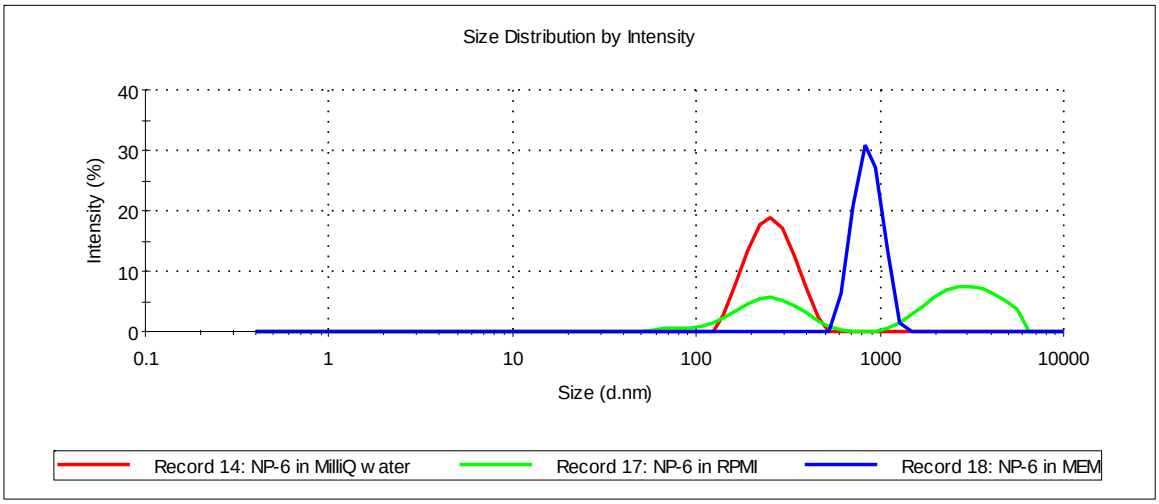

(E)

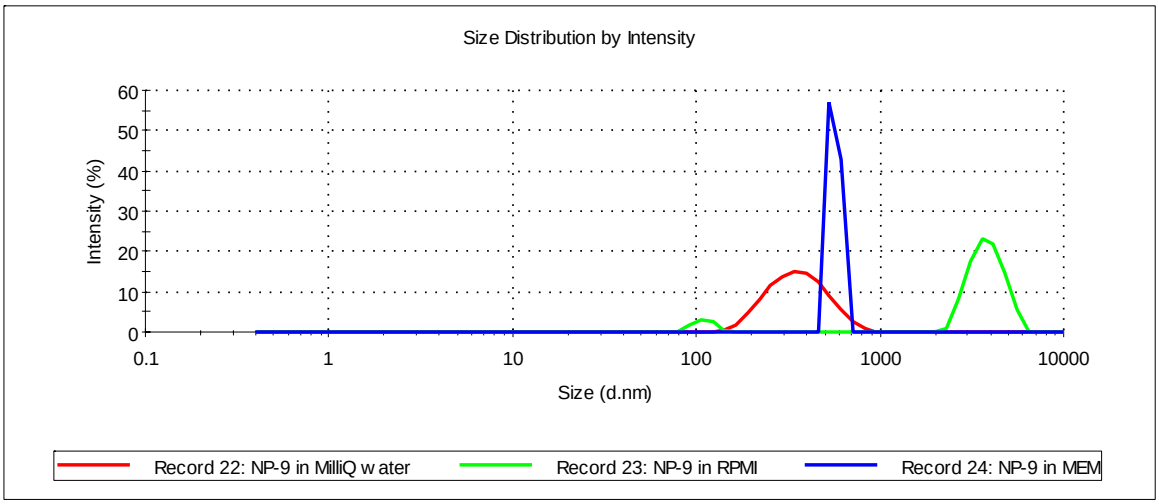

Figure 3: (A) MTT assay for nanoparticles with increasing concentrations of chitosan on different cell types, (B-E) size distribution curves of nanoparticles (B) NP-0, (C) cNP-3, (D) cNP-6 and (E) cNP-9 in water and different culture media

4. Incubation medium

The impact of the medium applied during the incubation of the particles with the cells and especially its pH is expected to play an essential role. Chitosan is known to acquire a positive charge in acidic media [18], while chitosan-modified nanoparticles in neutral pH (as in cell culture medium) are found to have low or negligible surface charge. It is therefore essential to investigate the behaviour of the particles when subjected to pH fluctuation as would be the case in the human body. In this context, non-modified PLGA nanoparticles, NP-0, and chitosan-modified PLGA nanoparticles, NP-3, were diluted in 3 different media: RPMI, RPMI + (HEPES pH 7.4) in 1:1 mixture and RPMI + (HEPES pH 4.7), the experimental pH of the latter was found to be 6.5, and incubated with A549 cells for 6 h. LDH assay revealed no destructive effect of the nanoparticles, NP-0 and NP-3, on the cell membrane in neutral media as seen before; RPMI and RPMI + (HEPES pH 7.4), Figure 4, where chitosan is expected to be uncharged. On the other hand, a remarkable increase in LDH release was noticed and even more pronounced in NP-3 when (HEPES pH 4.7) was mixed with the culture medium. This suggests that the toxicity of chitosan is mediated by electrostatic interaction with the negatively charged membrane. Despite the influence of the particles on the membrane integrity, negligible effect on the cell proliferation was observed as recorded by the MTT assay (data not shown).

It was hence necessary to check the colloidal stability of the nanoparticles in the different media used in this test. Particle size measurements revealed a monomodal distribution of PLGA nanoparticles, NP-0, in all media, while a bimodal distribution was observed in case of chitosan-modified particles, NP-3, indicating higher affinity of the latter to interact with the culture media independent of the presence of HEPES buffer, Figure 4 B&C. Similarly, PLGA nanoparticles retained their negative ζ-potential whereas a broad distribution of charges was observed for chitosan in culture media giving a mathematical mean of nil ζ-potential.

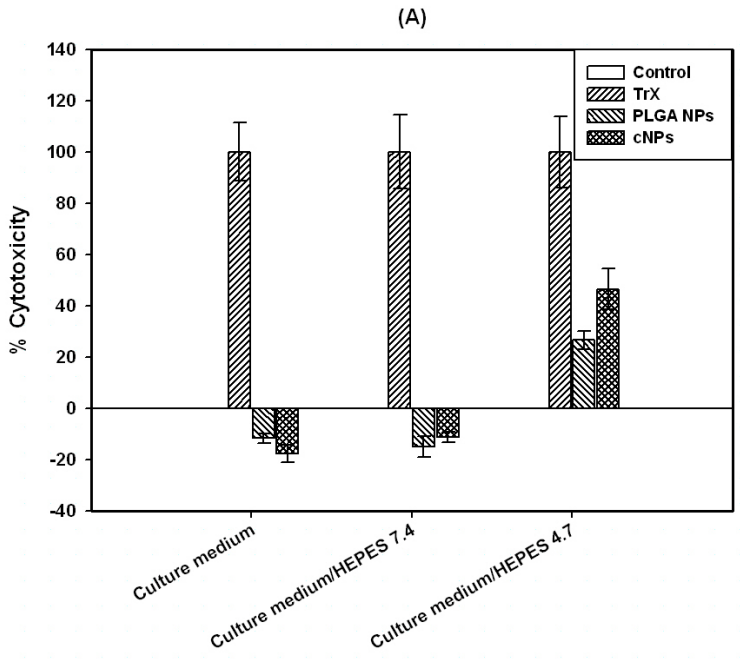

(B)

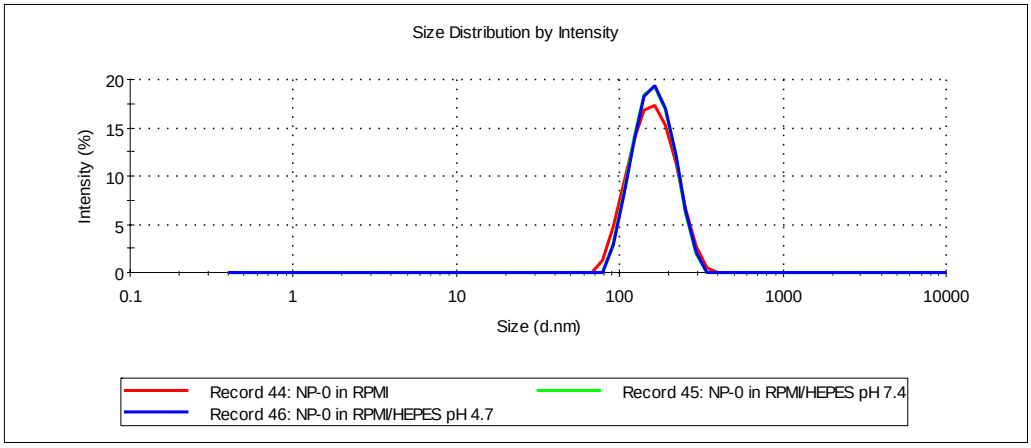

(C)

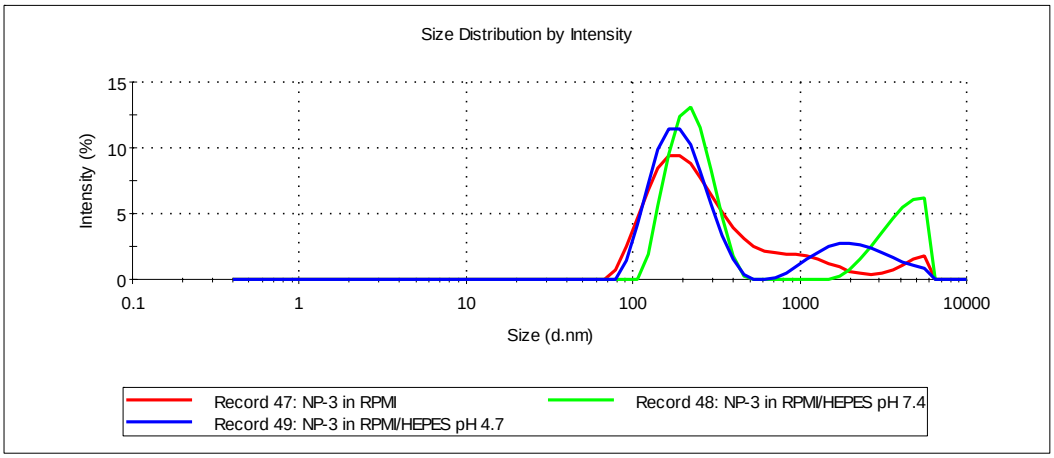

Figure 4: (A) LDH assay for PLGA and chitosan-modified PLGA nanoparticles incubated with A549 cells in different media, (B & C) size distribution curves of (B) PLGA NPs and (C) chitosan/PLGA NPS in these media

5. FCS in culture medium

Another important aspect regarding the influence of the culture medium on the toxicity of the particles is the presence of serum. A549 cells were incubated with nanoparticles, NP-3, suspended in RPMI both in presence and absence of 10% FCS; the cell viability was then determined. From Figure 5A, one can notice a slight reduction in viability in absence of FCS, which might indicate the protective role of serum. Several authors reported the adsorption of negatively charged serum proteins on the positively charged nanoparticles surfaces, therefore shielding or masking their original (probably harmful) effect on the cells [27]. Accordingly, it was necessary to investigate the colloidal stability of the nanoparticles in the culture medium both in presence and absence of FCS. Measurement of the particle size indicates the presence of some agglomerates (~ 1 μm) whereas a significant amount of the particles retain their original state in the nanosize range independent of the presence of serum, Figure 5B. On the other hand, in absence of serum the ζ-potential was found to have a mean value of zero indicating a risk of colloidal instability, while in serum-supplemented medium a broad undetermined range of surface charges was detected, Figure 5C, which clearly reveals the strong uncontrolled interaction of the serum proteins with the nanoparticles surfaces.

6. Viability assays (MTT vs ATP assay)

MTT assay is a widespread method to assess cell viability; a more recent method is the ATP assay. In order to check their validity to investigate the toxicity of our nanoparticles, a comparative experiment was done using nanoparticles with different chitosan content; NP-0, NP-3, and NP-6. As shown in Figure 6, viability of A549 cells incubated with nanoparticles were similar to the control as tested with the ATP assay, whereas a slight reduction in viability by ~15-25% was determined with the MTT assay. Despite the

difference in magnitude (which is always expected due to the difference in assay principle and protocol), both assays showed the same tendency.

(A)

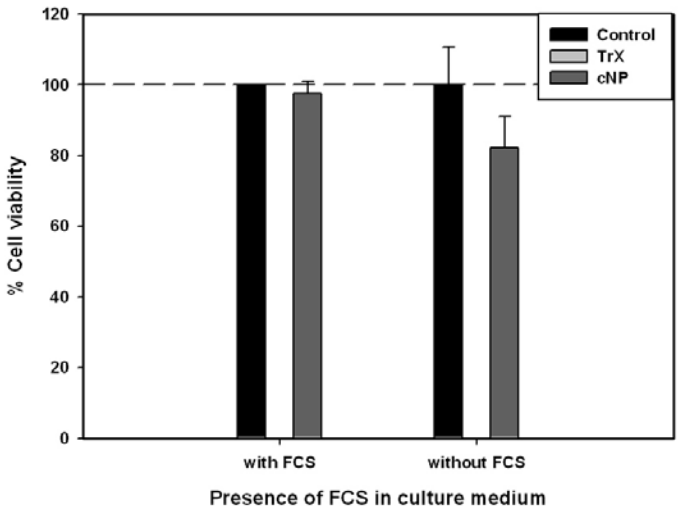

(B)

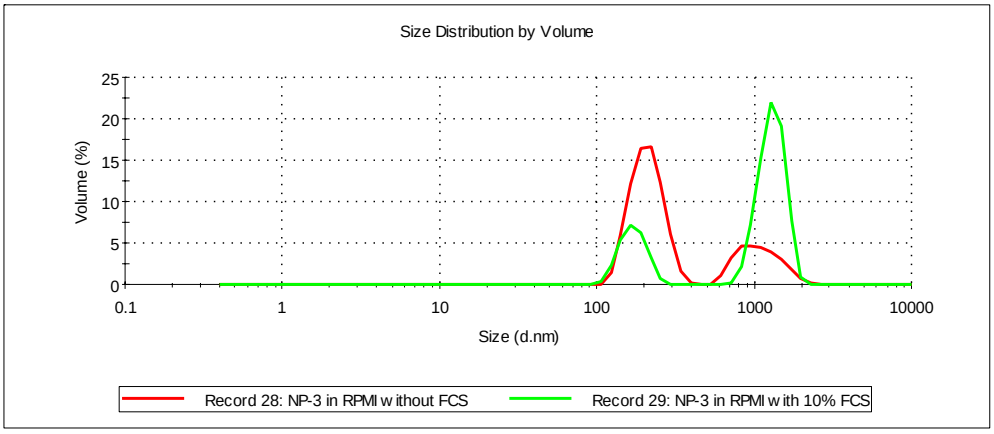

(C)

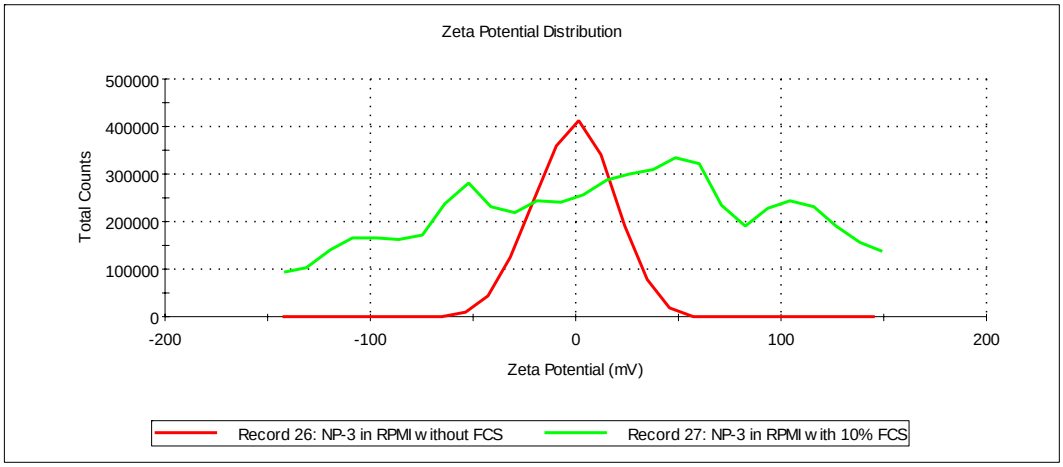

<u>Figure 5:</u> Effect of the presence of FCS in the culture medium on (A) the viability of A549 cells, (B) size distribution and (C) ζ-potential of chitosan/PLGA nanoparticles

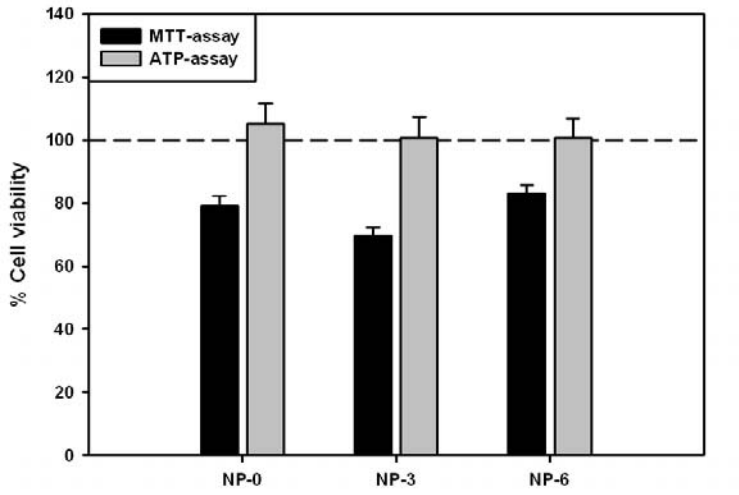

Figure 6: Cytotoxicity testing of chitosan-modified PLGA nanoparticles by different viability assays (MTT- and ATP-assays)

7. Colloidal stability of nanoparticles in culture media by SFM

In order to get a deeper insight on the nanoparticle behavior in different culture media as well as nanoparticles-serum surface interaction, the morphology of nanoparticles in different culture media, RPMI and MEM, was examined by SFM. Figure 7 represents a general overview on the rearrangement of the particles, containing increasing amounts chitosan, in RPMI and MEM. Generally speaking, one can remark that the culture media tend to form dendritic networks when dried on mica surfaces applied during the investigation (diffusion limited aggregation. Network arrangements formed in case of MEM are much larger in size compared to those formed in case of RPMI, Figure 7 A&B. It can be also noticed that PLGA nanoparticles, NP-0, remain evenly dispersed and can be clearly distinguished from the dendritic arrangements of the culture media, Figure 7 C&D. On the other hand, chitosan-modified particles were observed to be imbedded in the dendritic networks of the medium and usually surrounded by various small structures, which are most probably representing smaller protein units, Figure 7 E-H.

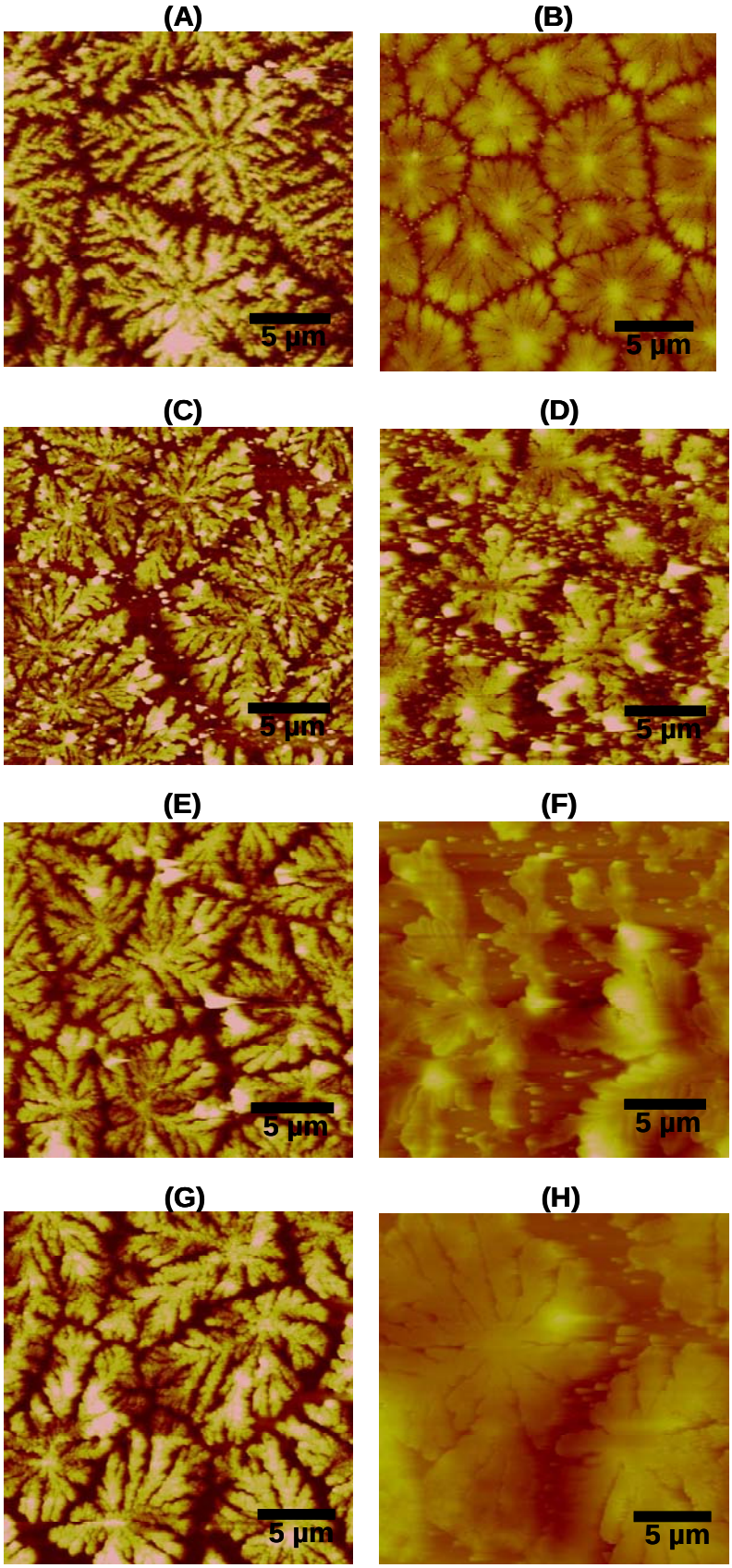

Figure 7: Surface morphology of (A) RPMI, (B) MEM, (C) NP-0 in RPMI, (D) NP-0 in MEM, (E) NP-3 in RPMI, (F) NP-3 in MEM, (G) NP-6 in RPMI and (H) NP-6 in MEM as examined by SFM

Closer look to the nanoparticle surface in both media is depicted in Figure 8. The surface of PLGA nanoparticles, NP-0, remain smooth and the particles retain their spherical well-defined shape either in RPMI or MEM as seen from the height, amplitude and phase images, Figure 8A. However, chitosan-modified particles, NP-3 and NP-6, are characterized by rough, non-uniform surfaces, Figure 8 B&C. Phase images reveal a distinct change in phase around each nanoparticle, indicating the absorption of other molecules from the medium to the nanoparticle surface.

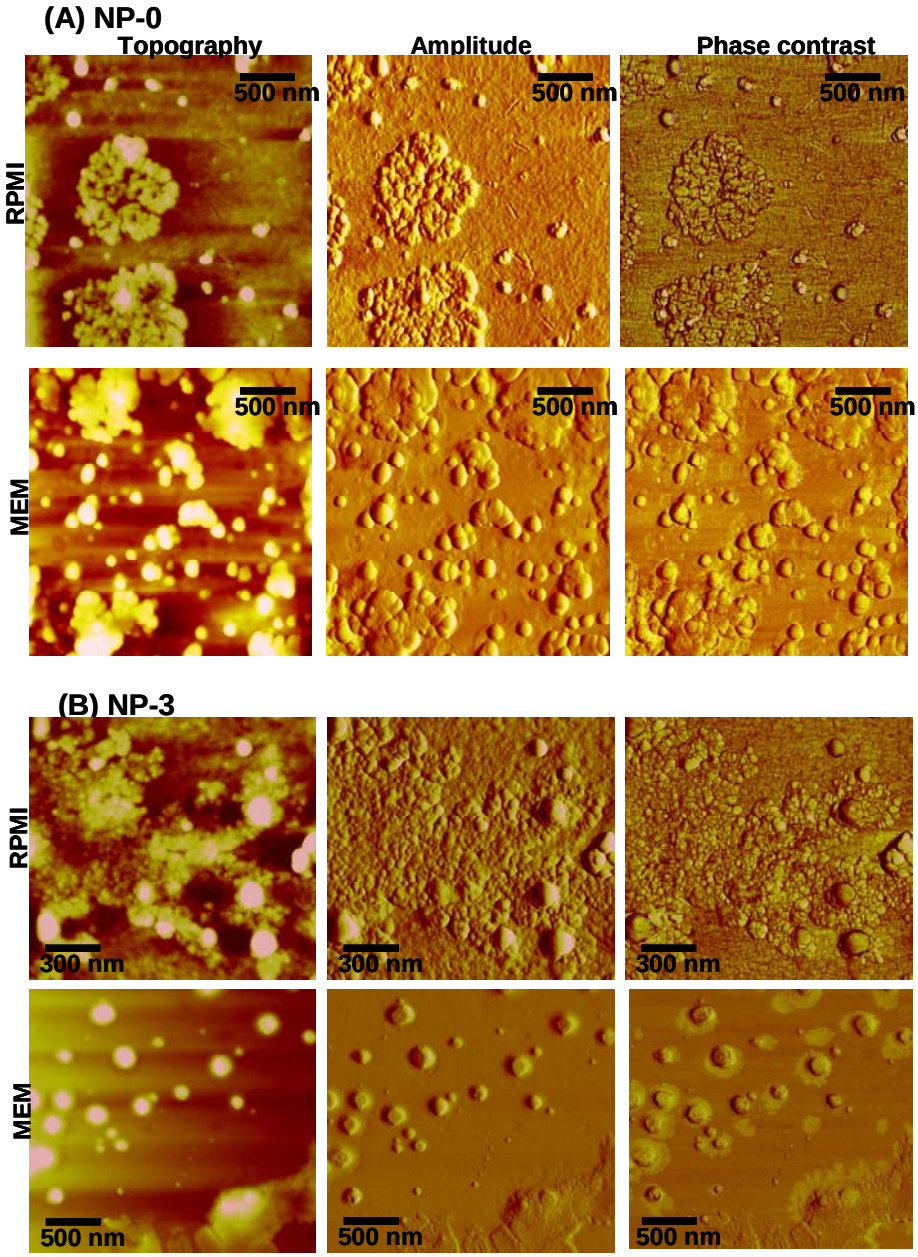

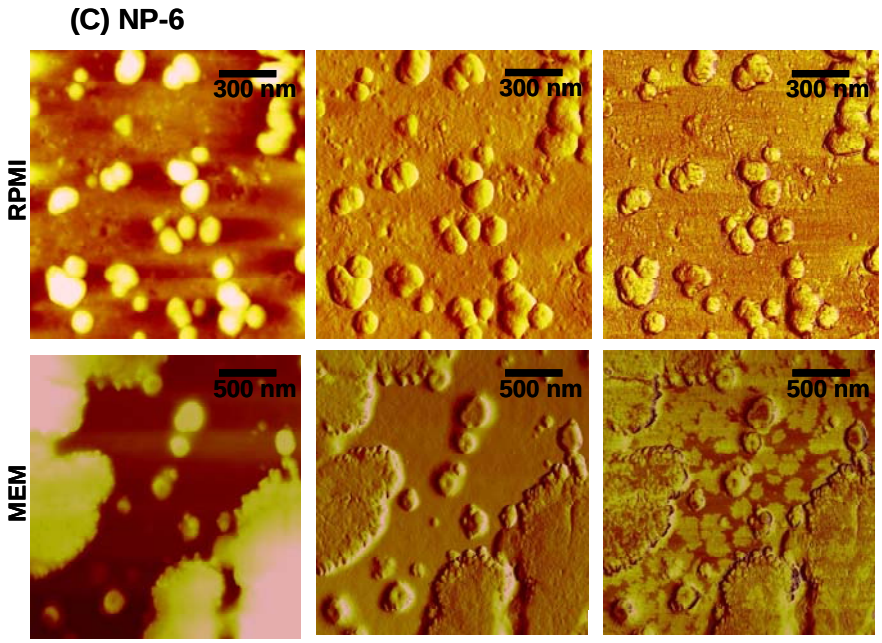

Figure 8: Surface morphology of (A) NP-0, (B) NP-3 and (C) NP-6 in RPMI and MEM as examined by SFM. Arrows demonstrate nanoparticles either dispersed (NP-0) or surrounded by medium components (NP-3, NP-6)

8. TEER measurements

Chitosan-modified nanoparticles, NP-3, were incubated in different concentrations with Calu-3 cells, the TEER values were measured after 2 and 4 h. The reduction in TEER values is calculated as % of the initial values measured prior to the addition of particles. As shown in Figure 9, diluted nanoparticle concentrations (0.02 – 0.3 mg/ml) resulted in slight decrease in the TEER values to ~ 80 % of the baseline values, which is similar to the reduction caused in case of the control. Higher nanoparticle concentrations (1.3 mg/ml) induced a distinct temporary reduction in TEER values to ~ 45 % after 2 h which started to recover again even in presence of the particles. Measurement of TEER values 24 h after starting the test reveals complete recovery of the monolayer integrity at all concentrations tested.

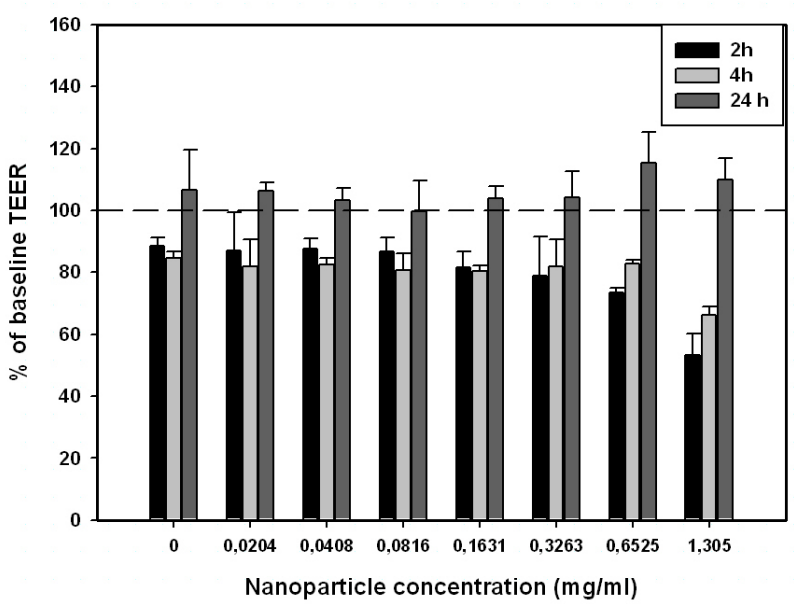

Figure 9: Change in the TEER values of Calu-3 cells after incubation with chitosan-modified PLGA nanoparticles in different concentrations for different time periods

Discussion

Insights into the cytotoxic effects of nanoparticulate carriers are essential especially when they are intended to be applied on a subcellular level. PLGA is known to be benign to the cells and therefore have been frequently applied as drug and gene carrier in different forms like implantations, micro- and nanoparticles [5]. On the contrary, cationic polymers are reported to induce certain cell damage through their interaction with anionic components (sialic acid) of the glycoproteins on the surface of epithelial cells. The necrotic cell reaction is not accompanied by apoptosis; the nuclei retain their size and shape [24]. Nevertheless, chitosan was found to be less toxic than other cationic polymers such as poly-L-lysine and polyethyleneimine *in vivo* and *in vitro* [28, 29]. Therefore, chitosan was chosen to modify the surface of PLGA nanoparticles aiming to improve their binding potential with negatively charged plasmids and enhance their cellular uptake. The emulsion-diffusion-evaporation technique produced spherical, smooth surface nanoparticles of monomodal size distribution and increasing positive surface charge upon adding increasing concentrations of chitosan. The toxicity of these particles was measured

by assessing cellular damage. An indication of acute cellular damage is a reduction in metabolic activity, which is the principle of MTT and ATP assays, whereas LDH release reflects the damage/leakage of plasma membrane.

Cytotoxicity is known to be a function of the cell type, therefore, three cell lines were used in this study; COS-1, A549 and Calu-3 cells. The Calu-3 cells were incorporated in the study to investigate the effect of the particles on the integrity of the cell monolayer and the possible impact of the surface charge, whereas COS-1 and A549 cells were used as fast growing cancerous cell types. In case of COS-1 cells, cytotoxicity of chitosan-modified particles was found to be dose dependent, this feature did not hold for A549 cells in the investigated dose range. Similarly, the survival of COS-1 cells was negatively affected after incubation with particles containing higher amounts of chitosan, while A549 and Calu-3 cells were found to be more robust. The dependence of toxicity on cell type was previously reported by different other research groups [19, 30]. It is important to note that chitosan solutions had the same effect as our chitosan/PLGA nanoparticles when tested on A549 cells (data not shown). Similar results were obtained when different types of chitosans with increasing molecular weight were tested (data not shown).

Since the toxicity of cationic polymers is considered an interesting issue, several authors discussed the influence of polymer properties such as molecular weight, charge density, type of cationic functionalities, structure and sequence (block, random, linear, branched) and conformational flexibility [31-33]. Ferruti et al. [31] noted that PLL macromolecules with tertiary amine groups exhibit a lower toxicity than those with primary and secondary residues. On the other hand, Ryser [34] related the cytotoxicity to the charge density, the three dimensional structure and flexibility of the cationic macromolecule as it determines the accessibility of the charges to the cell surface. Accordingly, branched molecules were found to be more efficient in neutralizing the cell surface charge than molecules with linear or globular structures [32], while rigid molecules

have more difficulties to attach to the membranes than flexible molecules and the interaction is therefore limited [33]. This should be true for the particles as they limit the flexibility of the anionic species but was not observed in the experiment that did not result in different behavior between chitosan NP and chitosan molecules.

Toxicity was checked over 6 and 24 h; 6 h to give an indication of the toxicity of the particles over the time of an *in vitro* transfection experiment. Additionally, a 24 h time point has been tested to mimic the tissue-therapeutic contact time, which is expected in an *in vivo* experiment where clearance would take longer. Furthermore, the 24 h-exposure is important as the cells would be within an exponential growth phase in this period meaning that any toxicity, due to inhibition of proliferation and/or cell death, would be clearly visible in the assay. The cells showing short term toxicity were not studied for long term incubation because of the already present toxicity. However, even the A549 cells showed a decrease of viability after 8h to 85% survival rate what is not considered problematic in terms of an application.

One of the interesting points to be discussed is the relation of particle toxicity with the composition and pH of the medium, yet this factor was rarely investigated. It is generally expected that diverse *in vivo* routes of administration can present different toxicological outcomes that vary with the surrounding pH. In our case, this can be considered a key factor, where the toxicity is thought to be due to the positive charge of the particles and the surface charge of the NP is pH dependent. Normally, optimum conditions for cell cultures maintain pH 7.4, at which chitosan is mostly non-ionized and hence apparently non-toxic. The decrease of pH by adding HEPES buffer of pH 4.7 reduced the overall experimental pH of the medium to ~ 6.5, the survival rate of the cells under these conditions was high enough to perform the study but was relatively lower than cells grown in culture medium only. The relative reduction in pH allows a considerable amount of chitosan molecules to be ionized, the positive charge acquired on the nanoparticle surface enhance their

interaction with the plasma membrane, which was clearly demonstrated by the increase in LDH release indicating membrane damage. This suggests that the toxicity of chitosan is mediated by electrostatic interaction with the negatively charged membrane. The presence of the particles impacts on the toxicity in addition to the unfavourable conditions with the medium at pH 6.5. These conditions may further facilitate the toxic impact of the particles on the cells what is reflected also in the increased toxicity of the PLGA particles.

The colloidal behaviour of nanoparticles in different buffers and culture media is rarely studied or considered with respect to acute toxicity, although the surface properties of the particles are considered to be a relevant factor for cytotoxicity and cellular uptake. Generally speaking, the main goal of using nanoparticles is their improved cellular uptake compared to larger size carriers. Nevertheless, in our study, a considerable fraction of the particles are forming agglomerates in culture media as revealed by particle size measurements and morphological examination by SFM. This agglomeration is thought to reduce the effective concentration of the particles in the nanosize range, which in turns correlates with the reduced toxic effect of NP with higher chitosan content on A549 and Calu-3 cells. Therefore, it is not possible to refer our results exclusively to their nanoscale properties. Besides, many authors referred the cytotoxic effects of polycations to their charge interaction with cell membrane. However, ζ-potential measurements demonstrated that this positive surface charge does not exist any longer due to high ionic strength, the presence of divalent ions and the possible surface association of serum proteins to the nanoparticle surface, even when higher concentrations of chitosan were applied to the nanoparticles. Hence, any discussion of cytotoxicity on charge basis might be misleading regarding the relevant determinant and not taking into account the Debye length. The presence of a variety of nanoscale components in the culture media often complicates the measurement and interpretation of size and ζ-potential measurements. Many researchers tried to avoid the problem of the colloidal instability of the nanoparticle in culture media

by using other buffers. However, this is also thought to be far away from the *in vivo* conditions and any findings based on this do not allow speculating the real behaviour of the particles in complex environments. Therefore, there is still a need to establish more physiologically relevant *in vitro* testing models that can efficiently substitute *in vivo* nanotoxicology studies [4].

We have demonstrated that SFM can be a promising approach to visualize the distribution of the nanoparticles within the air dried culture medium. The changed surface morphology or at least the change of the close environment of the chitosan coated particles compared to the PLGA particles can be clearly seen. In addition, the distribution of the particles gives another hint to the presence of interactions within the medium. PLGA particles were evenly distributed whereas the chitosan particles were always found within the solid residues of the dried media indicating the favored interaction with the included materials. It is reasonable to assume that the interactions of nanoparticles with serum proteins and the diverse components of the culture media mask not only the charge of the particles but also their recognition by the cells as foreign bodies and accordingly their harmful effects. However, the overall arrangement in dendritic structures is not representative for the general interactions because the arrangement of the molecules will be influenced by the drying process of the sample, the changing concentrations and the hindered diffusional processes. Therefore, a next step should be the SFM measurement of the nanoparticles in culture media under liquid to get a better insight in the situation in the medium and to avoid possible artifacts. Furthermore, studying nanoparticle-cell surface interactions is an ongoing topic.

Tight junctions are located at the boundary between apical and basolateral domains in epithelial cells and appear as a continuous apical belt around the cell periphery. The presence of tight junctions between neighbouring epithelial cells prevents the free diffusion of hydrophilic molecules across the epithelium by the paracellular route. An sensitive

indicator for sublethal toxicity is the loss of integrity of tight junctions. TEER measurement is a method to investigate changes in tight junction's structure. Our results indicate a temporary, concentration-dependent opening of the tight junctions of Calu-3 cells when exposed to chitosan-modified nanoparticles. Similarly, Smith et al. [35] found that chitosan cause a dose-dependent reduction in transepithelial electrical resistance of Caco-2 monolayers of up to 83% and that chitosan-mediated tight junction disruption is caused by a translocation of tight junction proteins from the membrane to the cytoskeleton.

Our findings can be summarized in the following; the toxicity of chitosan-modified PLGA NP is dependent on the cell type and was found to be in the order COS-1 > A549 > Calu-3 cells. The colloidal stability of the nanoparticles is remarkably reduced when suspended in the culture media. Due to the formation of agglomerates, a significant reduction in the amount of nanosized fraction decreases the actual effective concentration of the particles along the study. This is supported by the data of the chitosan particles with different chitosan amounts. The higher the amount (ζ-potential) the keener are the particles to agglomeration in medium and the less toxic they are on A549 cells. For COS-1 cells there seems to be no impact of lower charges (or uncharged); only the highest chitosan concentration shows a different toxicity level. Besides, the adsorption of multicomponents of the culture medium on the NP surface (as visualized by SFM) limits their recognition by the cells as foreign bodies, and hinders the real surface interaction between the nanoparticle and the cell. This, together with the reduction in nanoparticle effective concentration, might explore the reduced toxicity and supports the idea of underestimated nanotoxicity in general. On the other hand, stimulation of chitosan ionization by reducing the pH of the incubation medium relatively increases the positive surface charge of the particles and in turns destabilize the cell membrane. This clearly demonstrates the role of charge in NP-cell surface interaction.

Although our chitosan/PLGA nanoparticles did not show evident harmful effects to the investigated cell lines, the real interactions between the nanoparticles and the target cells on subcellular and molecular levels are still poorly understood. Therefore, the identification of fundamental cellular responses to nanoparticles (such as generation of reactive oxygen and activation of redox-sensitive signalling cascades) is still necessary to complement the toxicological testing with a mechanistic approach.

CONCLUSIONS

From this study, it can be concluded that the cytotoxicity of chitosan-modified PLGA nanoparticles is a function of the cell line. Nevertheless, the toxicity is under estimated due to the colloidal instability in culture media, reduction in effective nanoparticle concentration on the nanosize range, in addition to adsorption of medium components to the nanoparticle surface. Slight shift of the surrounding pH allows ionization of chitosan and increase in surface charge of the nanoparticles, which as a consequence lead to more pronounced loss of membrane integrity of the cells.

REFERENCES

[1] S. Azarmi, W.H. Roa, R. Löbenberg, Targeted delivery of nanoparticles for the treatment of lung diseases. Advanced Drug Delivery Reviews 60(8) (2008) 863-875.

[2] S. Jin, K. Ye, Nanoparticle-Mediated Drug Delivery and Gene Therapy. Biotechnology Progress 23(1) (2007) 32-41.

[3] T. Xia, M. Kovochich, J. Brant, M. Hotze, J. Sempf, T. Oberley, C. Sioutas, J.I. Yeh, M.R. Wiesner, A.E. Nel, Comparison of the Abilities of Ambient and Manufactured Nanoparticles To Induce Cellular Toxicity According to an Oxidative Stress Paradigm. Nano Letters 6(8) (2006) 1794-1807.

[4] H.C. Fischer, W.C.W. Chan, Nanotoxicity: the growing need for in vivo study. Current Opinion in Biotechnology 18(6) (2007) 565-571.

[5] J. Panyam, V. Labhasetwar, Biodegradable nanoparticles for drug and gene delivery to cells and tissue. Advanced Drug Delivery Reviews
Biomedical Micro- and Nano-technology 55(3) (2003) 329-347.

[6] M.N.V. Ravi Kumar, U. Bakowsky, C.M. Lehr, Preparation and characterization of cationic PLGA nanospheres as DNA carriers. Biomaterials 25(10) (2004) 1771-1777.

[7] N. Nafee, S. Taetz, M. Schneider, U.F. Schaefer, C.M. Lehr, Chitosan-coated PLGA nanoparticles for DNA/RNA delivery: effect of the formulation parameters on complexation and transfection of antisense oligonucleotides. Nanomedicine: Nanotechnology, Biology, and Medicine 3(3) (2007) 173-183.

[8] M. Lee, J.W. Nah, Y. Kwon, J.J. Koh, K.S. Ko, S.W. Kim, Water-soluble and low molecular weight chitosan-based plasmid DNA delivery. Pharm. Res. 18(4) (2001) 427-431.

[9] K. Corsi, F. Chellat, L. Yahia, J.C. Fernandes, Mesenchymal stem cells, MG63 and HEK293 transfection using chitosan-DNA nanoparticles. Biomaterials 24(7) (2003) 1255-1264.

[10] L. Illum, Chitosan and its use as a pharmaceutical excipient. Pharm. Res. 15(9) (1998) 1326-1331.

[11] V. Dodane, M. Amin Khan, J.R. Merwin, Effect of chitosan on epithelial permeability and structure. International Journal of Pharmaceutics 182(1) (1999) 21-32.

[12] M.M. Issa, M. Koping-Hoggard, P. Artursson, Chitosan and the mucosal delivery of biotechnology drugs. Drug Discovery Today: Technologies 2(1) (2005) 1-6.

[13] M. Amidi, S.G. Romeijn, G. Borchard, H.E. Junginger, W.E. Hennink, W. Jiskoot, Preparation and characterization of protein-loaded N-trimethyl chitosan nanoparticles as nasal delivery system. Journal of Controlled Release 111(1-2) (2006) 107-116.

[14] M. Amidi, S.G. Romeijn, J.C. Verhoef, H.E. Junginger, L. Bungener, A. Huckriede, D.J.A. Crommelin, W. Jiskoot, N-Trimethyl chitosan (TMC) nanoparticles loaded with influenza subunit

antigen for intranasal vaccination: Biological properties and immunogenicity in a mouse model. Vaccine 25(1) (2007) 144-153.

[15] R. Martien, B. Loretz, M. Thaler, S. Majzoob, A. Bernkop-Schnürch, Chitosan-thioglycolic acid conjugate: An alternative carrier for oral nonviral gene delivery? J. Biomed Mater Res 82A(1) (2007) 1-9.

[16] S. Hohne, R. Frenzel, A. Heppe, F. Simon, Hydrophobic Chitosan Microparticles: Heterogeneous Phase Reaction of Chitosan with Hydrophobic Carbonyl Reagents. Biomacromolecules (2007).

[17] H. Hwang, I.-S. Kim, I.C. Kwon, Y.-H. Kim, Tumor targetability and antitumor effect of Docetaxel loaded hydrophobically modified glycol chitosan nanoparticles. Journal of Controlled Release 128 (2008) 23-31.

[18] S.A. Agnihotri, N.N. Mallikarjuna, T.M. Aminabhavi, Recent advances on chitosan-based micro- and nanoparticles in drug delivery. Journal of Controlled Release 100(1) (2004) 5-28.

[19] T. Kean, S. Roth, M. Thanou, Trimethylated chitosans as non-viral gene delivery vectors: Cytotoxicity and transfection efficiency. Journal of Controlled Release 103(3) (2005) 643-653.

[20] D. Guggi, N. Langoth, M.H. Hoffer, M. Wirth, A. Bernkop-Schnurch, Comparative evaluation of cytotoxicity of a glucosamine-TBA conjugate and a chitosan-TBA conjugate. International Journal of Pharmaceutics 278(2) (2004) 353-360.

[21] M. Huang, E. Khor, L.-Y. Lim, Uptake and cytotoxicity of chitosan molecules and nanoparticles: effects of molecular weight and degree of deacetylation. Pharm. Res. 21(2) (2004) 344-353.

[22] L. Qi, Z. Xu, X. Jiang, Y. Li, M. Wang, Cytotoxic activities of chitosan nanoparticles and copper-loaded nanoparticles. Bioorganic & Medicinal Chemistry Letters 15(5) (2005) 1397-1399.

[23] H. Yin, H.P. Too, G.M. Chow, The effects of particle size and surface coating on the cytotoxicity of nickel ferrite. Biomaterials 26(29) (2005) 5818-5826.

[24] D. Fischer, Y. Li, B. Ahlemeyer, J. Krieglstein, T. Kissel, In vitro cytotoxicity testing of polycations: influence of polymer structure on cell viability and hemolysis. Biomaterials 24(7) (2003) 1121-1131.

[25] H. Lv, S. Zhang, B. Wang, S. Cui, J. Yan, Toxicity of cationic lipids and cationic polymers in gene delivery. Journal of Controlled Release 114(1) (2006) 100-109.

[26] S. Taetz, N. Nafee, J. Beisner, K. Piotrowska, C. Baldes, T.E. Mürdter, H. Huwer, M. Schneider, U.F. Schaefer, U. Klotz, C.M. Lehr, The Influence of Chitosan Content in Cationic Chitosan/PLGA Nanoparticles on the Delivery Efficiency of Antisense 2'-O-Methyl-RNA Directed Against Telomerase in Lung Cancer Cells. European Journal of Pharmaceutics and Biopharmaceutics In Press, Accepted Manuscript.

[27] C. Schulze, A. Kroll, C.-M. Lehr, U.F. SchÃ¤fer, K. Becker, J.r. Schnekenburger, C. Schulze Isfort, R. Landsiedel, W. Wohlleben, Not ready to use - overcoming pitfalls when dispersing nanoparticles in physiological media. Nanotoxicology 2(2) (2008) 51-61.

[28] B. Carreno-Gomez, R. Duncan, Evaluation of the biological properties of soluble chitosan and chitosan microspheres. International Journal of Pharmaceutics 148(2) (1997) 231-240.

[29] S.C.W. Richardson, H.V.J. Kolbe, R. Duncan, Potential of low molecular mass chitosan as a DNA delivery system: biocompatibility, body distribution and ability to complex and protect DNA. International Journal of Pharmaceutics 178(2) (1999) 231-243.

[30] H. Mueller, M.U. Kassack, M. Wiese, Comparison of the Usefulness of the MTT, ATP, and Calcein Assays to Predict the Potency of Cytotoxic Agents in Various Human Cancer Cell Lines. Journal of Biomolecular Screening 9(6) (2004) 506-515.

[31] P. Ferruti, S. Knobloch, E. Ranucci, E. Gianasi, R. Duncan, A novel chemical modification of poly-l-lysine reducing toxicity while preserving cationic properties. Proc Int Symp Control Rel Bioact Mater 24 (1997) 45-46.

[32] S. Choksakulnimitr, S. Masuda, H. Tokuda, Y. Takakura, M. Hashida, In vitro cytotoxicity of macromolecules in different cell culture systems. Journal of Controlled Release 34(3) (1995) 233-241.

[33] A. Singh, B. Kasinath, E. Lewis, Interaction of polycations with cell-surface negative charges of epithelial cells. Biochim Biophys Acta 1120 (1992) 337-342.

[34] H. Ryser, A membrane effect of basic polymers dependent on molecular size. Nature 215 (1967) 934-936.

[35] J. Smith, E. Wood, M. Dornish, Effect of Chitosan on Epithelial Cell Tight Junctions. Pharm. Res. 21(1) (2004) 43-49.

Chapter 6

cNPs/OMR nanoplexes as inhalation therapy for lung cancer

Nebulization and cellular uptake on air interface cultures*

***This chapter is prepared to be published as a journal article:**

N. Nafee, M. Schneider, U.F. Schäfer, and C.-M. Lehr. Nanoplexes of antisense oligonucleotides as inhalation therapy for lung cancer: nebulization and cellular uptake on air interface cultures.

Abstract

Purpose: Aerosol nanoparticulate delivery to the lungs is always associated with serious challenges among which is the nebulization of nanoparticles. In this chapter, we aimed to select the most appropriate techniques for nebulization of the nanoparticles that preserve their colloidal properties as well as the efficiency of the associated antisense oligonucleotide. In addition, a new alternative to the conventional liquid cell culture models is the air-interface-culture model (AIC), which enables direct contact of the lung epithelial cells with air while the culture medium is supplied to the cells only from the basolateral side. Therefore, this *in vivo* mimicking culture system is applied to investigate the deposition and uptake of nanoparticles/nanoplexes on the cell monolayer.

Methods: Two different nebulizers, a hydraulic liquid microsprayer and an electronic mesh nebulizer were tested. The one preserving the colloidal properties of the particles was selected for further studies. Thereafter, the nanoplexes were deposited on the surface of air interface cultured A549 cells. The uptake behavior and possible cytotoxicity on the cell monolayer were investigated.

Results: The hydraulic microsprayer offered greater colloidal stability to the nanoparticles during nebulization compared to the electronic mesh nebulizer. A significant improvement in the uptake of nanoplexes versus naked oligonucleotides was observed when deposited on air interface cultured A549 cells, indicating the feasibility of the delivery system for pulmonary application.

Conclusions: This study shows the feasibility of NP/OMR nanoplexes as inhalation therapy for the treatment of lung cancer. Studying the uptake after air interface deposition represents a step forward to the *in vivo* studies.

Background

In the context of pulmonary delivery, polymeric nanoparticles could represent a non-invasive alternative either for the local targeting of airway epithelium or for systemic absorption through the alveolar deposition. The majority of pulmonary drug delivery systems were based on microparticles in the form of dry powder inhalation [1], while few studies have recently shown interest in nanoparticle technology [2, 3]. The application of non-biodegradable polymers like polystyrene or silica in the lung remains questionable especially in cases where multiple dosing is required. Thus, a tendency toward the use of biodegradable polymers is always preferable. However, aerosol nanoparticulate delivery to the lungs - especially those based on biodegradable polymers - is always associated with several serious challenges among which is the nebulization of nanoparticles with minimum alteration in their colloidal characteristics, integrity and the full efficiency of the delivered drug.

In comparison to other delivery systems like liposomes, polymeric nanoparticles are expected to exhibit a greater stability against the forces generated during the nebulization process. Several studies with liposomes have shown that the shear forces generated during jet nebulization as well as the high energy produced by ultrasonic nebulization can disturb liposomal integrity thus leading to rupture and leakage of the drug compound [4, 5]. However, many researches reported the susceptibility of micro- and nanoparticles to aggregation during the nebulization [6]. The behavior of the nanoparticles suspension during nebulization is assumed, inter alia, to be a function of the original size and surface characteristics of the particles and their concentration. A variety of inhalation devices are currently on the market including metered dose inhalers (MDI), dry powder inhalers (DPI) in addition to modern nebulizers based on pressure-driven atomisation, ultrasonic generation and electrospraying. The proper choice of the nebulizer that generates uniform

fine flow of the particles suspension with minimum susceptibility of particle aggregation is a prerequisite for efficient pulmonary delivery.

Most studies involving *in vivo* animal testing or *ex vivo* lung perfusion models utilise different types of nebulizers while very few are concerned with checking the effect of this process on the particle integrity and uniformity.

A new alternative to the conventional liquid cell culture models is the air-interface-culture model (AIC), which enables direct contact of the lung epithelial cells with air while the culture medium is supplied to the cells only from the basolateral side. This *in vivo* mimicking culture system is expected to give a better and more realistic idea about the deposition and uptake of nanoparticles/nanoplexes on the cell monolayer [7]. The uptake of nanoparticles in liquid cultures is known to be affected by their sedimentation rate on the cell surface; not the whole amount of particles added to the culture medium is in contact with the cells at once. As shown in Figure 1A, a significant amount remains suspended in the medium and probably removed after the incubation period without any contact with the cells. The amount of deposited particles is a function of their size, density and colloidal stability in the incubation medium. In this case the nanoparticle uptake depends on the amount of deposited particles on one hand and on the nanoparticle characteristics on the other hand, keeping in mind that the uptake can be a saturable process. On the other side, direct deposition of nanoparticles on the cell surface via nebulization on AIC, Figure 1B, neglects the effect of sedimentation rate as all the particles are almost accumulating on the cell monolayer, giving impression of better contact with the cell membrane and improved uptake. However, the hydrophilic/hydrophobic properties of the particles affect the water shell on the nanoparticle surface and accordingly their interaction with the thin liquid layer on the cell surface as mentioned above, which in turns can have a remarkable impact on the uptake.

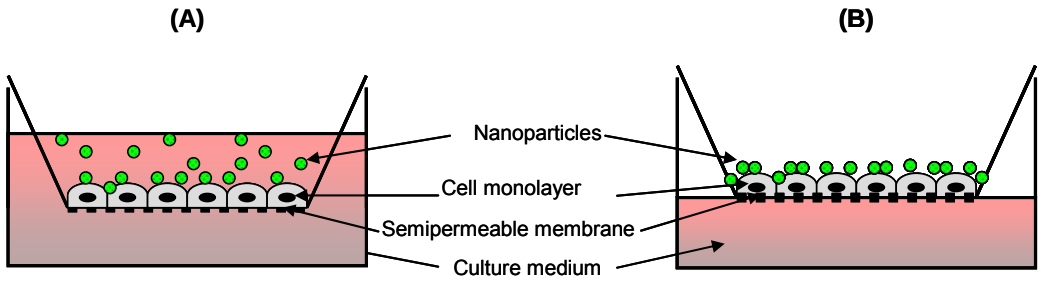

Figure 1: Schematic presentation of nanoparticle deposition on (A) Liquid-liquid culture, and (B) AIC

In chapter 4, we demonstrated the potential of chitosan-modified PLGA nanoparticles to bind the negatively charged antisense oligonucleotide 2'O-Methyl RNA (OMR) and to improve their cellular uptake by human lung cancer cell lines A549 on a liquid interface. In this chapter, we aimed to select the most appropriate techniques for nebulization of the nanoparticles that preserve their colloidal properties as well as the efficiency of the associated antisense oligonucleotide. Thereafter, the nanoplexes will be deposited on the surface of air interface cultured A549 cells. The uptake behavior and possible cytotoxicity on the cell monolayer will be investigated.

Materials and Methods

Materials

Poly(D,L-lactide-*co*-glycolide) 70:30 (Polysciences Europe GmbH, Eppelheim, Germany), polyvinyl alcohol; Mowiol® 4-88 (Kuraray Specialities Europe GmbH, Frankfurt, Germany), ultrapure chitosan chloride: Protasan® UP CL113 with a molecular weight of < 150 kDa (FMC BioPolymer AS, Oslo, Norway), 4',6-Diamidino-2-phenylindole dihydrochloride (DAPI, λ_{Ex} = 374 nm, λ_{Em} = 461 nm) and ethyl acetate (Fluka Chemie GmbH, Buchs, Switzerland) were used as obtained. The antisense oligonucleotide, 2'O-MethylRNA with a phosphorothioate (ps) backbone (5′-2′-O-methyl

[C(ps)A(ps)GUUAGGGUU (ps)A(ps)G]-3′) was obtained from (Biomers.net GmbH, Ulm, Germany). For the uptake studies, the carboxyfluoresceinamine-labeled derivative 5′-FAM-OMR was used. RPMI 1640 supplemented with L-glutamine and 10% fetal calf serum (PAA Laboratories GmbH, Pasching, Austria) was used as cell culture medium. Rhodamine-labeled ricinus communis agglutinin I (RRCA, λ_{Ex} = 522 nm, λ_{Em} = 577 nm) from Vector Laboratories Peterborough, England, was applied for cell membrane staining.

Methods

1. Preparation of nanoparticles

Cationically modified nanoparticles, cNP, were prepared using the emulsion diffusion evaporation technique previously described. To prepare the nanoplexes, cNP were mixed with an aqueous solution of the oligonucleotide 2OMR in a weight ratio cNP : 2OMR (50:1) at room temperature and vortexed for 30 s followed by 15 min incubation at room temperature. The nanoplexes formed were nebulized as described with the nanoparticles.

2. Nebulization of nanoparticles/nanoplexes

2.1. Colloidal characterization after nebulization

Two different nebulizers were used in this study: the hydraulic liquid microsprayer Penn Century® (Model IA-1C, Penn Century Inc., Philadelphia, USA) and the electronic mesh nebulizer, eFlow® (Pari, Starnberg, Germany), Figure 2 A & B, respectively. Samples of the nanoparticles suspension/nanoplexes were nebulized and collected in falcon tubes for further investigations. The colloidal characteristics and the particle morphology were determined using the Malvern Zetasizer Nano (Malvern Instruments,

Malvern, UK) and scanning probe microscopy (Digital Instruments, Veeco, Santa Barbara, California, USA), respectively.

(A) **(B)**

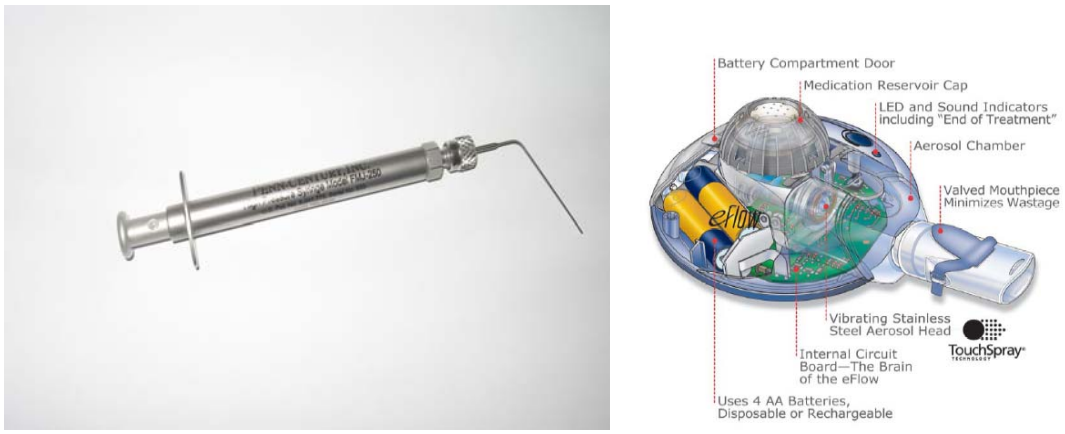

Figure 2: (A) Penn Century nebulizer, (B) eFlow, Pari nebulizer.

2.2. Cytotoxicity of nanoparticles after nebulization applied as suspension

The effect of chitosan modified PLGA nanoparticles on the cell viability and the membrane integrity was studied by the MTT and LDH assays, respectively. Human lung carcinoma A549 cell lines (100,000 cells/ml) were seeded in 24-well plates using RPMI supplemented with 10% FCS as culture medium. The cells were incubated at 37^{o}C, 95% RH and 10% CO_2 and allowed to adhere overnight. Samples of the nanoparticles before and after nebulization were incubated with the cells for 6h. After the incubation period, the supernatants were used for the LDH assay whereas the cell surface was washed twice with warm, sterile phosphate buffer saline (PBS) then incubated with fresh culture medium. On the next day the cells were incubated with MTT solution for 3-4 h. The formazan crystals were dissolved using acidified isopropanol. The absorbance was measured at 550 nm. The viability was determined as a percentage of the control cells cultivated in culture medium. Measurements were performed in quadruplicates.

2.3. Cellular uptake of cNP/OMR nanoplexes after nebulization applied as suspension

The uptake of the nanoplexes before and after nebulization was investigated using A549 human lung carcinoma cells. The cells were seeded on LabTec chamber slides (Nunc GmbH, Wiesbaden, Germany) at a density of 100,000 cells/ml. Nanoparticles incubated with fluorescently labeled oligonucleotides 5'-FAM-2'-OMR were mixed with the culture medium RPMI supplemented with 10 % FCS then added to the cells. After 6 h of incubation, the medium was replaced by normal cell culture medium. After 24 h, cell membranes were stained red with RRCA and then fixed with 4% paraformaldehyde in PBS. The uptake was then examined by confocal laser scanning microscopy (CLSM) as will be described. For comparison control cells incubated with medium and with the labeled oligonucleotide in the medium were investigated as well.

2.4. Confocal Laser Scanning Microscopy

Fluorescence imaging was performed using a BioRad MRC-1024 confocal laser scanning microscope equipped with an argon/krypton laser. The objective used was an oil immersion objective 40x NA=1.3. The excitation was performed using $\lambda = 488$ nm.

Furthermore, a Zeiss510LSM META NLO system (Jena, Germany) was used. The set-up made use 100x objective and of an argon ion laser line at $\lambda = 488$ nm to excite the oligonucleotides, a HeNe-laser with $\lambda = 524$ nm to excite the Rhodamin-labeled RCA (cell membrane staining) and a pulsed Ti:Sapphire laser operating at $\lambda = 730$ nm (~150 fs pulses, 80 MHz repetition rate) to excite DAPI based on the absorption of two or more photons.

The green fluorescent particles were located with respect to the red stained cell membrane and the blue stained cores.

3. Nanoparticle deposition on air interface culture

3.1. Air interface culture

A549 cells were seeded at 200,000 cells/ml onto the membrane culture insert (Costar Transwell 3460, pore size 0.4 μm, Corning, Cambridge, MA, USA). Initially, culture medium was added to both apical (Ap) and basolateral (BL) sides. The formation of cell monolayer was assessed microscopically and by measuring the transepithelial resistance (TEER) reflecting the development of tight junctions in the cell layer. A549 cells were cultured in liquid phase until the TEER showed constant values of ~ 50 Ω after subtraction of the resistance of the empty filter. Then, the culture medium was removed from the Ap side and cell monlayers continued to grow on AIC for ~ 5 days.

3.2. Cytotoxicity of nanoparticles/nanoplexes after air deposition

Nanoparticles (0.9 mg/ml) as well as their nanoplexes with 2OMR (50:1) in NaCl solution 10 mM were sprayed on the surface of AI-cultured A549 cell monolayer using the Penn Century®. In addition, AIC cells as well as cells treated with NaCl solution were used as control. After 6h of incubation with the samples, NaCl solution (200 μl/well) were added to the Ap side to extract the LDH released and the LDH assay was carried out as previously described. Samples from the BL side were also collected to check the amount of LDH in the lower compartment. Acute and prolonged toxicity due to nebulization and/or NP deposition were determined by monitoring the LDH release after 0, 2, and 24 h. In addition, cell viability was checked by ATP assay as described in the previous chapter.

3.3. Uptake of cNP/OMR nanoplexes after air deposition

Nanoplexes of cNPs with FAM-labeled-OMR in the weight ratio 50:1 were prepared in 3 different media; MilliQ water, NaCl solution 10 mM and HEPES buffer 25 mM. AI-cultured A549 cells were sprayed with nanoplexes and incubated for 6 h. The uptake of

nanoplexes (indicated by the green fluorescence) was examined by CLSM after staining the cell membrane (red) with RRCA and the nuclei (blue) with DAPI as previously described.

Results and Discussion

1. Nebulization of nanoparticles

1.1. Colloidal properties of nebulized nanoparticles

It is well known that the particle deposition in the respiratory system is greatly influenced by the aerodynamic particle behaviour (including size, density, hygroscopicity, shape, and electrostatics). Therefore, the efficiency of a nebulizer is mainly judged by the determination of Mass Median Aerodynamic Diameter (MMAD). In general, particles with an aerodynamic diameter of 3 μm are mainly deposited in the alveolar region, beyond this level bronchial deposition starts to increase. Most of the studies are always interested in determining the MMAD to show the efficacy of the nebulization process; however, very few investigate the colloidal stability of the nanoparticles within the aerosolised droplets. Nevertheless, the stability of the nanoparticles is crucial for the use of nanoscale carriers. In this study, nanoparticle suspensions were nebulized using the microsprayer Penn Century® as well as the electronic mesh nebulizer eFlow® (Pari). Figure 3A-C demonstrates the stability of the nanoparticles in term of size, charge and morphology after nebulization using the hydraulic microsprayer Penn Century; the particles preserve their integrity, spherical shape, mean diameter and surface charge despite the small change in their polydispersity.

In contrast, the eFlow® (Pari) utilizes advanced technology in order to increase the efficiency and effectiveness of medication delivery while significantly decreasing standard

treatment times. The device contains a perforated flat stainless steel membrane with tapered holes (several hundreds to several thousands).

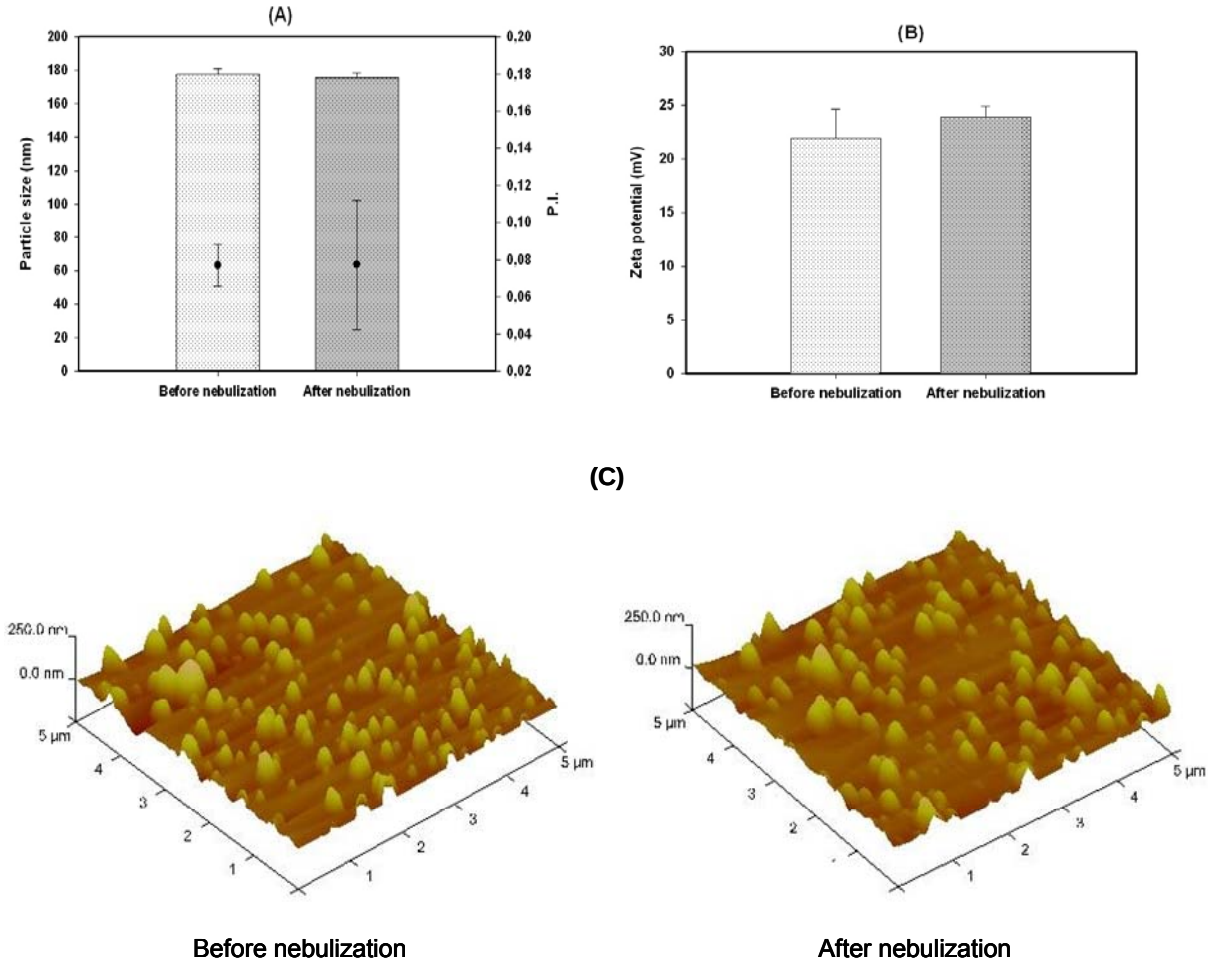

Figure 3: Nebulization of nanoparticles using the microsprayer Penn Century® (A) particle size & size distribution, (B) ζ-potential and (C) particle morphology as observed by SPM.

A piezoelectric actuator is used to induce the vibration of the membrane. The liquid is drawn through these tapered apertures to give a droplet size specified by the manufacturer as having a volume median diameter (VMD) ranging from 2.5 - 4.5 µm. In our experiments, two different aerosol heads characterized by two mesh sizes and resulting different particles distributions 25L and 30L were used. Measurements of the nanoparticle size after nebulization using the Malvern Zetasizer Nano revealed minor changes in the mean nanoparticle diameter (monomodal size distribution) when the mesh 25L was used (Figure 4A), however, a distinct drop in the count rate was observed together with the

appearance of agglomerates of the particles floating on the surface of the sample collected after nebulization. Examination of this sample by the SPM (Figure 4C) demonstrates the presence of dispersed nanoparticles as well as aggregates of deformed nanoparticles. The effect was more distinct when the mesh 30L was used during nebulization; the mean size and charge of the particles were almost doubled; Figure 4A & B, and huge aggregates of fused particles (> 1 μm) were observed by the SPM, Figure 4C. Particle aggregation may not only affect the properties of the suspension during nebulization, but also influence the overall dose to be applied. In addition, aggregates could block the apertures of the aerosol generating nozzle system, thereby affecting the aerosol formation. Particle adhesion to the surface of the nebulizer and the formation of multimodal particle size distributions have also been reported for polycation-DNA polyplexes when a vibrating mesh nebulizer was used [8]. The forces acting on nebulized droplets such as electrostatic charges and high shear forces could be responsible for particle destabilization. The energy involved in the generation of the aerosol and the elevated temperatures contribute to a high frequency of particle contact and accordingly promote a tendency towards aggregations.

Previous studies demonstrated clearly that a certain degree of surface hydrophilicity was essential to prevent particle aggregation within aerosolized fluid droplets during nebulization [6]. On the other hand, it was also observed that anionic nanoparticles are more stable during nebulization compared to positively charged nanoparticles [2].

Based on the previously shown findings, we decided to continue our investigations using the Penn Century®.

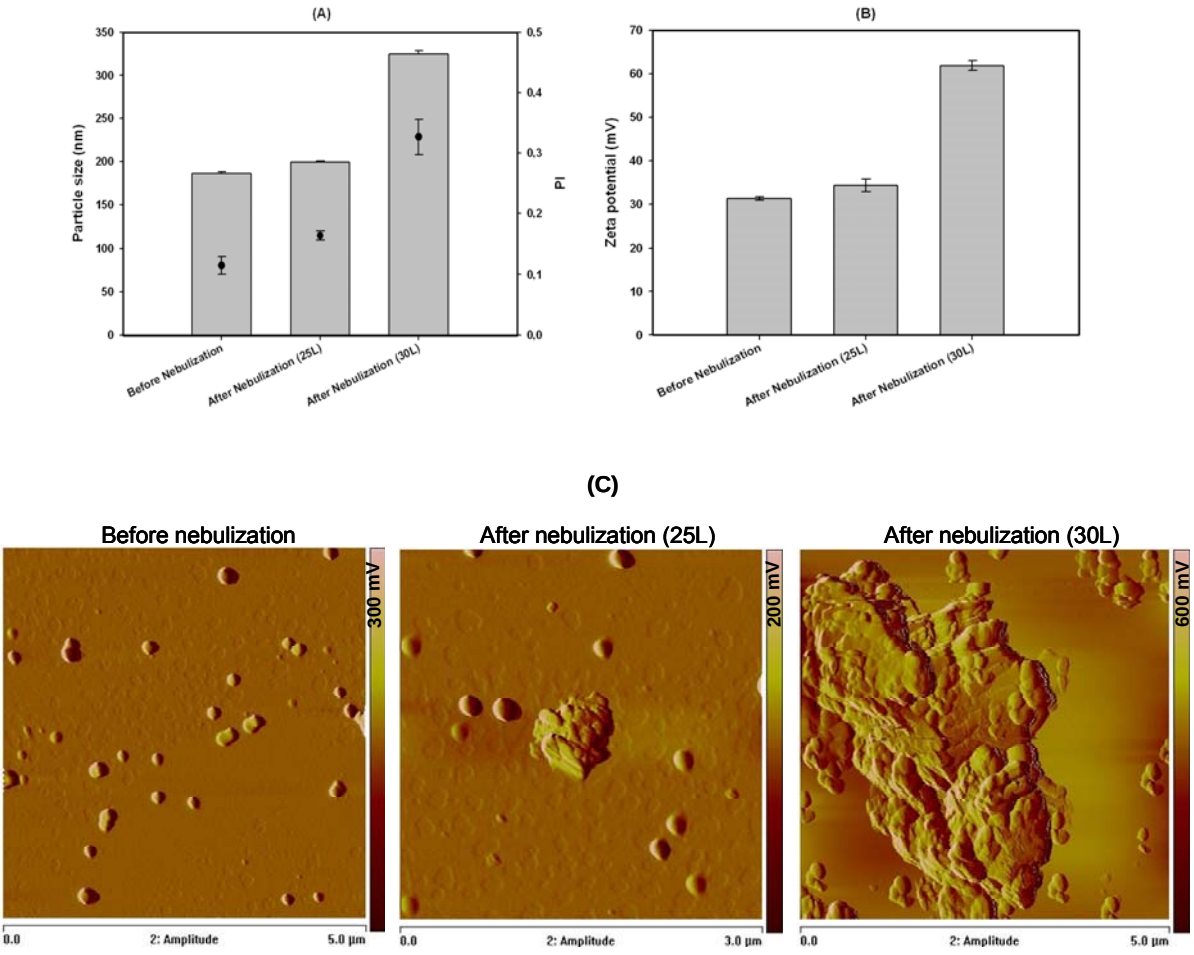

Figure 3: Nebulization of nanoparticles using the electronic mesh nebulizer eFlow® (A) particle size and size distribution, (B) ζ-potential and (C) particle morphology as observed by SPM.

1.2. Cytotoxicity of the nebulized nanoparticles

As for any substance or treatment, the possible effect of the nebulization on the cytotoxicity needs to be carefully investigated (e.g. surface modification). This especially holds for nanoparticulate material. Therefore, after checking the colloidal stability of chitosan modified nanoparticles during nebulization with the Penn Century®, it was important to check the effect of the nebulization process on the cytotoxicity of the nanoparticles. For this reason, original nanoparticles as well as nanoparticles collected after nebulization with the Penn Century® were tested on A549 cell lines using MTT and LDH assays. The incubation of the cells with the nanoparticles (whether nebulized or not)

for 6 h had no effect on the cell viability compared to the control cells in the culture medium, Figure 5A, indicating that nebulization of the nanoparticles had no harmful effect on cell viability. Similarly, negligible changes in the integrity of the cell membrane were noticed from LDH assay, Figure 5B.

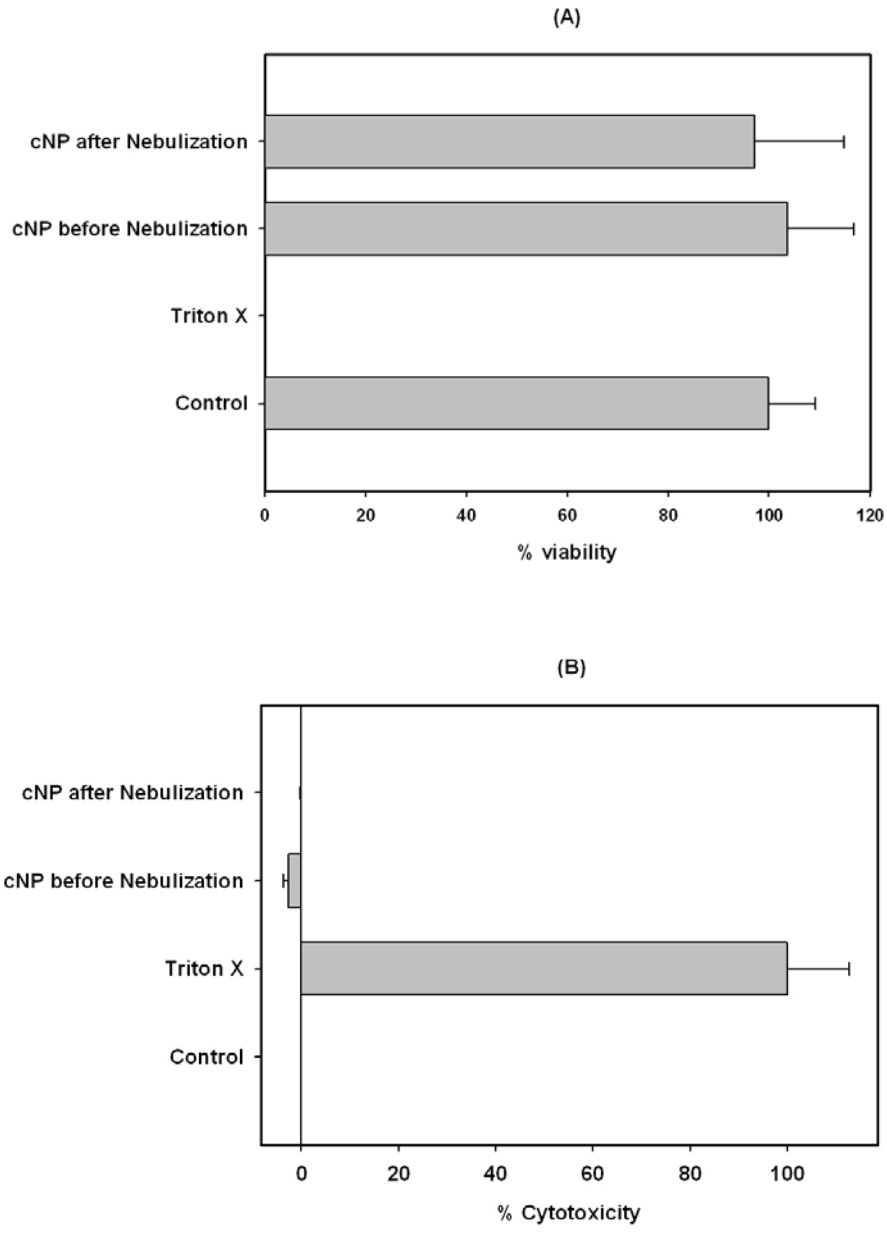

Figure 5: Cytotoxicity study of nanoparticles before and after nebulization (A) MTT assay, (B) LDH assay.

1.3. Uptake of OMR/cNP nanoplexes pre- and post-nebulization

The main objective behind our study is improving the uptake of the antisense oligonucleotide inside the lung cancer cells. Therefore, it was very important to investigate whether the nebulization process would affect the cellular uptake of these nanoplexes as a prerequisite prior to *ex vivo* or *in vivo* applications. A549 cells were incubated with non-nebulized FAM-OMR/cNP nanoplexes and nanoplexes collected after nebulization with Penn Century ®. The internalization of the FAM-OMR indicated by the green fluorescence in the cells (cell membrane stained red with RRCA) was demonstrated by CLSM. In comparison to the control cells and those incubated with the FAM-OMR alone, a significant increase in the green fluorescence connected to the uptake of nanoplexes was observed, Figure 6A-C.

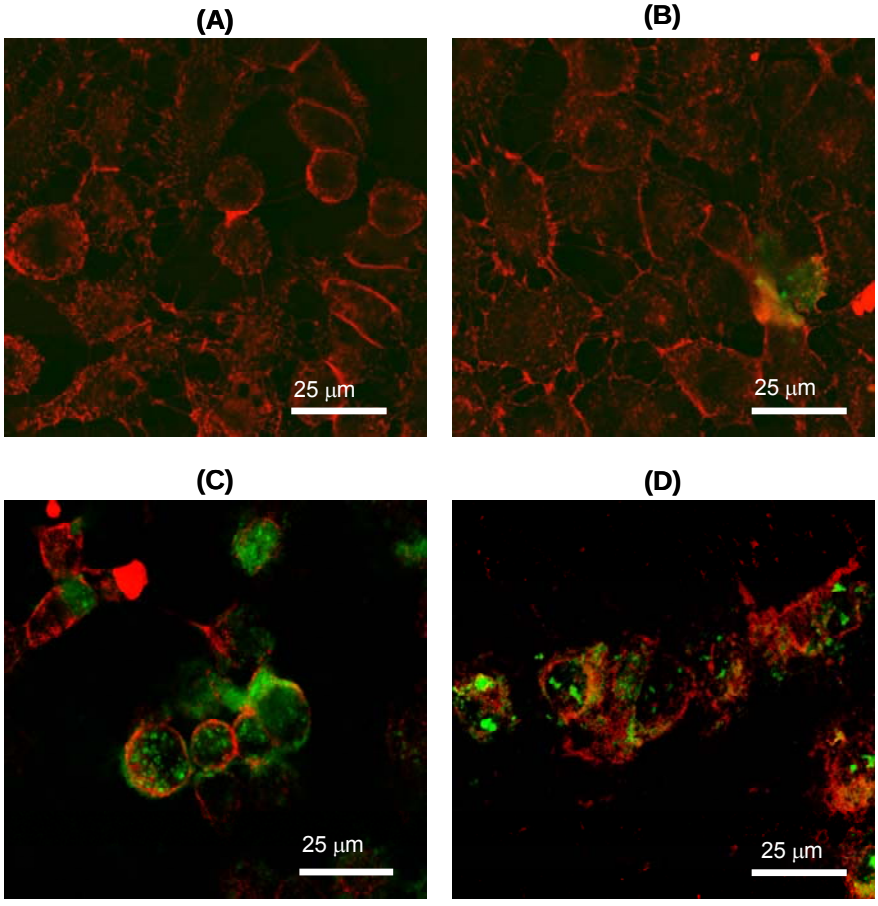

Figure 6: Uptake of cNP/OMR nanoplexes in A549 cell lines (A) control cells, (B) FAM-OMR, (C) cNP/FAM-OMR nanoplexes before nebulization and (D) cNP/FAM-OMR nanoplexes after nebulization.

The ability of the nanoparticles to act as a delivery system for OMR was already shown in chapter 4 with non-aerosolized particles [9]. Further studies indicated that nebulization of our nanoparticles using the Penn Century preserve the colloidal stability of the particles, the cell viability and membrane integrity. In addition, the potential of binding of cNP/OMR nanoplexes to A549 cells was maintained after nebulization, Figure 6D.

2. Air interface deposition of nanoparticles

2.1. Cytotoxicity of nanoparticles after air deposition

In the previous part, we demonstrated that nebulized nanoparticles are benign to the cells when cultured on a liquid-liquid interface. However, the nebulization process itself can cause certain stress on the cell monolayer when grown at air interface. Besides, nebulized nanoparticles are directly deposited on the AI-cultured cell surface opposite to those suspended in the culture medium above the cells and need certain time to sediment and come into direct contact with the cells.

Preliminary studies on nebulization of nanoparticles in suspension form produced a high mechanical pressure on the cell monolayer, as illustrated in the membrane cross section, Figure 7A, showing severe destruction of the monolayer independent of the sample applied. For this reason, the spraying procedure was modified in order to minimize the pressure on the cells and preserve the cell membrane integrity. Microscopical examination of the membrane cross sections showed no disruption in the cell monolayer, Figure 7B.

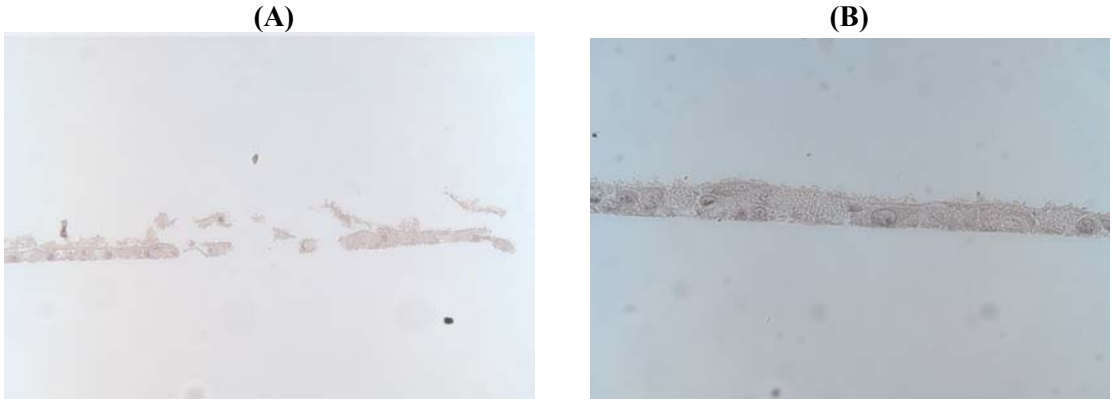

Figure 7: Membrane cross section showing destruction of A549 cell monolayer after nebulization (A) preliminary trial and (B) modified nebulization technique

Furthermore, LDH assay (performed directly after spraying, 2 and 24 h later) showed LDH levels released in case of nanoparticles/nanoplexes comparable to the control. This proves that the membrane integrity was retained after nebulization and along the study period, Figure 8A. Similarly, checking the cell viability under the same condition by detecting the ATP level showed no remarkable differences between the cells sprayed with NaCl solution, cNPs and their nanoplexes with the oligonucleotides, Figure 8B.

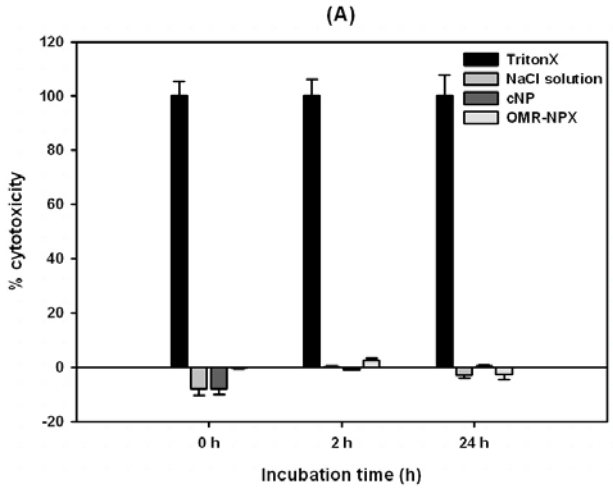

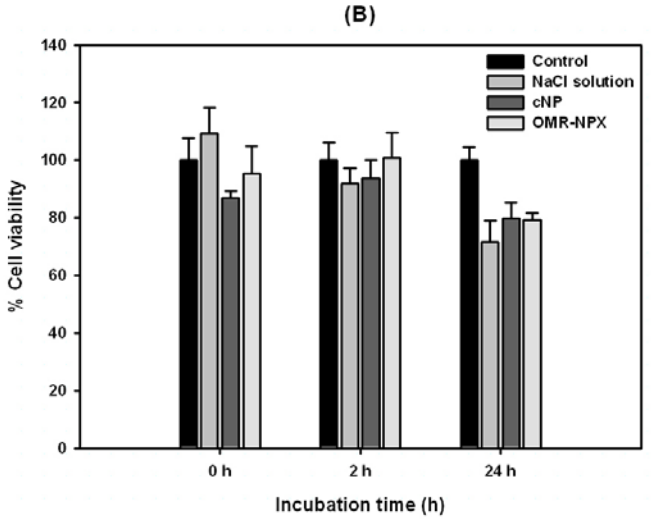

Figure 8: Effect of nebulization on air interface cultured A549 cells: (A) LDH assay, (B) ATP assay

2.2. Uptake of nanoplexes after air deposition

As previously mentioned, higher amounts of nanoparticles/nanoplexes can be deposited on the cell surface via nebulization compared with those in conventional liquid phase loading; accordingly, different uptake behavior could be predicted.

The uptake of naked oligonucleotide solution and their nanoplexes with chitosan-modified PLGA nanoparticles on AI-cultured A549 cells was studied. CLSM images, Figure 9 A-C, shows AI-cultured A549 cells after incubation with FAM-OMR and the nanoplexes for 6 h. the images revealed the significantly higher amount of FAM-OMR internalized when applied as nanoplexes, Figure 9C, compared to the FAM-OMR solution sprayed alone, Figure 9B. In addition, the XZ-sections showed the localization of nanoplexes in the cytoplasm as spots or point shaped, while naked oligonucleotides are mostly attached to the membrane.

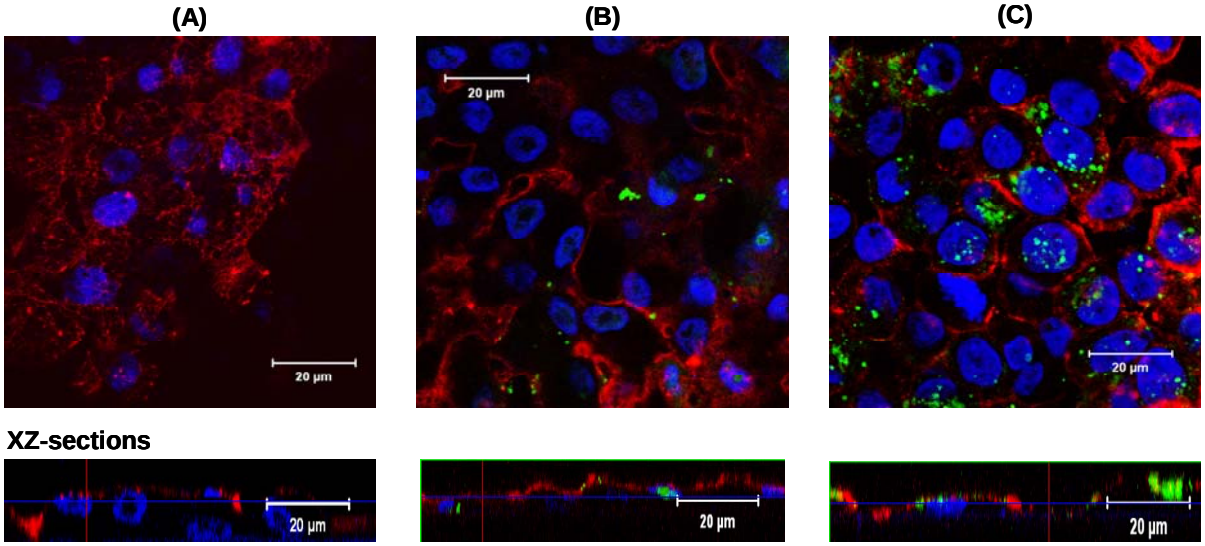

Figure 9: Uptake of FAM-OMR after nebulization on AI-cultured A549 cells: (A) Control, (B) FAM-OMR solution in water, and (C) FAM-OMR/cNP nanoplexes in water

The influence of the medium used to prepare the nanoplexes on the uptake was verified by substituting water with NaCl solution 100mM and HEPES buffer 25 mM. As shown in Figure 10, the uptake was also improved by applying the nanoplexes instead of the oligonucleotides alone. Nanoplexes prepared in NaCl solution are observed to fill the cytoplasm around the cores and probably a considerable amount in the cores as well, as illustrated in the CLSM image and the corresponding XZ-section underneath, Figure 10C.

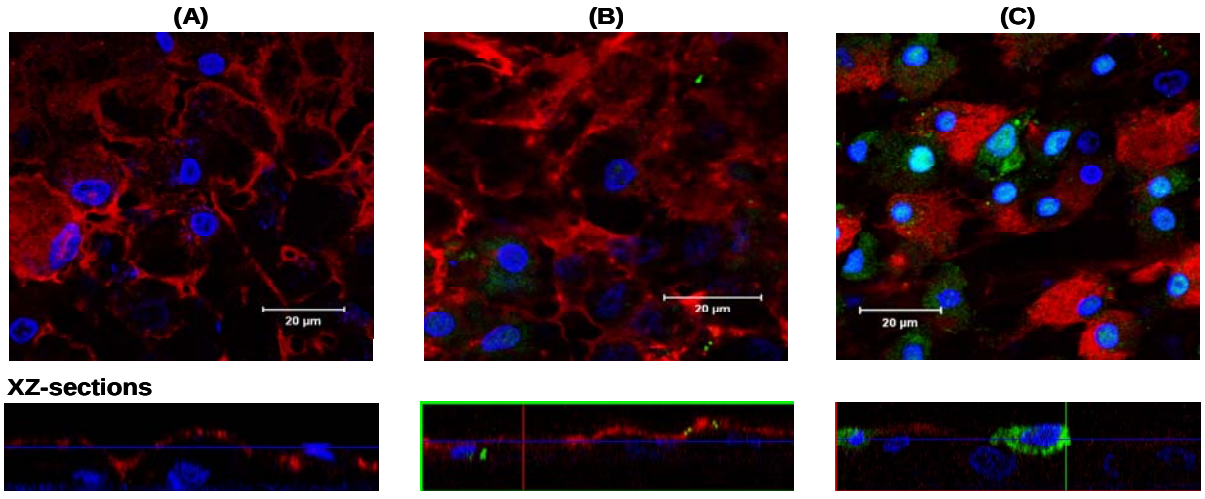

Figure 10: Uptake of FAM-OMR after nebulization on AI-cultured A549 cells: (A) Control, (B) FAM-OMR solution in NaCl solution, and (C) FAM-OMR/cNP nanoplexes in NaCl solution

The same enhancement in uptake by using the nanocarrier system was also noticed when the nanoplexes were prepared in HEPES buffer, Figure 11.

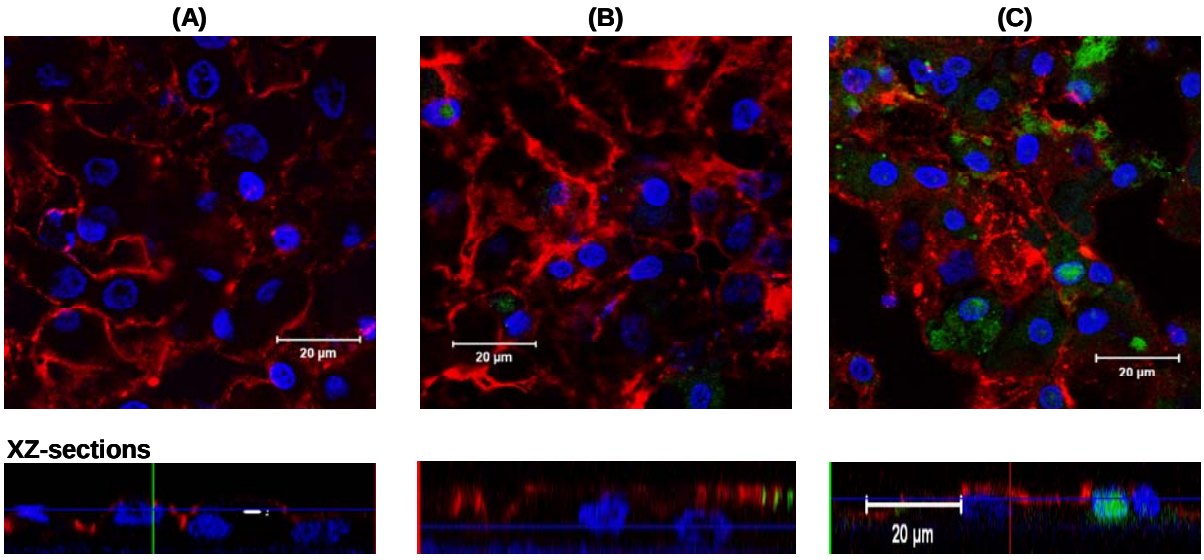

Figure 11: Uptake of FAM-OMR after nebulization on AI-cultured A549 cells: (A) Control, (B) FAM-OMR solution in HEPES buffer, and (C) FAM-OMR/cNP nanoplexes in HEPES buffer

Generally speaking, several aspects can influence the nanoparticle uptake through AIC compared to conventional liquid cultures. Cells grown on air interface are known to be covered by a thin liquid film on their surface. The existence of an aqueous lining layer covering the surface of the conducting airways and a surfactant film at the air-liquid interface was previously demonstrated [10]. The surfactant lining layer (10–20nm in thickness) that covers the alveolar surface is composed of 90% in weight of water-insoluble long chain phospholipids and 10% in weight of specific proteins [11]. The principle role of these pulmonary surfactants is to stabilize the gas-exchange region of the lung by reducing the surface tension at the air-liquid interface of the alveoli. Once deposited within the lung lining via nebulization, nanoparticles are expected to interact with this surfactant film. It was found that regardless of the nature of the nanomaterials surfaces, they will be submersed into the lining fluids after their deposition [12]. Many groups were interested in studying the interaction of nanocarriers with lung surfactants [13-

15]. Such interaction is thought to be dependent on the physicochemical properties of the particles from one side and on the cell type from the other side. Inhaled nanomaterials that are either lipid-soluble or soluble in intracellular or extracellular fluids undergo chemical dissolution in situ. Low molecular weight hydrophobic molecules are thought to be rapidly absorbed (within seconds) by passive diffusion through the lung epithelial membrane [16]. Low molecular weight hydrophilic molecules can be absorbed by active transport via specific transporters, or by passing through the tight junctions [17]. Inhaled nanomaterials that are insoluble in mucus and lining fluid, are not able to be rapidly absorbed, and may undergo physical translocation.

In general, cells grown on air interface can build up a tight monolayer through the formation of tight junctions between the cells. Pulmonary cell lines like Calu-3 cells are characterized by remarkably high TEER values > 1000 Ωcm^2, reflecting the formation of a very tight monolayer. On the other hand, A549 cells in AIC build up only TEER < 200 Ωcm^2. By immunostaining of tight junction protein zonula occludens (ZO-1), they show a broken tight junction belt. This is obviously expected to influence the paracellular uptake and the transport rate of the nanoparticles across such a monolayer.

Studying the uptake of nanoparticles and/or nanoplexes on AIC represents a real big step towards the *in vivo* expectations. The ability of our nanocarrier system to be internalized and in a significant amount under these conditions while preserving the integrity of the cell monolayer enables to predict efficient pulmonary delivery in future *ex vivo* studies using lung perfusion models or *in vivo* studies on experimental animals.

Conclusions

Efficient aerosol delivery of the nanoparticles necessitates the proper choice of the nebulizer as well as the application procedure. Essential parameters to be considered are

the colloidal stability of the particles, good spreadability, the full efficiency of the delivered payload and preservation of an intact cell monolayer. Nanoparticles nebulized using the hydraulic liquid microsprayer reserve their characteristics, morphology, their safety as well as their efficacy to form nanoplexes with antisense oligonucleotide and their potential to promote their intracellular uptake. However, electronic mesh nebulizer caused particle aggregation and fusion. An *in vivo*-mimicking step was to investigate the uptake of nanoplexes on air interface-cultured A549 cells. A significant improvement in uptake of nanoplexes versus naked oligonucleotides was observed, indicating the feasibility of the delivery system for pulmonary application.

REFERENCES

[1] H. Courrier, N. Butz, T. Vandamme, Pulmonary drug delivery systems: recent developments and prospects. Crit Rev Ther Drug Carrier Syst 19(4-5) (2002) 425-498.

[2] L.A. Dailey, E. Kleemann, M. Wittmar, T. Gessler, T. Schmehl, C. Roberts, W. Seeger, T. Kissel, Surfactant-Free, Biodegradable Nanoparticles for Aerosol Therapy Based on the Branched Polyesters, DEAPA-PVAL-g-PLGA. Pharm. Res. 20(12) (2003) 2011-2020.

[3] N. Hernández-Trejo, O. Kayser, H. Steckel, R.H. Mueller, Characterization of nebulized buparvaquone nanosuspensions—effect of nebulization technology. Journal of Drug Targeting 13(8) (2005) 499-507.

[4] K.K.M. Leung, P.A. Bridges, K.M.G. Taylor, The stability of liposomes to ultrasonic nebulisation. International Journal of Pharmaceutics 145(1-2) (1996) 95-102.

[5] P.A. Bridges, K.M.G. Taylor, Nebulisers for the generation of liposomal aerosols. International Journal of Pharmaceutics 173(1-2) (1998) 117-125.

[6] L.A. Dailey, T. Schmehl, T. Gessler, M. Wittmar, F. Grimminger, W. Seeger, T. Kissel, Nebulization of biodegradable nanoparticles: impact of nebulizer technology and nanoparticle characteristics on aerosol features. Journal of Controlled Release 86(1) (2003) 131-144.

[7] H. Lin, H. Li, H.-J. Cho, S. Bian, H.-J. Roh, M.-K. Lee, J.S. Kim, S.-J. Chung, C.-K. Shim, D.-D. Kim, Air-liquid interface (ALI) culture of human bronchial epithelial cell monolayers as an *in vitro* model for airway drug transport studies. Journal of Pharmaceutical Sciences 96(2) (2007) 341-350.

[8] J. Lynch, N. Behan, C. Birkinshaw, Factors Controlling Particle Size during Nebulization of DNA-Polycation Complexes. Journal of Aerosol Medicine 20(3) (2007) 257-268.

[9] N. Nafee, S. Taetz, M. Schneider, U.F. Schaefer, C.M. Lehr, Chitosan-coated PLGA nanoparticles for DNA/RNA delivery: effect of the formulation parameters on complexation and transfection of antisense oligonucleotides. Nanomedicine: Nanotechnology, Biology, and Medicine 3(3) (2007) 173-183.

[10] J. Gil, E.R. Weibel, Extracellular lining of bronchioles after perfusion-fixation of rat lungs for electron microscopy. Anat Rec 169 (1971) 185-200.

[11] J. Goerke, Pulmonary surfactant: functions and molecular composition. Biochimica et Biophysica Acta (BBA) - Molecular Basis of Disease 1408(2-3) (1998) 79-89.

[12] M. Geiser, S. Schuerch, P. Gehr, Influence of surface chemistry and topography of particles on their immersion into the lung's surface-lining layer. Journal of Applied Physiology 94(5) (2003) 1793-1801.

[13] D. Stuart, R. benberg, T. Ku, S. Azarmi, L. Ely, W. Roa, E.J. Prenner, Biophysical Investigation of Nanoparticle Interactions with Lung Surfactant Model Systems. Journal of Biomedical Nanotechnology 2 (2006) 245-252.

[14] L. Mu, P.H. Seow, Application of TPGS in polymeric nanoparticulate drug delivery system. Colloids and Surfaces B: Biointerfaces 47(1) (2006) 90-97.

[15] A. Meyboom, D. Maretzki, P.A. Stevens, K.P. Hofmann, Interaction of pulmonary surfactant protein A with phospholipid liposomes: a kinetic study on head group and fatty acid specificity. Biochimica et Biophysica Acta (BBA) - Molecular and Cell Biology of Lipids 1441(1) (1999) 23-35.

[16] J.S. Patton, P.R. Byron, Inhaling medicines: delivering drugs to the body through the lungs. Nat Rev Drug Discov 6(1) (2007) 67-74.

[17] J.S. Patton, Mechanisms of macromolecule absorption by the lungs. Advanced Drug Delivery Reviews 19(1) (1996) 3-36.

SUMMARY

Lung cancer is one of the leading causes of cancer-related death worldwide. Current cancer therapy usually involves intrusive processes including chemotherapy, radiation and surgery.

Gene therapy provides a novel strategy for cancer treatment; promising approaches focus on such therapies that target specific proteins and pathways involved in the growth and proliferation of cancer cells. Much interest has recently been focused on ***telomerase***, a ribonucleoprotein that adds telomeric repeats to the end of the telomeres and therefore prevents telomere shortening occurring during replication of the cell cycle. Telomerase activity is required for continuous cell proliferation and allows cells to overcome senescence. Therefore telomerase inhibition using antisense oligonucleotides may represent a promising strategy for anticancer treatment. In our study, we chose the antisense oligonucleotide ***2´-O-methyl-RNA*** (OMR) as a potent and sequence-selective inhibitor of telomerase.

The major challenge in nucleotide-based therapy is the development of appropriate vectors. Nowadays, nanocarriers have gained great attention as promising drug/gene delivery systems, among which nanoparticles have shown broad applicability. Our main aim was hence to evaluate the potential of the biodegradable PLGA nanoparticle (NP) as carrier for OMR and the efficacy of the nano-delivery system as inhalation therapy for treatment of lung cancer. In order to improve the binding and uptake efficiency, the surface of PLGA nanoparticles was modified with the cationic polymer, chitosan, to establish an electrostatic interaction.

The working plan was as follows:

- ***Improvement of the physicochemical properties of the nanoparticles***

In this part (Chapter 2), we investigated the effect of polymer concentration, process parameters on the colloidal characteristics of the NP. As a result, a wide range of particle sizes (136 – 520 nm) and surface charges (13 – 60 mV) could be obtained. This reveals the flexibility and tune-ability of our delivery system in dependence of the payload.

- ***Purification of the nanoparticles***

The removal of excessive polymers and stabilizers from the NP suspension is a prerequisite for their *in vivo* application. Significant amounts of surfactants might lead to impaired lung function, inflammation or poor transfection efficiency. In this thesis, small-scale purification of NP was based on the centrifugal ultrafiltration while large-scale purification was done by size exclusion chromatography. Both techniques allowed efficient separation of the nanoparticles from the residual polymers while preserving the colloidal characteristics of the NP. In addition, the amount of the excessive polymers was quantified by colorimetric assays, revealing that all of the chitosan is bound while only 66 % of the stabilizer was consumed for the NP synthesis.

- ***Effect of surface charge of NP on their binding and uptake in lung cancer cell lines and their efficiency as carrier for the antisense oligonucleotides (OMR):***

A net positive charge on the NP surface is intended to increase both their binding potential with the negatively charged oligonucleotides and their tranfection efficiency. However, a linear correlation between the surface charge and the transfection efficiency cannot be assumed. Therefore, the uptake efficiency of fluorescently labeled NPs containing increasing concentrations of chitosan (and accordingly carrying higher surface charges) was studied in two human pulmonary cancer cell lines. The results showed better uptake in A549 cells compared to Calu-3 cells. Surface modification with chitosan significantly improved the nanoparticles uptake in comparison to PLGA NPs; however,

increasing chitosan concentration above certain limit remarkably reduces the uptake efficiency. In addition, the binding potential with OMR increased by increasing the charge of the NP, indeed, a common saturation point was reached at equal OMR:NP ratio. The uptake of OMR:NP nanoplexes followed the same tendency as the fluorescent NPs alone. Despite the essential role of chitosan in improving the cellular uptake, self-assembled nanoplexes of OMR with chitosan solution were found to bind preferentially to the cell surface, while a poor internalization was observed.

- ***Cytotoxicity of chitosan-modified PLGA NP***

Although a positive surface charge of the NPs plays an essential role in cellular uptake, it is also known to have a negative influence on the cell membrane integrity and cell viability. Thus, it was necessary to verify the safety of our chitosan-modified PLGA nanoparticles on different cell lines. The study revealed that cytotoxicity of cNPs is a function of the cell line, being acceptable for A549 and Calu-3 cells (viability ~ 80%), even at longer incubation times (~ 24 h) and higher concentrations of chitosan on the NP surface. Nevertheless, the toxicity is thought to be underestimated due to the colloidal instability of the NPs in culture media, reduction in effective nanoparticle concentration in the nanosize range, in addition to adsorption of medium components to the nanoparticle surface. Slight shift of the surrounding pH allows ionization of chitosan and increase in surface charge of the nanoparticles, which as a consequence lead to more pronounced loss of membrane integrity of the cells.

- ***Nebulization of chitosan-modified PLGA NPs & uptake of OMR/NP nanoplexes on air-interface cultures (AIC)***

The application of our delivery system for cancer therapy involves its use in the form of inhalation product. Therefore, the proper choice of the nebulization technique that effectively delivers the system in the airways while preserving the colloidal characteristics, integrity and the full efficiency of the delivered payload is quite of interest. For this

purpose, two nebulizers were applied; a hydraulic liquid microsprayer and an electronic mesh nebulizer. Nanoparticles were stable after nebulization with the microsprayer, whereas agglomerates were obtained in case of the electronic mesh nebulizer.

An *in vivo*-mimicking step was to investigate the uptake of nanoplexes on AIC. In this part, naked oligonucleotides as well as their nanoplexes were sprayed on the surface of air interface-cultured A549 cells. A significant improvement in uptake of nanoplexes versus naked oligonucleotides was observed, indicating the feasibility of the delivery system for pulmonary application.

In conclusion, chitosan-modified PLGA nanoparticles can be considered as promising carrier for nucleotide-based drugs. Surface modification of nanoparticles with chitosan significantly improved the intracellular delivery of the oligonucleotides without being harmful for the cellular systems, which are prerequisites for their functionality. The efficacy of the delivery system on AIC reveals its suitability for *in vivo* applications, making real steps towards a new generation of cancer therapeutics.

Curriculum Vitae

Name	**Noha Nafee**
Date of birth	May 4th, 1971
Place of birth	Alexandria, Egypt
Email address	n.nafee@mx.uni-saarland.de nnadel_pharm@yahoo.com

EDUCATION:

1989	High School Diploma from the French School; École des Religieuses Franciscaines "Coeur Immaculé De Marie", Alexandria, Egypt.
1994	B.Sc. of Pharmacy, grade "Distinction" (honor), Faculty of Pharmacy, University of Alexandria, Alexandria, Egypt.
2002	M.Sc. of Pharmaceutical Sciences, grade "Distinction", Faculty of Pharmacy, University of Alexandria, Alexandria, Egypt. Thesis: "Formulation and evaluation of mucoadhesive drug delivery systems".

WORKING EXPERIENCE:

2005 - current	Ph.D. candidate, Biopharmaceutics and Pharm. Technology, Saarland University, Saarbrücken, Germany.
2005 - 2007	DAAD fellowship for Ph.D. research in Biopharmaceutics and Pharm. Technology, Saarland University, Saarbrücken, Germany.
2002 - 2005	Assistant lecturer, Department of Pharmaceutics, Faculty of Pharmacy, Alexandria University, Alexandria, Egypt.
1996 – 2002	Demonstrator, Department of Pharmaceutics, Faculty of Pharmacy, Alexandria University, Alexandria, Egypt.

SCIENTIFIC PUBLICATIONS:

1. **N. Nafee**, S. Taetz, M. Schneider, U. F. Schaefer, C.-M. Lehr. "Chitosan-coated PLGA nanoparticles for DNA/RNA delivery: Effect of the formulation parameters on complexation and transfection of antisense oligonucleotides". *Nanomedicine: Nanotechnology , biology, and medicine* 3:173-183 (2007).

2. **N. Nafee**, M. Schneider, U. F. Schaefer, C.-M. Lehr. Relevance of the colloidal stability of chitosan-modified PLGA nanoparticles on their cytotoxicity profile. *Intrenational Journal of Pharmaceutics* (submitted)

3. S. Taetz, **N. Nafee**, J. Beisner, K. Piotrowska, C. Baldes, T.E. Mürdter, H. Huwer, M. Schneider, U. F. Schaefer, U. Klotz, C.-M. Lehr. "The influence of chitosan content in cationic chitosan/PLGA nanoparticles on the delivery efficiency of the antisense 2'O-Methyl RNA directed against telomerase in lung cancer cells". *Eur. J. Pharm. Biopharm.* (in press)

4. J. Beisner, M. Dong, S. Taetz, **N. Nafee**,, K. Piotrowska, U. F. Schaefer, C.-M. Lehr, U. Klotz, T.E. Mürdter. *Mol Cancer Ther.* (submitted)

5. **N. Nafee**, F. Ismail, N. Boraie, L. Mortada. Mucoadhesive Delivery Systems. I. Evaluation of mucoadhesive polymers for buccal tablet formulation. *Drug Development and Industrial Pharmacy*, 30(9) 985-993 (2004).

6. **N. Nafee**, F. Ismail, N. Boraie, L. Mortada. Mucoadhesive Delivery Systems. II. Formulation and in vitro/in vivo evaluation of buccal mucoadhesive tablets containing water-soluble drugs. *Drug Development and Industrial Pharmacy*, 30(9) 995-1004 (2004).

7. **N. Nafee**, F. Ismail, N. Boraie, L. Mortada. Mucoadhesive buccal patches of miconazole nitrate: in vitro/in vivo performance and effect of ageing. *International Journal of Pharmaceutics*, 264 (1-2) 1-14 (2003).

8. **N. Nafee**, F. Ismail, N. Boraie, L. Mortada. Design and characterization of mucoadhesive buccal patches containing cetylpyridinium chloride. *Acta Pharmaceutica*, 53 (3) 199 – 212 (2003).

BOOK CHAPTERS:

- **N. Nafee**, M. Schneider, C-M. Lehr. (2008) Charge modification of pharmaceutical nanocarriers: biological implications. In Multifunctional pharmaceutical nanocarriers. V. Torchilin, Ed.; Springer, New York, USA.

- **N. Nafee**, V. Bhardwaj, M. Schneider. (2008) Transport across biological barriers. In Nanotherapeutics – drug delivery concepts in nanosciences, A. Lamprecht, Ed.; WSPC: Singapore.

AWARDS:

- Award from the DPhG for the best oral presentation (1st prize, Doktorandentagung der Deutsche Pharmazeutische Gesellschaft DPhG, Nürnberg, Germany, 6 – 8 September 2006).

- Award from the competition Nano&Art for 'the visualizations related to the nano-future market' organized by Nano4women (Nano&Art – Der Wettbewerb, der Degussa AG, 8th February 2007).

CONTRIBUTION TO SCIENTIFIC CONFERENCES:

A) PODIUMS:

1. **Noha Nafee**, Sebastian Taetz, Marc Schneider, Julia Beisner, Christiane Baldes, Thomas E. Muerdter, Ulrich F. Schaefer, Ulrich Klotz, Claus-Michael Lehr. "Cellular delivery of oligonucleotide-based drugs using chitosan-modified PLGA nanoparticles for the treatment of lung cancer", *GTRV Summer School 2007*, 6-8 September 2007, La Grande Motte, France.
2. **Noha Nafee**, Marc Schneider, Ulrich F. Schaefer, Claus-Michael Lehr. "Cationically modified PLGA nanoparticles for DNA/RNA delivery", *Doktorandentagung der Deutsche Pharmazeutische Gesellschaft (DPhG)*, 6–8 September 2006, Nürnberg, Germany.

B) POSTERS:

1. **Noha Nafee**, Sebastian Taetz, Marc Schneider, Julia Beisner, Christiane Baldes, Thomas E. Muerdter, Ulrich F. Schaefer, Ulrich Klotz, Claus-Michael Lehr. "Chitosan-coated PLGA nanoparticles as a flexible and efficient carrier for antisense oligonucleotides", *34th Annual Meeting & Exposition of The Controlled Release Soceity*, 7-11 July 2007, Long Beach, California.
2. **Noha Nafee**, Marc Schneider, Claus-Michael Lehr. „Cytotoxicity of chitosan-coated PLGA nanoparticles for DNA/RNA delivery", Poster number DD-T-110, *3rd Pharmaceutical Sciences World Congress*, 22-25 April 2007, Amsterdam, The Netherelands.
3. Sebastian Taetz, **Noha Nafee**, Marc Schneider, Christiane Baldes, Kamilla Piotrowska, Thomas E. Muerdter, Ulrich F. Schaefer, Ulrich Klotz, Claus-Michael Lehr. "Cationic chitosan/PLGA nanoparticles effectively deliver antisense 2'O-MethylRNA into A549 cells to inhibit telomerase activity". Poster number DD-W-078, *3rd Pharmaceutical Sciences World Congress*, 22-25 April 2007, Amsterdam, The Netherelands.
4. **Noha Nafee**, Marc Schneider, Claus-Michael Lehr. „Improvment of cellular uptake of antisense oligonucleotides by cationically modified PLGA nanopaticles for the treatment of lung carcinoma". *Annual Meeting of the Nano2Life*, 19-22 March 2007, Saarbrücken, Germany.
5. **Noha Nafee**, Sebastian Taetz, Marc Schneider, Christiane Baldes, Kamilla Piotrowska, Thomas E. Muerdter, Ulrich F. Schaefer, Ulrich Klotz, Claus-Michael Lehr. "Cationically modified PLGA nanoparticles and their potential of binding to antisense oligonucleotides". Poster number 756, *33rd Annual Meeting of The Controlled Release Soceity*, 22-26 July 2006, Vienna, Austria.
6. **Noha Nafee**, Fatma Ismail, Nabila Boraie, Said Khalil. "Polyelectrolyte complexes of chitosan with biodegradable polyanions for the colonic drug delivery" Poster number 1046, *33rd Annual Meeting of The Controlled Release Soceity*, 22-26 July 2006, Vienna, Austria.
7. Sebastian Taetz, **Noha Nafee**, Christiane Baldes, Kamilla Piotrowska, Marc Schneider, Thomas E. Muerdter, Ulrich F. Schaefer, Ulrich Klotz, Claus-Michael Lehr. "Cationically modified PLGA nanoparticles and their potential of binding to antisense oligonucleotides". Poster number 636, *33rd Annual Meeting of The Controlled Release Soceity*, 22-26 July 2006, Vienna, Austria.
8. **Noha Nafee**, Marc Schneider, Ulrich F. Schaefer, Claus-Michael Lehr. "Cationic, chitosan-coated PLGA nanoparticles for DNA/RNA delivery. (I) Manipulation of the formulation parameters". Poster number P0-80, *2nd EUFEPS/APGI Conference on Optimizing drug delivery and formulation: evaluation of drug delivery systems: issues and perspectives*, 20-23 November 2005, Paris-Versailles, France.

9. **Noha Nafee**, Nabila Boraie, Fatma Ismail, Said Khalil. “Formulation and evaluation of buccal bioadhesive tablets containing water-soluble drug”. *AAPS Annual Meeting and Exposition*, 31 October, 2000, Arlington, USA.

Acknowledgements

*First of all, I would like to express my sincere gratitude to **Allah (God)** for guiding me on the track, for supporting me in the hard moments, for giving me the effort and time to do this work. Allah.. may you make this thesis helpful to others.*

*Many thanks to my doctor-father **Prof. Dr. Claus-Michael Lehr** for offering me the chance to join your group and work under your supervision, for providing me with scientific guidance, laboratory facilities and financial support. You really gave me the opportunity to improve my skills, develop my carrier and broaden my knowledge. Many thanks for your trust, your confidence and your never-ending encouragement and moral support.*

*A lot of special thanks and appreciation to my supervisor **Jun. Prof. Dr. Marc Schneider** for... it is really hard to enumerate what you did, I owe you a lot… I just can say thank you for everything... It was enough for me your smile everyday and your words 'never ever give up' to keep me on the road… I am really proud to be your first PhD student… and very grateful for the friendly and comfortable atmosphere that you created at work, for letting me feel that we are not just a supervisor and his student but that we are one team, in one boat… for defending me when necessary, for the funny and fruitful discussions we ever had, for your big trust and faith in me… I hope to keep our relationship in the future as close as it always was and wish you the best of the success and happiness in your life.*

*My respect and thanks to **Dr. Ulrich Schäfer** for his interesting scientific guidance, valuable suggestions, patience and precious time that he generously gave me. Many thanks to you and your wife, **Monika Schäfer**, for taking care of me on personal level, to provide me with all the facilities as much as you can during my first time in Germany. You were always a kind father for me in this foreign country and I wish you will always be.*

*I would also like to convey my appreciation to my first officemates; **Samah Anabousi**, **Javiana Luengo** and **Susanna Kossek** that I miss so much for the friendly atmosphere that we always had in the office and their support in my first days in Saarbrücken… To my present officemates, **Claudia Philippi**, **Fransisca Leonard** and **Daniela Sossong** for their pleasant company and the nice moments that we share.*

*To my dear friend **Stefania Carino**, thank you for the great nights and days that we spent together sharing thoughts, opinions, moods, easy and hard moments. I miss our lunches together but always practicing the Italian specialities that you showed me and that I like a lot. I am very happy to meet you, to know you in deep, to still keep our friendship even after you left and hopefully for ever.*

*Many thanks to my colleagues in the institute **'Biopharmacy & Pharmaceutical Technology', Saarland University,** for their cooperation, their kind help and support especially my coworker **Sebastian Taetz** for our fruitful collaboration… To our expert technicians **Petra König**, **Leon Muijs** and **Heike Stumpf** for their generous help with the cell culture handling, the flow cytometry and the confocal microscopy… To **Kristin Friebel** for her productive contribution in the uptake studies, her nice company and her friendly attitude… To **Peter Meiers** for his help with the devastating computer troubles…To our helpful and cooperative secretaries **Isabelle**, **Karin**, **Gabriele** and the former kind **Gisela**, to all of you my deep feelings of love and thanks.*

*To my dear professors, friends and colleagues back home in the **Department of Pharmaceutics, Faculty of Pharmacy, Alexandria University in Egypt**, for preparing me and putting me on the track… You share part in every success I achieved here in Germany and in my whole life, with all what I learned from you, all your guidance and support.*

*My warmest Hugs to my sweetheart, my daughter **Aya**. Thank you for sharing this 'adventure' with me with fascinating courage and patience, for baring my hard times, my sadness and my nervosity. You gave up your society; your school, your best friends and relatives to come with me here where you know nobody and have no clue to any German word. You did it just for me, for my best… Thank you for always being the responsible person that I can trust and rely on, for withstanding my absence at home till the late hours almost everyday without complains… I promise to reward you with more care and time from now on… I know, it was a big challenge for both of us, I am deeply happy that we finally made it together, every nice and hard moment together… I wish you all the success and happiness in your future life, you really deserve the best.*

Aya… big kisses just for you.

*To my late **mother**, although you passed away, you are always inside me, inspiring me as you always did in my life. I wish we could share this moment together but I hope you are proud of me.*

*To my dear **father**, my whole **family** in Egypt thank you all for your love, kind support, faith and encouragement.*

*Many sincere thanks to all my friends in Germany, especially Dr. **Yasser Elnakady** and **Wael Elmenofy**, you were more than brothers for me; I would not imagine it without you… To **Saad Shaaban** and his wife **Shaimaa** and to **Mohamed Hamdoon** thank you for every nice moment and good meals we shared together.*

*The German Academic Exchange Service **(DAAD)** is gratefully acknowledged for the financial support during the first two years of my stay in Germany and The **'Deutsche Kerbshilfe'** for the financial support of the Telomerase project.*

To everyone that was not mentioned, please forgive me and to all of you all my respect, appreciation and thanks.